MECHANISM OF WEAR PROTECTION OF Al-ALLOYS USING XANES

by

BEIBEI WANG

Presented to the Faculty of the Graduate School of

The University of Texas at Arlington in Partial Fulfillment

of the Requirements

for the Degree of

MASTER OF SCIENCE IN MATERIAL SCIENCE AND ENGINEERING

THE UNIVERSITY OF TEXAS AT ARLINGTON

August 2009

ACKNOWLEDGEMENTS

This research has been made possible by invaluable help, input and support from several people. First I wish to thank my advisor, Dr. Pranesh B.Aswath who has been my guide and mentor in the past 2 years. His support, help and guidance, combined with his patience and pleasant and inspiring personality as well as his exceptional knowledge in his field have been the key reason behind the progress in his work.

I would like to thank the help and support of my graduate committee members, Dr. Choong-Un Kim, and Dr. Michael Jin.

I would like to thank the faculty members of the materials science and engineering department at University of Texas at Arlington for their generous sharing of their knowledge and resource through out my graduate studies at this university. I would like to thankful acknowledge the MSE staff, Mrs. Jennifer Standlee, who has always greeted me with a smile and has been more than helpful in many instance, and Mrs. Libia A. Cuauhtli whose help has insured the timely progress of this research work. My special thanks to Dr. Jiechao C. Jiang and David Yan who provided me with training on numerous equipments in the characterization lab as well as their significant help.

My deepest gratitude goes to my former and current colleagues, Dr. Xin Chen, Dr. Ramoun Mourhatch, Dr Anuradha Somayaji, Dr. Hande Demirkiran, Bo-Hoon Kim, Mihir Patel, Eray Erkan, Hansika Parekh, Arunya Suresh and TJ Adeogba in the tribology research group and the MSE department who not only have been great team members, and helpful with everything, but have also become among some of my best friends.

July 14, 2009

ABSTRACT

MECHANISM OF WEAR PROTECTION OF Al-ALLOYS USING XANES

Beibei Wang, M.S

The University of Texas at Arlington, 2009

Supervising Professor: Pranesh B. Aswath

The mechanism of wear protection of Al-Si alloys in wear tests using lubricants containing Zinc dialkyl-dithiophosphate (ZDDP), Dialkyl dithiophosphate (DDP) , Amine phosphates, Thiadiazole, Antimony 0, 0-dialkylphosphorodithioate (SbDDP) was studied. Using techniques such as XANES this study examined the tribological behavior of these compounds and the characteristics of the tribofilms formed by them.

High frequency reciprocating rig (HFRB) tests were conducted with lubricant containing these five antiwear additives were compared in both base oil and fully formulated oil. The tribofilms formed were then analyzed by a variety of techniques such as Scanning electron microscopy of the film and the composition was examined using EDS. The tribofilms were also chemically analyzed using X-ray absorption near edge structure (XANES) spectroscopy. Results indicate that the Al matrix does not assist in the formation of a tribofilms. However a transfer film formed from the steel ball and the lubricant chemistry on the precipitates provide protection on the surface. Lubricant chemistries that contain both S and P provide the best protection while the chemistries with either only P or S have very poor wear outcomes.

TABLE OF CONTENTS

LIST OF ILLUSTRATIONS

Figure Page

LIST OF TABLES

CHAPTER 1

INTRODUCTION

Aluminum alloy engine blocks are widely used in the auto industry, providing approximately a 50% weight savings over cast iron blocks. One of the primary goals of car manufacturers is to reduce the weight of the engine-block, and hence to improve the fuel efficiency and reduce harmful emission into the environment. Unfortunately, aluminum cannot be used effectively for the cylinder bore wall due to its poor tribological properties. To overcome this wear problem, the wear resistance of aluminum can be improved through alloying with silicon to increase the overall strength of aluminum. The lightweight characteristics, high strength and low cost make silicon content aluminum-silicon (Al-Si) alloys important materials of choice for automotive applications [1].

Automobile lubricants have been used to reduce wear, improve running efficiency, and hence prolong the life of an engine for nearly a century. The additives have been extensively used as viscosity improvers, pour-point depressants, antiwear additives, extreme pressure additives, detergents, and dispersant. These additives have also been extensively developed to meet different technical and environmental requirements for different parts in a car engine. The main problem of the lubricants is that they can interact with combustion products which results in their contamination, oxidation, and formation of deposits on contacting and rubbing surface. These problems will cause serious corrosion and wear to engine.

Zinc dialkyl-dithiophosphates (ZDDPs) is the most commonly used and best antiwear and antioxidant additive for engine lubricants (Figure 1).

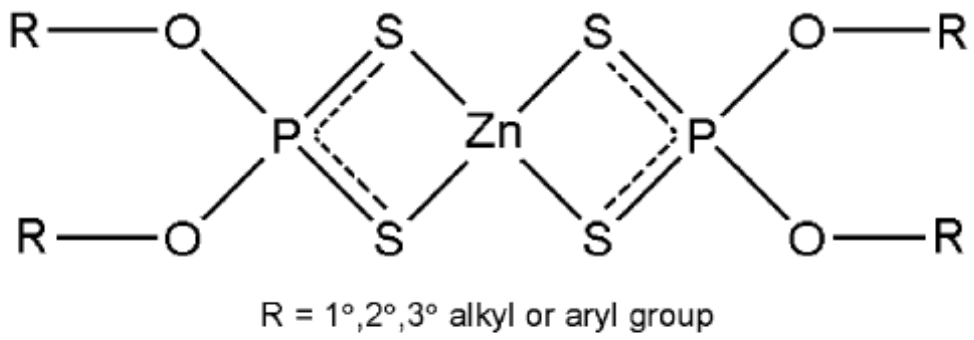

Figure 1.1 The structure of zinc dithiophosphate. The R group dictates whether it is an alky- or aryl-dithiophosphate.

It is widely accepted that ZDDPs breakdown and react with the steel by Zn→Fe iron exchange and subsequent formation of an amorphous chemisorbed film containing zinc, phosphorus, oxygen and sulfur and also iron in the form of polyphosphates and sulfates of zinc and iron at temperature above 80℃[2-8]. This sacri ficial film is responsible for minimizing asperity contact and wear [9]. Other studies using X-ray absorption near edge structure (XANES) spectroscopy, at the L-edge, indicated that this film was composed of a mixture of two layers, with the outer layer consisting of long chain polyphosphates and the inner layer composed of short chain polyphosphates [10]. However, despite years of work, the mechanism of formation and action of the antiwear films are still poorly understood. In spite of these prominent merits, ZDDP has some drawbacks. The demerits of ZDDP are problems with toxicity, waste disposal, filter clogging, pollution, and deposition on the lubricated surfaces. In particular, the antiwear additives with metal elements like Zn in ZDDP are susceptible to hydrolysis. Therefore, the contamination of the finished fluid with water can lead to the breakdown of the bond that holds zinc oxide. This reaction results in clogging filters, catalysts, and traps, depositing all ask forming elements on the surface of substrate, and degrading performance. As a consequence, the pressure drop across the trap or the catalyst converter is increased and the harmful emissions aren't converted into the harmless products. This requires

more frequent maintenance or replacement in order to keep high levels of effectiveness and durability in the various exhaust gas treatment system. The use of environmentally friendly ashless additives without any heavy metal elements is desirable because of the environmental and toxicological considerations.

1.1 Motivation of Research

In an effort to reduce weight of an engine aluminum-silicon (Al-Si) alloys are used to replace cast ion parts in automobile engines. In comparison to cast ion, Al-Si alloys have advantages including resistance to corrosion, good thermal conductivity, less weight.

However, little work has focused on the lubrication of Al-Si alloys. Some authors have indicated that in the presence of additives, a reduced-friction layer, soap or polymer forms from a reaction between aluminum and the additive, or from an additive by-product [11-15]. Fuller et al [16] performed experiments with a reciprocating wear tester with a sliding-cylinder-on-block geometry. The authors used a 1.2wt%ZDDP solution in base oil, aluminum 6061(A6061, Si content~0.7%)/A6061 and A390/A390 pin and block couples. The authors found that after only 30 min of rubbing time, the ZDDP tribofilms form on the Al-alloy surfaces and they are nearly identical to those that form on steel. Konishi et al [17] used a pin-on-disk wear tester under fully formulated conditions, and used an A390/A390 couple, 0.2wt% ZDDP in mineral and synthetic base oil. The author found that the wear rate was reduced when ZDDP was added to base oil comparing with base oil only. They claim that is due to the formation of a ZDDP-containing protective film. Wan et al [18] test is a sliding point contact using a steel ball on an aluminum 2024 plate (A2024, Si content~0.5%).The authors used a mixed alkyl-chain ZDDP and varied the concentration in the base oil up to 5%.The authors claimed that increasing the ZDDP concentration increased the wear, and the friction coefficient was not altered. Kawamura and Fujita[19] did a cross-pin-type wear test about boundary, drip-supplied lubrication conditions on aluminum 390(A390, Si content~18%) and they used additives containing phosphates, phosphates and ZDDPs. Individual solutions contained 5% concentration of either primary,

secondary or aryl ZDDPs in paraffinic base oil. The authors claimed that the lubrication effect is due to an adsorption effect or to the formation of a friction polymer, and not due to a chemical reaction between the A390 surface and ZDDP.

Their findings described above contain differing conclusions. Some of their results showed that adding ZDDP to base oil had little effect in preventing wear. The study of wear resistance of Al-Si alloys rubbing against themselves or against steel is becoming more important because Al-Si alloys are being used to replace some cast iron parts in combustion engines. In this test, we have used five kinds of lubricants : Dialkyl dithiophosphate (DDP),Amine phosphates, Thiadiazole ,Antimony 0, 0-dialkylphosphorodithioate (SbDDP) and Zinc dialkyl-dithiophosphate (ZDDP) to examine the possibility of forming an antiwear film on related Al-Si alloys under base oil or fully formulated oil lubrication conditions .This will provide us insight about Al-Si alloys and help to understand whether these lubricant additives can reduce wear by decomposing and forming a film in the same way as in cast iron engines. The tribofilms formation on the surface provides insight the mechanism of wear protection.

1.2 Objectives of Research

This research work is aimed at examine the mechanism of wear protection of Al-Si alloys under the lubrication condition. An essential part of this study includes understanding the antiwear action of five kinds of lubricants :Dialkyl dithiophosphate (DDP), Amine phosphates, Thiadiazole, Antimony 0, 0-dialkylphosphorodithioate (SbDDP) and Zinc dialkyl-dithiophosphate (ZDDP) by studying the formation mechanisms of antiwear films. We divided these chemical to four groups and compared:

(1) ZDDP vs SbDDP in base oil/ fully formulated oil, we want to compare whether the different cation species have any influence on the formation of antiwear film.(2) ZDDP vs DDP in base oil/ fully formulated oil ,we want to compare the difference between ash and ashless antiwear additives and whether the absence of intrinsic cationic species has any influence on the formation of tribofilms;(3) DDP vs Amine phosphate in base oil/ fully formulated oil ,we want to compare the thiophosphate and amine phosphate ashless antiwear additives;(4) Thiadiazole vs

Amine phosphate in base oil/ fully formulated oil ,we want to compare the sulfur and phosphate ashless antiwear additives. We use the base oil and fully formulated oil want to know how these additives reaction at ideal and real condition in engine. The characterization methods employed will further deepen our understanding of these lubricants from different properties standpoints. These characterization methods include several mechanical and chemical surface analysis methods: HFRB, Optic Profilometer, SEM/EDS, and XANES. These methods will look at the chemical compositions of the films through out the depth of the films as well as mechanical properties of these films.

1.3 Structure of Research

This thesis is presented in five chapters. Each chapter is included here with an outline and summary of contents detailed in the chapter later:

Chapter 1, Introduction: this chapter introduces the reader to the motivation and objectives behind the whole research work. It also includes a summary of what can be gained from such a study from research point of view.

Chapter 2, background: this chapter gives an overview tribology in internal combustion engines, engine oils, and different types of wear phenomena, lubrication and wear in internal combustion engines, including different lubrication regimes. A review of the lubrication of cast iron/steel surface by ZDDPs, and a review of the lubrication of aluminum-silicon alloys by ZDDPs.

Chapter 3, Experimental procedures: Experimental methods and testing and characterization techniques used in this study. Five kinds of lubricants were used: Dialkyl dithiophosphate (DDP), Amine phosphates, Thiadiazole, Antimony 0, 0-dialkylphosphorodithioate (SbDDP) and Zinc dialkyl-dithiophosphate (ZDDP) in base oil and fully formulated oil, and HFRB tests were conducted to examine the wear resistance and characteristics of the films forming on Al-Si alloys in the present of these lubricants .These test methods includes: Optic Profilometer, SEM/EDS, XANES.

Chapter 4 Results and discussion, describes an extensive investigation into the wear performance of specify alloy used in this study. The morphology of film surface was evaluated using SEM and EDS. The chemical species present in the films were investigated by XANES and the antiwear performance was evaluated based on the wear scar volumes measured on the aluminum-silicon alloys disks. The mechanism of wear protection in Al-Si alloys is present on a function of the chemistry of the antiwear additives used.

Chapter 5, Mechanism.

Chapter 6, Conclusions.

CHAPTER 2

BACKGROUND

2.1 Overview: Tribology of Engines

Tribology is the science and technology of interacting surfaces in relative motion. It includes the study and application of the principles of friction, lubrication and wear, is a new field of science defined in 1967 by a committee of the Organization for Economic Cooperation and Development. “Tribology” is derived from the Greek word “tribos” meaning rubbing or sliding [20].Wear is the major cause of material wastage and loss of mechanical performance and any reduction in wear can result in considerable saving. To reduce friction and wear, the engine tribologist is required to achieve effective lubrication of all moving engine components, with minimum adverse impact on the environment. This task is particularly difficult given the wide range of operating condition of load, speed, temperature, and chemical reactivity experienced in an engine.

Improvement in the tribological performance of engine can yield:

- Reduced fuel consumption
- Increased engine power output
- Reduced oil consumption
- A reduction in harmful exhaust emissions
- Improved durability, reliability, and engine life
- Reduced maintenance requirements and longer service intervals

With such large numbers of reciprocating internal combustion engines in service, even the smallest improvements in engine efficiency, emission levels, and durability can have a major effect on the world economy and the environment in the medium to long term [21].

2.2 Friction and Wear in Engines

2.2.1 Definition and Mechanisms

Wear has been recognized as meaning the phenomenon of material removal from a surface due to interaction with a mating surface. Wear is normally measured by measuring the mass or volume of the material removed due to contact between two surfaces [22].Wear is the result of material removal by physical separation due to microfracture, by chemical dissolution, or by melting at the contact interface. Focusing on the wear mechanism from the viewpoint of contact configurations, there are four fundamental and major wear modes: adhesive wear, abrasive wear, fatigue wear and corrosive wear.

2.2.1.1 Adhesive Wear

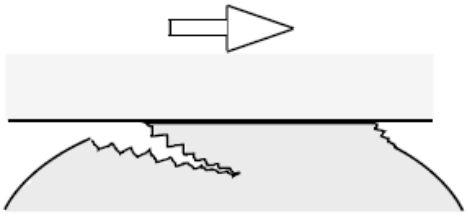

Figure 2.1 Adhesive wear

Adhesive wear is a very serious form of wear characterized by high wear rates and a large unstable friction coefficient. If the contact interface between two surfaces under plastic contact has enough adhesive bonding strength to resist relative sliding, large plastic deformation caused by dislocation is introduced in the contact region under compression and shearing. As a result of such large deformation in the contact region, a crack is initiated and is propagated in the combined fracture mode of tensile and shearing. When the crack reaches the contact interface, a wear particle is formed and adhesive transfer is completed. This type of wear which occurs when there is enough adhesive bonding at the contact interface is called

adhesive wear. Adhesive wear is the most common in most tribological systems [23] (figure 2. 1).

2.2.1.2 Abrasive Wear

If the contact interface between two surfaces has interlocking of an inclined or curved contact, ploughing takes place in sliding. As a result of ploughing, a certain volume of surface material is removed and an abrasive groove is formed on the weaker surface. This type of wear is called abrasive wear. Abrasive wear occurs whenever a solid object is loaded against particles of a material that have equal or greater hardness. The particles either may be present at the surface of a second material (two-body wear) or may exist as loose particles between two surfaces (three-body wear). Abrasive wear can be measured as loss of mass by the Taber Abrasion Test according to ISO 9352 or ASTM D 1044[23](figure 2.2).

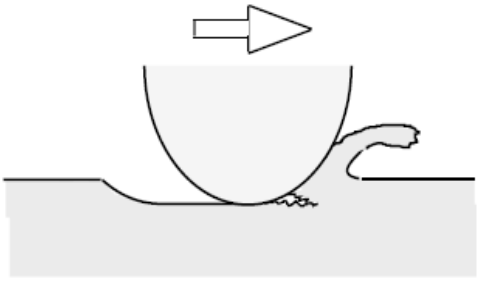

Figure 2.2 Abrasive wear

2.2.1.3 Fatigue Wear

There are other cases of wear where a certain number of repeated contacts are essential for the generation of wear particles. Wear generated after such contact is called fatigue wear. When the number of contact cycles is high, the high-cycle fatigue mechanism is expected to be the wear mechanism. When it is low, the low-cycle fatigue mechanism is expected [23] (figure 2. 3).

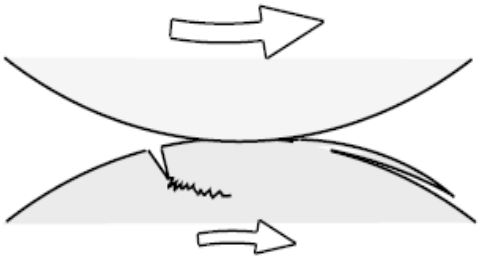

Figure 2.3 Fatigue wear

2.2.1.4 Corrosion Wear

When sliding takes place, especially in corrosive liquids or gases, reaction products are formed on the surface mainly by chemical or electrochemical interactions. If these reaction products adhere strongly to the surface and behave like the bulk material, the wear mechanism should be almost the same as that of the bulk material. In many cases, however, such reactions products behave very differently form the bulk material. Therefore, wear is quite different from that of the bulk material, and is dominated by the reaction products formed by the interaction of solid materials with the corrosive environment. This kind of tribochemical wear accelerated by corrosive media is called corrosive wear [23] (figure 2. 4).

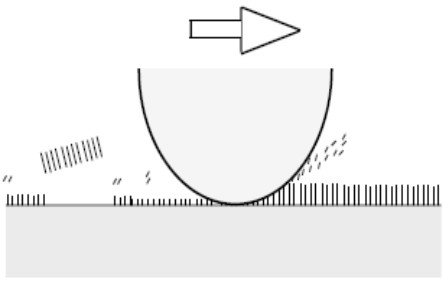

Figure 2.4 Corrosive wear

2.2.2 Wear Stage in Tribology

There are three wear stages during the wear process. The wear process begins with a break-in stage, during which steady-state conditions are building up (figure 2.5).This stage is always short compared to the whole lifetime of the component. During this stage, the mating surfaces conform to each other in such a way that the load is more favorably distributed over the surface. During the early break-in stages, the wear rate may be relatively high because asperities on both mating surfaces abrade the opposing surface, leading to generation of conforming surface, larger contact area and smaller contact as a result of loads being distributed over large areas. In lubricated contacts, low friction antiwear films have not been formed in the break-in stage.

Steady-state stage has low wear rates and stable friction values. A protective antiwear film is present during this steady state condition. This film in lubricated system works as a sacrificial layer against wear and compression and shearing forces. The steady state in these lubrication films will continue as long as the lubricant-surface tribological interactions favor new film formation and replenishment. In this state, wear rates will eventually alter clearances or surface properties to the extent that component fail when the lubricant is no longer able to participate in the tribochemical reactions that lead to formation and replenishment of a protective antiwear film. Therefore, it can bring a brief, final, catastrophic stage during which wear rates are high and severe surface damage occurs.

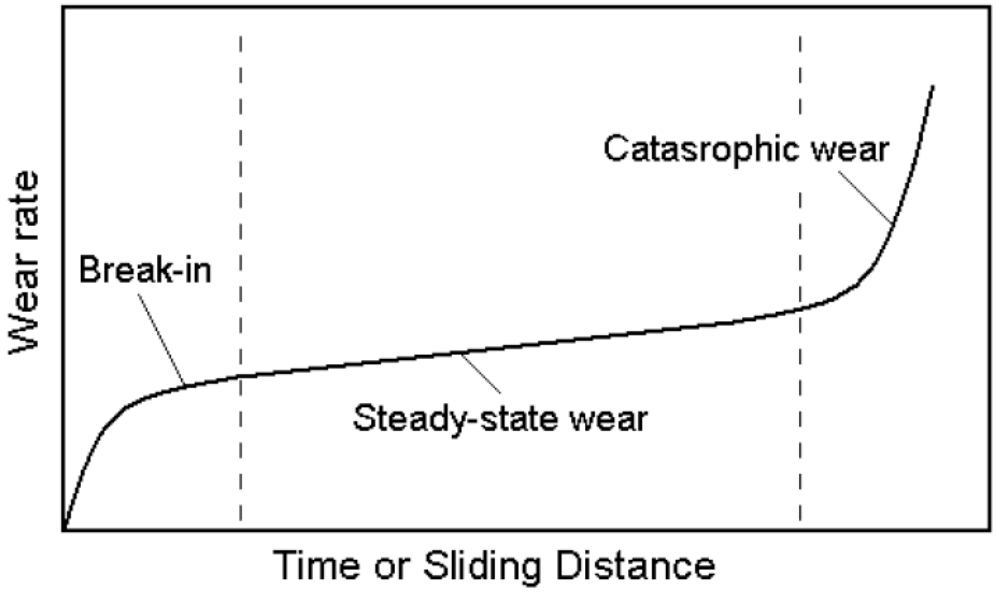

Figure 2.5 Typical wear stages appearing over longer service times in sliding contacts

2.3 Lubrication in Internal Combustion Engines

2.3.1 Lubrication Regimes

Lubrication is the process of introducing a layer of material (liquid, solid or a mix of both) in between two surfaces with relative motion and contact in order to reduce or prevent wear as well as to reduce friction. The material introduced to perform this task as the lubricant. There are three types of lubrication regimes occur depending on different load, surface roughness, amount of lubricants, etc. These lubrication regimes have been identified as fluid film lubrication, mixed lubrication and boundary lubrication regimes.

2.3.1.1 Fluid Film Lubrication

In fluid lubrication regimes, a thin film of liquid separates the solid components of a tribological system and the fluid film support the load. The physical properties of the lubricant such as viscosity, traction, load bearing capability, etc determine the performance of the lubricant in fluid film lubrication. There are two types of fluid film lubrication (a) hydrodynamics lubrication and (b) elastohydrodynamic lubrication. Hydrodynamic lubrication occurs where non-parallel interacting surfaces are present and provide for convergent fluid lubricant films between

the two surfaces. Elastohydrodynamic (EHD) lubrication occurs when the viscosity of the fluid film becomes a function of load while its effective thickness becomes insensitive to contact load under high contact loads. The fluid film will become not able to fully support the load and the surface asperities under the extreme contact loads and the lubrication regime becomes a mixed regime of boundary and EHD fluid film lubrication regimes.

2.3.1.2 Boundary Lubrication

Boundary lubrication occurs at very high contact loads and low sliding speeds. During this regime, asperities interactions occur and asperities on the two rubbing surfaces collide and therefore undergo deformation both elastic and plastic fracture. In engines, the antiwear chemistries present in the lubrication, react with the metal surface and form protective thin film in boundary lubrication. The antiwear film separates the two rubbing surfaces and it is usually low friction and wear resistance and protects the surface from further wear. In real surfaces in practical tribological systems, there are different sizes of asperities and the condition is more complicated, therefore a mixed regime of boundary and EHL lubrication modes exist in this system (figure 2.6).

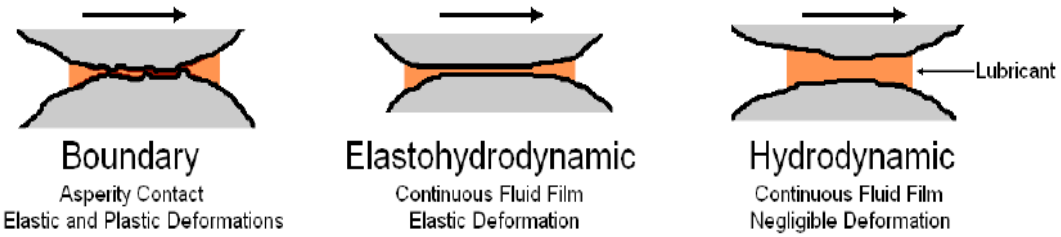

Figure 2.6 Schematic comparisons of different lubrication regimes

2.3.1.3 Friction Coefficient in Lubricated Contacts

Surface conditions and lubrication regime determine the tribological effects such as lubricant film thickness and coefficient of friction. Lubricated components of mechanical systems are usually working under hydrodynamic lubrication regimes. The coefficient of friction under these conditions is related to absolute viscosity of oil, relative speed, component geometry and load, etc by pertroff's formula (equation 2.3.1.3).

$$f = 2\pi^2 (r/c)(\mu N/P)$$

Equation 2.3.1.3

Where f is the coefficient of friction, μ is the absolute viscosity of the fluid lubricant, N is the shaft rotation speed, P is the load per unit of projected bearing area, r is the journal radius and c is the radial clearance. In hydrodynamic lubrication regime, according to Petroff's formula, there is a linear relationship between coefficient of friction and the dimensionless bearing characteristic parameter uN/P. The higher contact loads (higher than P) will squeeze out of the lubricant from the contact point as well as making asperity contact, it will results in the mixed mode and boundary lubrication regimes (see figure 2.7 Stribeck curve).

Observed from the Stribeck curve, under the boundary lubrication regime, friction follows the different trend with changing bearing characteristics. Increasing contact pressure will increase coefficient of friction under the boundary lubrication regime because it increases contact stresses between the asperities and therefore increasing the chance of their adhesion, and results in higher resistance against relative movement of the two surfaces and the coefficient of friction increases. Low speeds under boundary lubrication will increase the number of asperities in contact with one another the same effect as increasing the contact load.

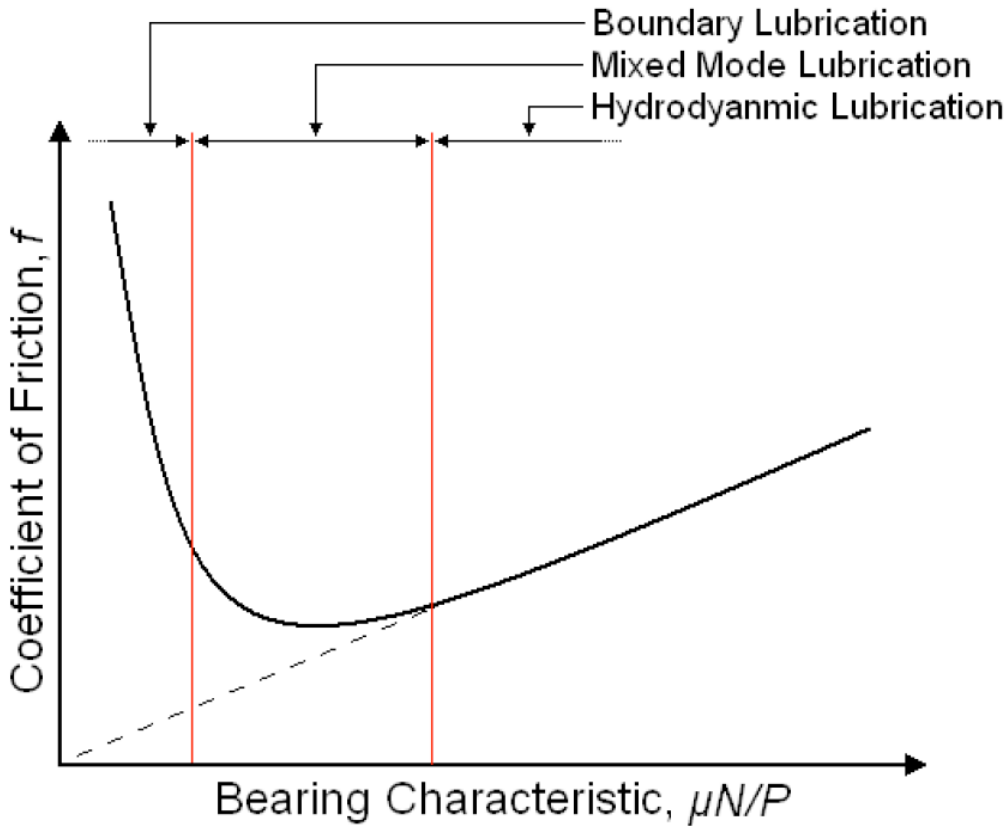

Figure 2.7 Stribeck curve

2.3.2 Antiwear Additives and Boundary Lubrication

A significant portion of wear in engines occurs during the brief start up and acceleration periods. The amount of oil present in bearing and on cylinder surface is not enough to provide effective fluid film lubrication when engine is started. lack of sufficient amount of lubricant results in asperity-asperity contact in these locations and the boundary lubrication regime is the dominant lubrication regime during this short period. Adding antiwear additives in oil to formed solid tribofilms on the surface can reduce the amount of wear occurring at this regime. When such protective films are formed, wear of mating materials is prevented and replaced by consumption of antiwear additive in the oil. Depending on the chemical nature of the antiwear additives, two types of antiwear effects have been identified by Martin, et al. [24, 25]

Tribology reaction leading to formation of tribofilms by chemical reaction processes involving an active participation of both the contact surface materials and environmental factors (atmosphere, water etc) and their chemical interaction with the antiwear additive. In this case depending on the type of the additives, two types of mechanisms are observed:

1. Additives chemically react with the surface directly, e.g. sulfur and chlorine chemical compounds, fatty acids, fluorinated compounds.

Antiwear action by the additives occurs through thermal and/or oxidative degradation process of the additive e.g. metal dithiophosphates and phosphorus containing organic compounds.

2. Polymeric and non-sacrificial films. In this case, contact surfaces do not chemically partake in the formation of the antiwear film, although the may catalyze the process. This process also involves formation of high molecular weight compounds through polymerization process e.g. complex esters, solid lubricant additive like oil soluble molybdenum compounds, borate additives, double bond containing molecule etc.

2.4 The Lubrication of Cast Iron/Steel Surfaces by ZDDPs

2.4.1 Chemical Characterization

The structure formula of ZDDP is shown in figure 2.4.1.1 represents alkyl and/or aryl groups in the structure. When R represents alkyl groups (alkyl ZDDPs), it can either be primary, secondary or tertiary alkyl chain [26].The ZDDP complexes are manufactured by reaction of alcohols, phosphorus pentasulphide and zinc salts [27].Whether the alkyl type R groups are of secondary or primary type as well as their chain length depends on the type of alcohols used in the manufacturing process of ZDDP. It has been found that ZDDP derivatives containing alkyl type R groups generally have lower thermal stability but are better antiwear additives and have better hydrolytic stability than ZDDP derivatives with aryl R groups [28].Among alkyl type ZDDPs, secondary alcohol ZDDP derivatives have been shown to be more effective antiwear additives than primary alcohol ZDDPs derivatives as they have lower thermal stability than primary alcohol ZDDPs [29].

Figure 2.8 Structure of ZDDP

Commercially manufactured ZDDP is usually a mixture of two types of ZDDPs, i.e. neutral and basic. Neutral ZDDP exists as equilibrium between monomer and dimmer in solution as seen from figure 2.9[30].

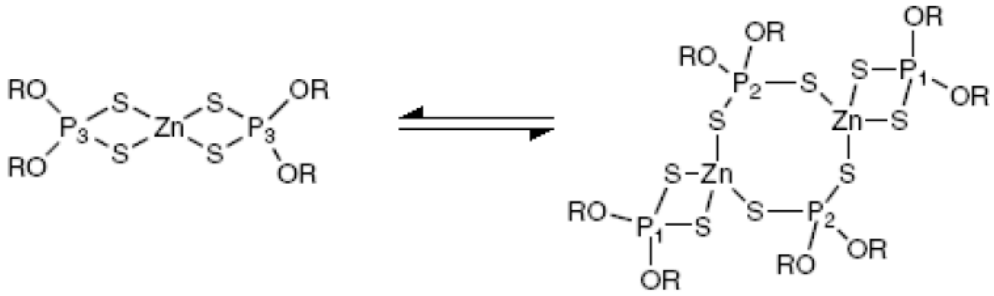

Figure 2.9 Neutral ZDDP

The crystal structure of basic ZDDP has remained a matter of speculation since a long time however good quality data was obtained from a single crystal at -100℃ for Butyl ZDDP,Zn4O[S2P(OBu)2]6.It revealed a Zn4O core with four Zinc atoms in an almost prefect tetrahedral arrangement about central oxygen as seen in figure 2.10[31].

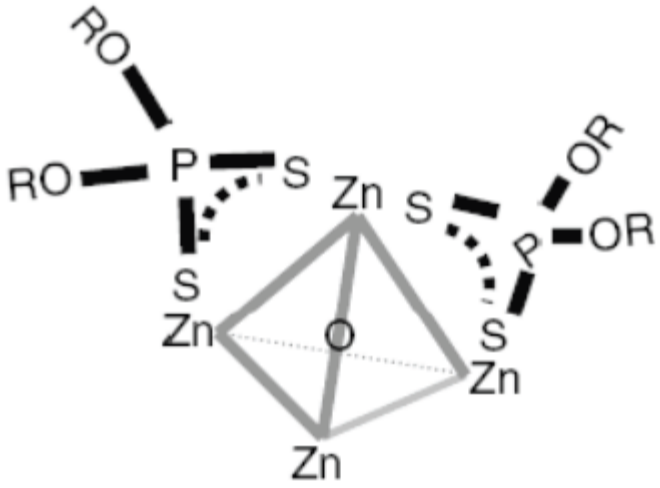

Figure 2.10 Crystal structure of basic ZDDP

2.4.2 Film Formation Mechanisms

The chemical nature of ZDDP films has been extensively studied using many different surface sensitive techniques such as X-ray photoelectron spectroscopy (XPS)[32],Auger electron spectroscopy(AES)[33],X-ray absorption near edge structure(XANES) analysis[34],extended X-ray absorption fine structure(EXAFS) analysis[35],energy dispersive X-ray (EDX) analysis[36],infrared(IR) spectroscopy[37],high pressure diamond anvil cell combined with IR[38],transmission electron microscopy (TEM)[39],and others. The reaction of ZDDP with metallic surfaces and oxides and the decomposition of ZDDP in solution(base oil) has also been studied using quantum chemical methods and molecular modeling[40],which suggest the reaction products that can be involved in, and in some cases are observed, during antiwear film formation.

Lot of effort has been put in to understand the mechanisms for the formation of ZDDP antiwear films, and there are many theories .Two combined mechanisms, which involve the ZDDP thermal decomposition and chemical reaction of degradation products, appear to be the most appropriate.

Armstrong et al [41] have investigated the structure of ZDDP's using semi-empirical quantum chemistry methods. And the calculation showed that the basic form has been concluded as the most stable structure of ZDDP .Further, they found that for ZDDP monomers the most stable structure is that in which O^{2-} is bound to the zinc atom, and the lowest power is needed for the attack of O^{2-} on one of the sulfur atoms in the dimmer or basic ZDDP molecules. Thus, during the reaction at the steel surface, the sulfur atoms are likely to be attacked by oxygen anions, lead to the cleavage of three bonds, two P-S bonds and one Zn-S bond, and as a result, break down the ZDDP molecule. They also found that sulfur species are diminished in the film, and exist primarily as sulfate or sulfides [42, 43].

Westerfield and Agnew [44] using a specially developed diamond anvil cell/FTIR completed work provided this insight on the film formation mechanism at high pressure and temperature. They used the intensity of the P-O stretching band to monitor the chemical change of ZDDP under pressure and temperatures up to as high as 12.3GPa and 200℃. They showed that the decomposition of ZDDP increased with increasing pressure and decreased after reaching a maximum at a pressure of 0.7GPa.This indicated that the decomposition of ZDDP might be initiated by the increase of pressure in the area of asperity contacts rather than by the induced frictional heat.

Willermet et al [45].have proposed a four-step process that describes the reaction mechanism of ZDDP from solution, under mild wear condition, to reaction products on steel surfaces:

(i) Adsorption of ZDDP on metallic surfaces.

(ii) Reaction of ZDDP with the metallic surface to form species of phosphates and phosphothionic moieties bound to the metal surface.

(iii) Formation of phosphate film precursors from antioxidant reactions of ZDDP.

(iv) Condensation of the phosphates/phosphothionates species occur and are then terminated by zinc-containing compounds or other metal ions in solution (such as from detergents).

The authors conclude that phosphates are formed by oxidative decomposition of ZDDP in which the antioxidant and antiwear chemistries are linked.

Yin. et.al [46] assumed their mechanism based on their results determined using XANES spectroscopy. The authors postulated a three-step mechanism:

(i) ZDDP is physisorbed on steel.

(ii)Thermal-oxidative process with oxygen or organic peroxides (from the oxidation of hydrocarbon base oil) results in the decomposition of ZDDP producing zinc metaphosphate (a long-chain polyphosphate), $Zn(PO_3)_2$, and small amounts of zinc sulphides.

(iii)Step three can proceed by two different pathways depending on the availability of cations (such as Fe) or on the reaction temperature.

(3a) the formation of pyrophosphates ($FeZnP_2O_7$).

(3b) the formation of orthophosphates $Fe_2Zn(PO_4)_2$.

The fast reaction pathway(2)dominates if the temperature is high or if there is a lack of metal irons in solution, and this step forms the metaphosphates. However, if the reaction is proceeding slowly because of the low reaction temperature or an abundance of iron and/or zinc cations, then pyrophosphate or orthophosphate forms (3a and 3b).The authors also claim that at the metal oxide-phosphate interface, metal irons create pyrophosphate or orthophosphates that result in the formation of a layered film with zinc polyphosphates at the surface and iron coordinated pyrophosphate and/or orthophosphates in the bulk. Different from Willermet et al, Yin et.al [47] conclude that long-chain polyphosphates form first, and with extended rubbing, these long-chain polyphosphates interact with the metal ions to form short-chain polyphosphates. Willermet et.al [48] suggested that short-chain polyphosphates form first, and then polymerized to long-chain polyphosphates.

Suominen-Fuller et al [49] gave new insight of the growth and formation of thermally generated ZDDP and tribologically derived films on steel, using XANES spectroscopy. They made a slight change to the three step mechanism of Yin et.al, and developed a five step pathway for the decomposition of ZDDP and formation of a polyphosphate film on steel.

(i) ZDDP is adsorbed onto metal surface.

(ii) ZDDP (in solution) is converted to phosphate intermediate termed Linkage Isomer (LI in solution).

(iii) LI(in solution) is absorbed to the metal surface.

(iv) Thermal-oxidation of adsorbed LIand ZDDP occurs by either O_2 or ROOH to form long-chain polyphosphates $Zn(PO_3)_2$.

(v) With continued rubbing, in the presence of water from the base oil, hydrolysis of polyphosphates occurs, creating short-chain polyphosphates.

Ferrari et al [50] proposed a similar mechanism of film formation. They claimed that zinc polyphosphate undergoes an oxidation process leading to the formation of Zn-O and Fe-O bonding and finally to the formation of a glass network. The authors gave a simple 2-step pathway:

(i) The removal of iron oxide.

(ii) Reaction of ZDDP with nascent iron substrate.

Martin et.al [51, 52] gave an alternative mechanism to those outlined above. They claimed that the mechanism is based on the hard and soft acids and bases (HSAB) principle and under tribological contacts form a third-body abrasive particle such as iron oxide. The authors explained an acid-base reaction between phosphates and iron oxides since Fe^{3+} is a harder Lewis acid than Zn^{2+} and therefore a cation exchange is very easily. Because phosphates are hard bases they will react with hard acids. The authors gave the reaction 1.1 under mild wear conditions (shear (θ), temperature (T), and pressure (P)):

$$5Zn(PO_3)_2 + Fe_2O_3 \text{--------} \rightarrow Fe_2Zn_3P_{10}O_{31} + 2ZnO \qquad [1.1]$$

Which indicates the digestion of the iron oxide to the formation of a mixed iron/zinc polyphosphate glass? The authors suggested that based on the Moh's scale iron oxides are much harder than zinc oxide and gave the reaction 1.2:

$$Zn(PO_3)_2 + Fe_2O_3 \text{--------} \rightarrow 2FePO_4 + ZnO \qquad [1.2]$$

The authors suggest that the chain-length of the polyphosphate structure will decrease with rubbing as Zn^{2+} cations are exchanged for the higher charged Fe^{3+} cations. Therefore, there are shorter-chain polyphosphates forming in the bulk of the film and long-chain polyphosphates forming at the surface of the film. Martin [51] also explains the role of sulfur in the tribochemical reaction. Based on the HSAB principle, organic sulfur species can react with ZnO to form ZnS, if a poly (thio) phosphate exists then ZnS can also form by reaction 1.3:

$$Fe_2Zn_3P_xS_{10-x}O_{31}+Fe_2O_3\text{------}\rightarrow Fe_2Zn\,(P_2O_7)_2+ZnS \qquad [1.3]$$

The author said that under the extreme wear conditions, the role of sulfur may be to act with nascent surface to form FeS, which can prevent adhesion between adjacent asperities and the further attack of the nascent surface by oxygen.

Although there is some difference between the mechanisms, there is significant agreement. First, ZDDP in solution adsorbs chemically or physically to the metal/oxide surface. Second, the decomposition products such as the linkage isomer also adsorb. Third, an oxidative process occurs which results in the degradation of the ZDDP molecule. The largest inconsistency is how the polyphosphate film forms. Yin et al [47] claimed that there is short-chain polyphosphate in the bulk of the film and long-chain polyphosphate at the surface of the film. Willermet et al [48] suggested that short-chain polyphosphate form first and then is polymerized to form long-chain polyphosphate. These theories suggest that short-chain polyphosphates are bound to the metal/oxide surface and then formed film having the long-chain polyphosphates. In all process, the phosphate structure is predominantly coordinated by zinc cations and a mixture of zinc and iron cations at the film/metal substrate interface.

2.5 The Lubrication of Aluminum-Silicon Alloys by ZDDPs

Generally, more and more aluminum-silicon (Al-Si) alloys are being considered to replace cast ion parts in automobile engines. Comparing with the cast iron parts they have many advantages including resistance to corrosion, good thermal conductivity, less weight, and moderate costs, etc. The introduction of silicon improves the wear resistance and reduces the

susceptibility to scuffing of aluminum. Silicon forms separate hard phase grains in the aluminum matrix, therefore providing better wear resistance.

There are several studies that are focused on the dry-sliding wear responses of Al-Si alloys. On the other side, very little research has been done on the lubrication of Al-Si alloys.

Fuller et al [16] performed experiments with a reciprocating wear tester with a sliding-cylinder-on-block geometry. The authors used a 1.2wt% ZDDP solution in base oil, aluminum 6061(A6061, Si content~0.7%)/A6061 and A390/A390 pin and block couples. They used X-ray absorption near edge structure (XANES) analysis; the author examined the wear scar for the presence of sulfur and phosphorus decomposition products of ZDDP. The authors found that only after 30 min of rubbing time, the ZDDP tribofilms form on the Al-alloy surfaces and they are nearly identical to those that form on steel. They pointed out that these films have a polyphosphate structure. And the authors also found that severe wear occurs on these alloys. Konishi et. al [17] used a pin-on-disk wear tester under fully formulated conditions , and used a A390/A390 couple,0.2wt% ZDDP in mineral and synthetic base oil. The author found that the wear rate was reduced when ZDDP was added to base oil comparing with base oil only. They used EPMA to analysis the wear scar and found that there are zinc, phosphorous and sulfur in the wear scar, and they assume that is due to the formation of a ZDDP-containing protective film. Wan et al [18] used sliding point contact using a steel ball on an aluminum 2024 plate (A2024, Si content~0.5%).The authors used a mixed alkyl-chain ZDDP and varied the concentration in the base oil up to 5%.The authors found that increasing the ZDDP concentration increased the wear, and the friction coefficient was not altered. The author clamed that ZDDP does not improve the wear conditions of aluminum because the film formed on aluminum is very fragile and it easily displaced. Kawamura and Fujita[19] did a cross-pin-type wear test about boundary, drip-supplied lubrication conditions on aluminum 390(A390, Si content~18%) and they used additives containing phosphates, phosphates and ZDDPs. Individual solutions contained 5% concentration of either primary, secondary or aryl ZDDPs in paraffinic base oil. The authors examined the wear scar using electron probe microanalysis

(EPMA) and found that there was no phosphorus or sulfur contained in the wear scar. And the author claimed that the lubrication effect is due to an adsorption effect or to the formation of a friction polymer, and not due to a chemical reaction between the A390 surface and ZDDP.

Their findings described above contain conflicting conclusions. Some of their results showed that adding ZDDP to base oil had little effect in preventing wear. The study of wear resistance of Al-Si alloys rubbing against themselves or against steel is becoming more important because Al-Si alloys are being used to replace some cast iron parts in combustion engines. Examination of possible ZDDP antiwear film formation on related Al-Si alloys under base oil or fully formulated lubrication conditions will provide us more insight about Al-Si alloys and help to know whether ZDDP can reduce wear by decomposing and forming a film in the same way in cast iron engines.

2.6 Tribological Testing

There are many ways to design and perform the tribological tests. Many factors affect the tribotests: characteristics of the materials couple, the type of lubricant, contact geometry, surface roughness, environment of the test, mechanical system variables (load, speed, etc).Tribology testing methods can be classified according to realism, i.e. how closely they reproduce the conditions of the real application and how representative they are of the machine component and the conditions they are designed to simulate. The wear characteristics of the cylinder-piston system in a car engine are investigated; a field test would include the car, driven under realistic service conditions in the service environment. A single piston and cylinder is the important machine components in wear test. In the for an automobile engine test, an example of a simplified component test can be a tribometer with a reciprocating piece of the actual piston ring sliding on a surface of a small portion of the cylinder sleeve cut from the actual cylinder of the engine [53].Another method to test is a model test. Such as pin on disk or ball on cylinder lubricity evaluators can be used. In our test, we used HFRR (high frequency reciprocating rig) to predict the behavior of engine oils in real engines to an acceptable extent.

CHAPTER 3

EXPERIMENTAL PROCEDURE

3.1 Testing Method for HFRB

In order to simulate boundary lubrication conditions and study the effects of the factors influencing the performance of the tribofilm and transfer film generated under such condition (e.g. Load, speed, chemistry and surface finish) a unique type of model wear tester used in this study is a high-frequency reciprocating rig (HFRB).Figure 3.1

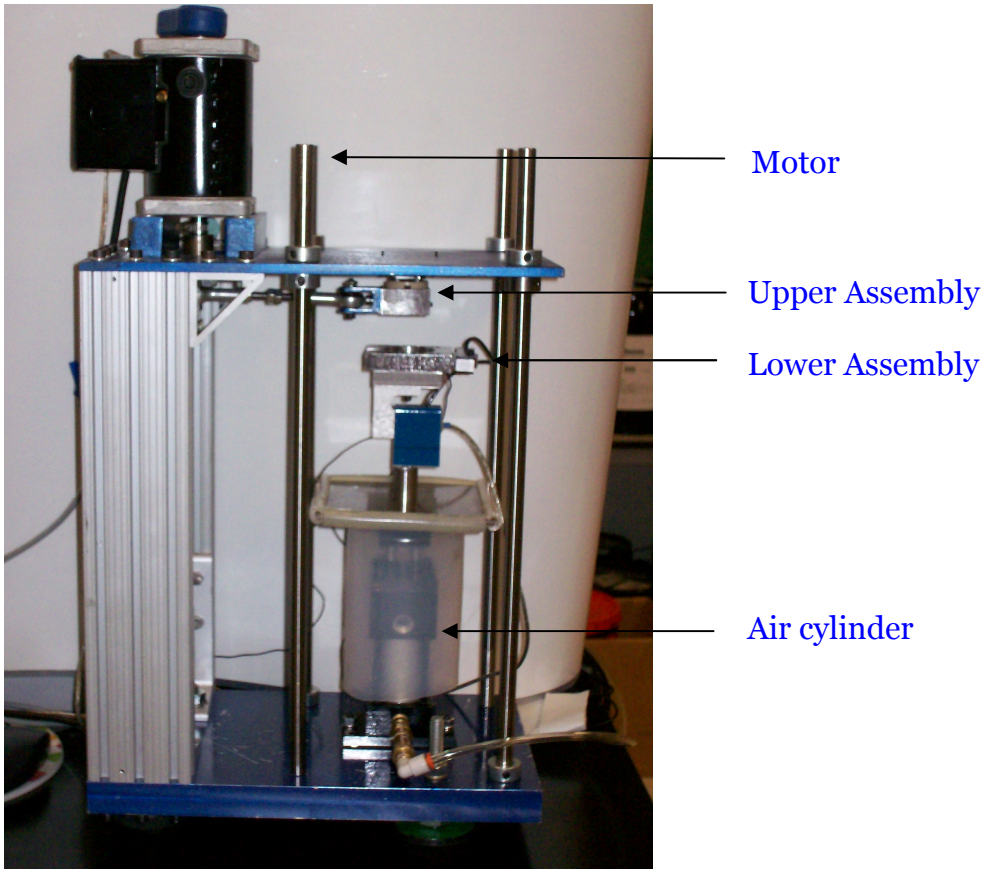

Figure 3.1 HFRB machine

The machine was divided into five major components:

1. Upper assembly

The upper assembly is a moving part and made from stainless steel, the upper assembly consists of three components. The first component is the rail guide and it guaranteed the linear motion required of the machine. The second component in the upper assembly is the counter sample holder mount. The mount bolts onto the rail guide and the drive system and it holds the counter sample holder. The third component in the upper assembly is the counter sample holder. The holder is designed to fit snugly inside the mount and held with a set screw. The counter sample is in direct contact with the heated oil in the oil bath and since it will tend to expand during testing, a small offset hole in the base of the holder provides access for easy removal of the counter sample. The neck of the counter sample was sized to allow a clearance of 1/8 inch between the upper assembly and the oil bath in the lower assembly. The counter sample holders' unique design makes it suitable for a variety of counter sample geometries such as ¼ inch diameter spheres and cylinders(both horizontal and vertical oriented).The samples are held in place with a set screw.

2. Lower assembly

The lower assembly is comprised of four components. The first part is oil bath. The oil bath houses the heater, the test sample and a thermocouple. The test sample is placed in a small recess in the center of the oil bath. Contained below are a thermocouple and an Ohmmeter lead for measuring electrical resistance. The oil bath, mounts to the lower fixture. The second component of the lower assembly is the lower fixture, which is bolted to the two rail guides. The lower fixture has an alcove on the top surface of the fixture, which contains two guide pins for mounting the oil bath. The pins ensure proper location of the oil bath and prevent rotation. Two small holes are drilled through the center of the recess and match with holes on the base of the oil bath. These holes allow wires to pass to the sensors mounted in the oil bath. The test sample sets in the upper recess of the oil bath and is initially held in place by the applied normal force and a low interference fit. Once the test begins and the sample and oil bath heated up,

thermal expansion of both pieces will further the interference. After the test is complete the sample can be removed by pushing it out using the holds for the sensors. Two low friction rail guides were used to mount the lower fixture on the center plate. The motivation for using two rail guides was to minimize bending and restrict any sideways motion. This will maintain the lower assembly motion in the same linear direction as the upper assembly, which allows accurate reading from the horizontal load cell.

3. Drive system

A 1/7 Hp 12-24V DC motor is used to drive the slider crank mechanism, which provides the linear motion, the stroke and the frequency required of the machine. At the end of the shaft of the motor is a removable head. This head serves as the crank of the mechanism and is designed with a 1mm eccentricity, giving an overall stroke of 2mm.The head is connected to a high speed rod end, which has ball bearing to minimize friction. The rod end screws onto a treaded rod with another rod end at the other end, where it attaches to the main assembly. The power requirements of the system are along with the power produced by the motor.

4. Support structure

The support structure consists of the top plate, bottom plate, vertical rods, rectangular aluminum tubing and base supports. The top plate supports the motor and the rail guide for the upper assembly. To prevent unnecessary vibrations, dampening machine supports are mounted the underside of the lower plate. These supports also act as levelers for the machine. The bottom plate holds the air cylinder as well supports the entire structure. The vertical rods are used to connect the top and bottom plates and, as mentioned above, the center plate slides on these rods. The rectangular aluminum tubing is used as an additional support that connects the top and bottom plates and also prevents any deflection in either plate. Aluminum was chosen to lessen the overall weight of the whole structure and was freely available.

5. Control components

One of the key features of the Test works design is its ability to accurately control and measure input forces, output forces, temperature, angular velocity, and electrical resistance.A5/6 inch

bore air cylinder is controlled by an electric regulator and attached to a 25 pond capacity load cell that measures the applied load and provides feedback to the air cylinder regulator. The air cylinder allows for dynamic adjustment of the applied load during testing, an important variable when trying to form tribofilms. The Test work drive system is controlled by an off the shelf controller, making the velocity dynamically controllable.

The control system of this machine includes three components. The first component is heating element. The test samples will be heated with a nichrome wire resistance heater. The nichrome wire has a high electrical resistance which reduces the size of the heating element. The coiled wire is encapsulated in an electrically insulative and chemically inert two parts epoxy that provides structural support and protection against oil and solvents used for cleanup. The power will be supplied from an AC step down transformer that has a maximum output of 13 VAC and 4.0 A. To achieve and maintain a specified testing temperature a closed loop PID control will be used. The power input to the heater will be controlled with an on/off relay on a process controller that uses readings from a thermocouple mounted to the sample as its feedback. To adjust the input power a potentiometer will be added in series to the 12.6 VAC input. The second component is motor control. A closed loop speed control system will be used to control the motor. The system has an economical SCR variable speed control that is not pulse modulated. SCR is a silicon-controlled rectifier (or semiconductor-controlled rectifier) is a 4-layer solid state device that controls current flow. The resistance to give the desired current and speed will be controlled with a digital closed loop microprocessor based control system (ASP20). This control features a true PID algorithm for extremely responsive and precise control over a wide variety of desired speed and applications and RS232 connectivity for programming it with the VEE software. The feedback to the control is given by a Hall-effect pick-up that is mounted on the motor shaft. The pulses given by the pick-up give the motor speed for the controller. The third component is loading system. An electrical pressure regular is used as the means to apply the vertical load. The pressure regulator is programmable to deliver a true ramped load. Start signals will come from the software and stop signals will come from

feedback from the load cell. When the loading reaches the programmed value, the alarm will signal the pressure regulator to stop. Since no data will be collected from the pressure regulator (force values are taken from the load cell), there is no need for RS232 connectivity.

3.1.1 Al-Si Alloy Chemistry

Disk: Al-Si alloy 4032 (Si=12.2 wt%, Cu=0.9wt%, Mg=1.05wt%, Ni = 0.9wt %)

Diameter: ½ inch

Thickness: 1/6 inch

Hardness: 84 HRB (Rockwell Hardness)

The discs were mechanically polished with 600 grit SiC paper and subsequently polished with 17.5 µm and 5 µm alumina in water on a Leco polishing wheel. The disks were then washed in hexane and stored in a dry container.

3.1.2 Ball Chemistry

Ball: Steel ball (52100 steel: C=1.1wt%, Cr=1.5wt%, Mn=0.35wt%, Si=0.35wt %)

Diameter: 1/4 inch

Hardness: 60-67 HRC (Rockwell Hardness)

The ball was washed in hexane and stored in a dry container before testing.

3.1.3 Lubricant Chemistry (Antiwear Additives)

Zinc dialkyl-dithiophosphate (ZDDP: 0.1wt% Phosphorous)

- Base oil
- Fully formulated oil

Dialkyl dithiophosphate (DDP: 0.1wt% Phosphorous)

- Base oil
- Fully formulated oil

Amine phosphate (0.1wt% Phosphorous)

- Base oil

- Fully formulated oil

  Thiadiazole (0.2wt %Sulfur)
- Base oil
- Fully formulated oil

  Antimony 0, 0-dialkylphosphorodithioate (SbDDP: 0.1wt% Phosphorous)
- Base oil
- Fully formulated oil

3.1.4 Test Condition

Load: 0.5 Kg

Around 18 ml solution

100℃

50 Hz

Time: 60 minutes

Travel distance per stroke: around 2 mm

Each test was repeated 3 or 4 times.

3.1.5 Sample Preparation and Testing Protocols

Antiwear films samples are generated by wear tests using the HFRB machine, both the disks and balls used in the tests were ultrasonicated and cleaned by hexane and the surface of the disk was brushed in order to remove any pre-existing wear debris and machine oil. An 18 ml specimen of fuel is placed in the test reservoir of an HFRB. The preferred test temperature is 100 ℃. When the fuel temperature has stabilized, a vibrator arm holding a nonrotating steel ball and loaded with 500 g mass is lowered until it contacts a test disk completely submerged in the fuel. The ball is caused to rub against the disk with a 2 mm stroke at a frequency of 50Hz for 60 min. The ball is removed from the vibrator arm and cleaned with hexane. The disks are used for

both wear volume measurements and different surface characterization techniques used for determining the properties of the antiwear films generated during different tests.

3.2 Measurement of Wear Scar

The wear volume is examined using the Wyko NT9100 Surface Profiler. Wyko surface profiler systems are non-contact optical profilers that use two technologies to measure a wide range of surface heights. Phase-shifting interferometry (PSI) mode allows you to measure smooth surfaces and small steps, while vertical scanning interferometry (VSI) mode allows you to measure rough surfaces and steps up to several millimeters high. In this study, we used VSI mode. The basic interferometric principles: light reflected from a reference mirror combines with light reflected from a sample to produce interference fringes, where the best-contrast fringe occurs at best focus. In VSI mode, the white-light source is filtered with a neutral density filter, which preserves the short coherence length of the white light, and the system measures the degree of fringe modulation, or coherence, instead of the phase of the interference fringes.

In VSI, the irradiance signal is sampled at fixed intervals as the optical path difference (OPD) is varied by a continuous translation of the vertical axis through focus. Low-frequency components are first removed from the signal; the signal is rectified by square-law detection, and then filtered. Finally, the peak of the low-pass filter output is located and the vertical position that corresponds to the peak is recorded. To increase the resolution of the measurement beyond the sampling interval, a curve-fitting interpolation technique is used.

The interferometric objective moves vertically to san the surface at varying heights. A motor with feedback from an LVDT (linear variable differential transformer) precisely controls the motion. Because white light has a short coherence length, interference fringes are present only over a very shallow depth for each focus position. Fringe contrast at a single sample point reaches a peak as the sample is translated through focus.

The system scans through focus (starting above focus) as the camera captures frames of interference data at evenly-spaced intervals. As the system scans downward, an interference signal for each point on the surface is recorded. The system uses a series of advanced

computer algorithms to demodulate the envelope of the fringe signal. Finally the vertical position corresponding to the peak of the interference signal is extracted for each point on the surface. The range refers to the greatest vertical distance the profiler can accurately measure. The limits of dynamic range for VSI mode is 2mm.

We assumed that the wear scar is like half of the cylinder. (Figure 3.2). We chose six different locations (Figure 3.3) of the wear scar, plotted the data using excel, calculated the area of wear scar using Kaleida Graph and made the average, and then multiply the wear length (Figure 3.5), we got the wear volume (mm^3).

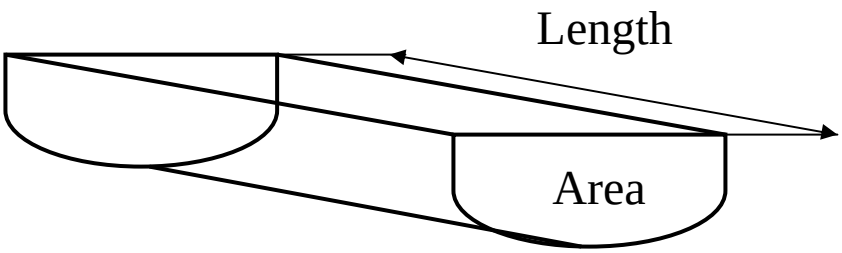

Figure 3.2 The volume of wear scar

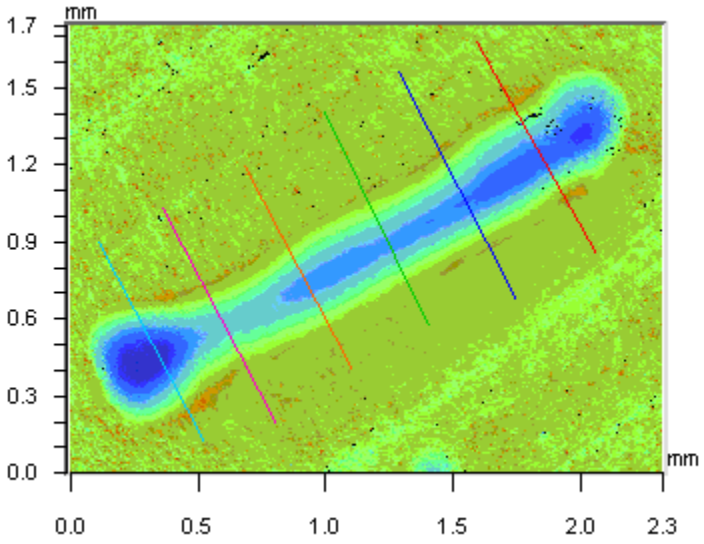

Figure 3.3 Different locations of wear scar

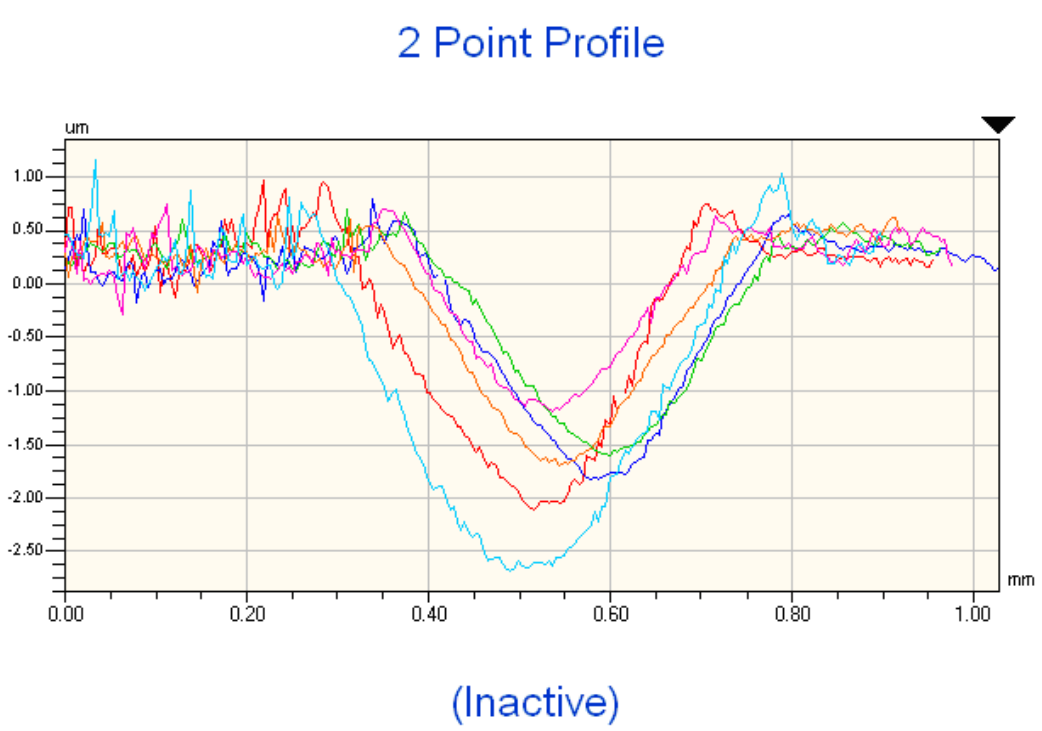

Figure 3.4 2 point profile of wear scar

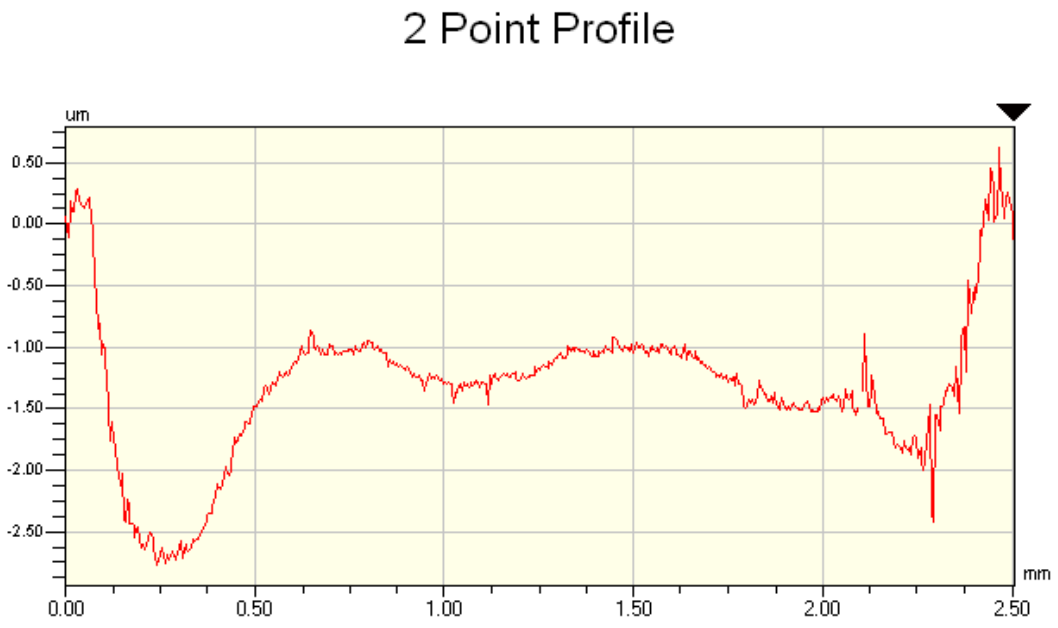

Figure 3.5 The length of the wear scar

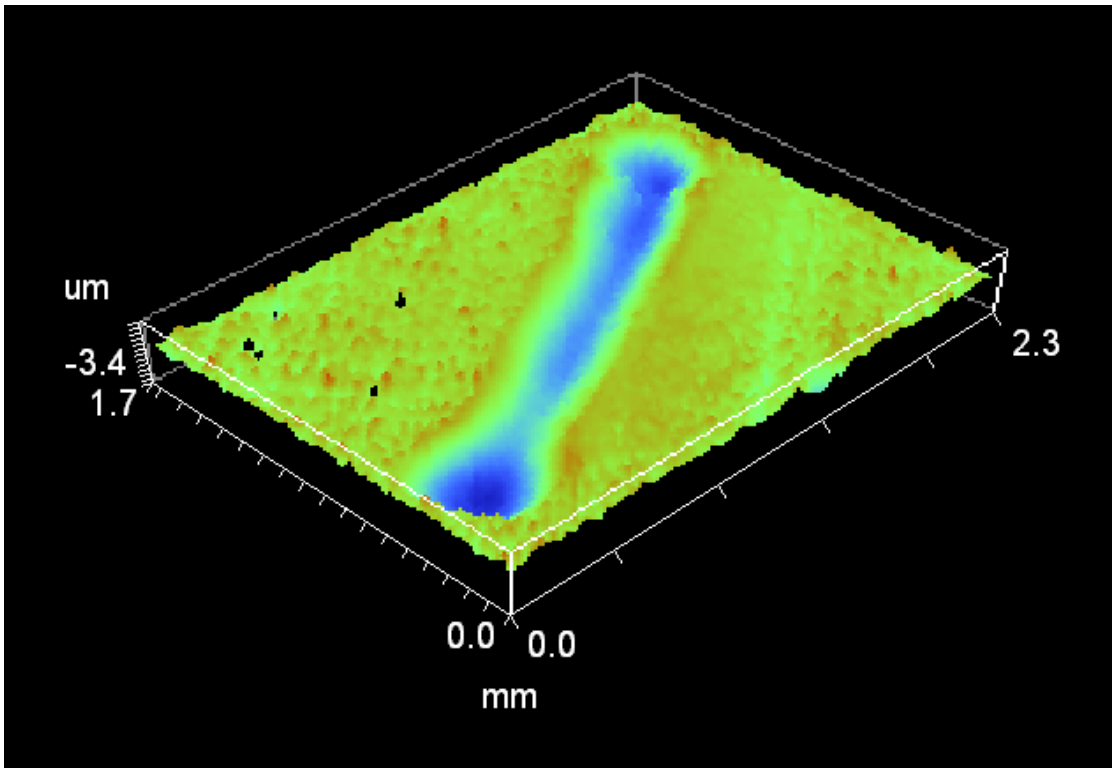

Figure 3.6 3D image of the wear scar

3.3 Surface Analysis: SEM/EDS

In order to examine the chemical composition and surface of the film generated from wear tests, JEOL JSM 845 scanning electron microscope (SEM) coupled with energy dispersive X-ray spectroscopy (EDS) was used. The acceleration voltage was set at 20KV and the working distance normally at 30cm. For every sample, once an area of uniform film formation is located on the surface of the wear track, an EDS spectrum was obtained from that area of the film surface in order to identify some of the elements present in the film.

3.4 Film Analysis: XANES

X-ray adsorption near edge structure (XANES) spectroscopy is an absorption spectroscopy technique that is capable of probing the local structure and bonding environment around selected atoms and can determine their formal valence; coordination environment and subtle geometrical distortions of them. Due to the development of synchrotron radiation as an X-

ray source, XANES spectroscopy has become a common analytical tool in the study of surface films. Synchrotron radiation is light emission produced by accelerated relativistic electrons moving in a circular orbit. Synchrotron sources provide flux many orders of magnitude greater than conventional X-ray sources [54]. It has a broad spectral range, easily tuneable using monochromators and highly stable over long energy ranges. Because the antiwear films are mainly amorphous in nature, and XANES does not require crystalline samples and thus has been used as a powerful analytical technique in the study of antiwear films.

The absorption spectrum displays an absorption edge associated with the excitation of a core shell electron(normally K-edge or L-edge).By exciting the multiple scattering resonances of the photoelectron at the atomic absorption site(absorbing atom) and scattering by neighbor atoms ,a spectrum taken of a condensed material exhibits an oscillatory structure. The peaks close to the absorption edge can be attributed to transitions to localized electronic states, with the edge position itself being related to the oxidation state of the absorbing atoms. The strong oscillation beyond the absorption edge is because of the multiple scattering of photoelectrons by the atoms in a local cluster around the absorbing atom.

3.4.1 XANES Experimental

XANES spectroscopy has two different modes:

Total electron yield (TEY): examine the surface layers (≈ 5 nm for L-edge and ≈ 50 nm for K-edge)

Fluorescent yield (FLY): examine the bulk beyond the outer surface layers (≈ 50 nm for L-edge and ≈ 300nm for K-edge)

Use these two modes to analysis the chain length and chemical composition and structure environment variation through the depth of the films.

The XANES experiments were run two different beam lines:

Variable line spacing plane grating monochromator (VLS-PGM) 11ID-2, Spherical Grating Monochromator (SGM) beamline at the Canadian Light Source (CLS) facility, Saskatoon, Saskatchewan, Canada. The specification of each beamline are shown in Table 3.1[54].

Table 3.1: Specification of the beamlines used in this study

Beamline	SGM	VLS-PGM
Energy Range	200-1900eV	5.5-250eV
Slit Size	50μm	50μm
Resolution used	0.1eV for Fe and O	0.1eV for P ,Al and S

CHAPTER 4

RESULTS AND DISCUSSION

4.1 Microstructure of Al-Si Alloy

The Al-Si alloy chosen is Al-Si alloy 4032 with 12.2wt% Si, 0.9wt%Cu, 1.05wt%Mg, 0.9wt %Ni. Examination of the binary Al-Si phase diagram indicates limited solubility of Si in the Al-matrix; in addition there is very limited solubility of Ni in the Al-matrix. In addition the solubility of Mg in Al is also limited to below 1% in Al as is Cu. On the other hand the high amount of Si present in the alloy can result in the formation of Mg_2Si precipitate as well as a Al_3Ni with some Si in it .The matrix of this alloy is primarily pure Al with minor a mount of Cu and Mg dissolved in solid solution with the precipitates being made up of pure Si and Mg_2Si, Al_3Ni.

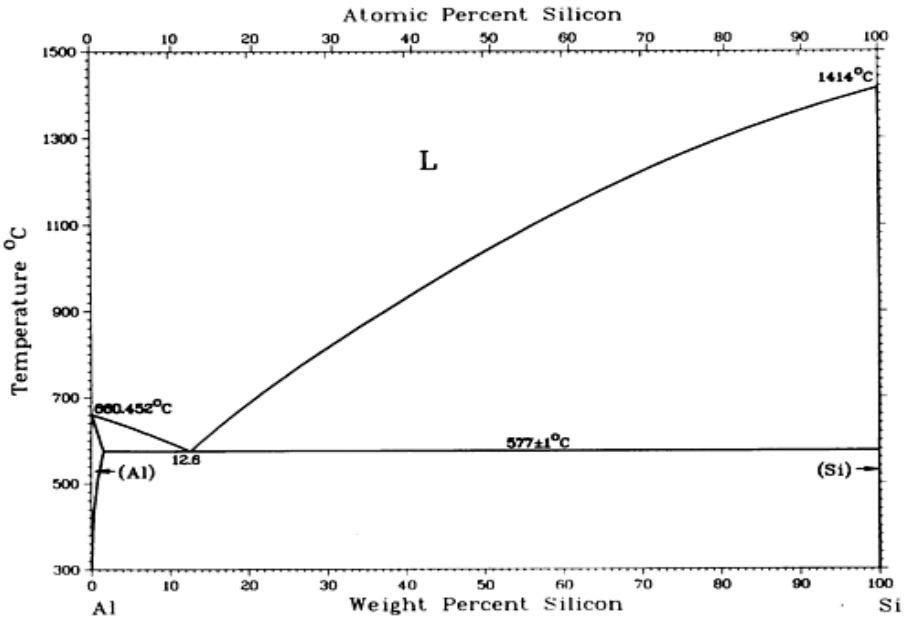

Figure 4.1 Al-Si Phase diagraph

4.2 Wear Behavior

4.2.1 Zinc Dialkyl-dithiophosphate Compared with Antimony 0, 0-dialkylphosphorodithioate

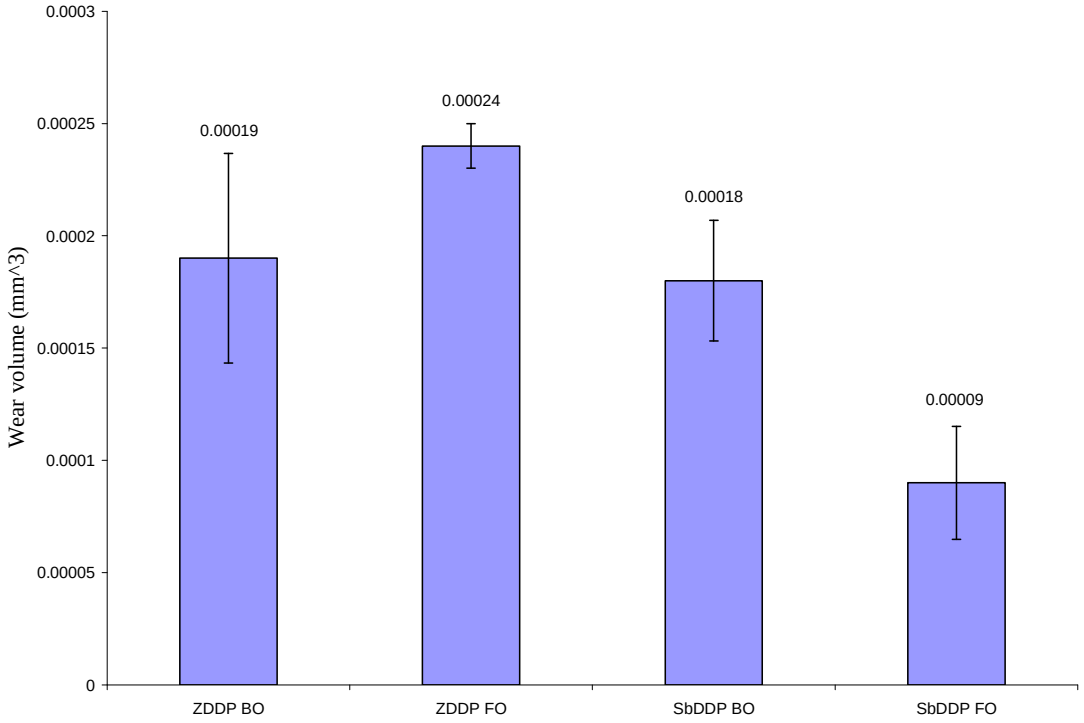

Figure 4.2 wear volume data for tests on four different formulations, containing ZDDP, SbDDP in base oil/fully formulated oil.

ZDDP contains Zn; SbDDP contains Sb. The figure shows that SbDDP is better than ZDDP in antiwear performance. ZDDP in fully formulated oil exhibits antagonistic effect while SbDDP in fully formulated oil exhibits good synergistic antiwear effect.

4.2.2 Zinc Dialkyl-dithiophosphate Compared with Ashless Dialkyl Dithiophosphate

ZDDP is an antiwear additive that contains metal Zn that contributes to the ash content of the oil, DDP is an ashless additive as it does not contain metal cation, from the figure 4.3, and we can see that DDP is better than ZDDP in antiwear performance. In comparison to steel, where we have shown better and thicker tribofilm and improved wear performance because the Fe from substrate helps in the cross-linking of polyphosphate film [55]. DDP in fully formulated oil exhibits synergistic antiwear effect.

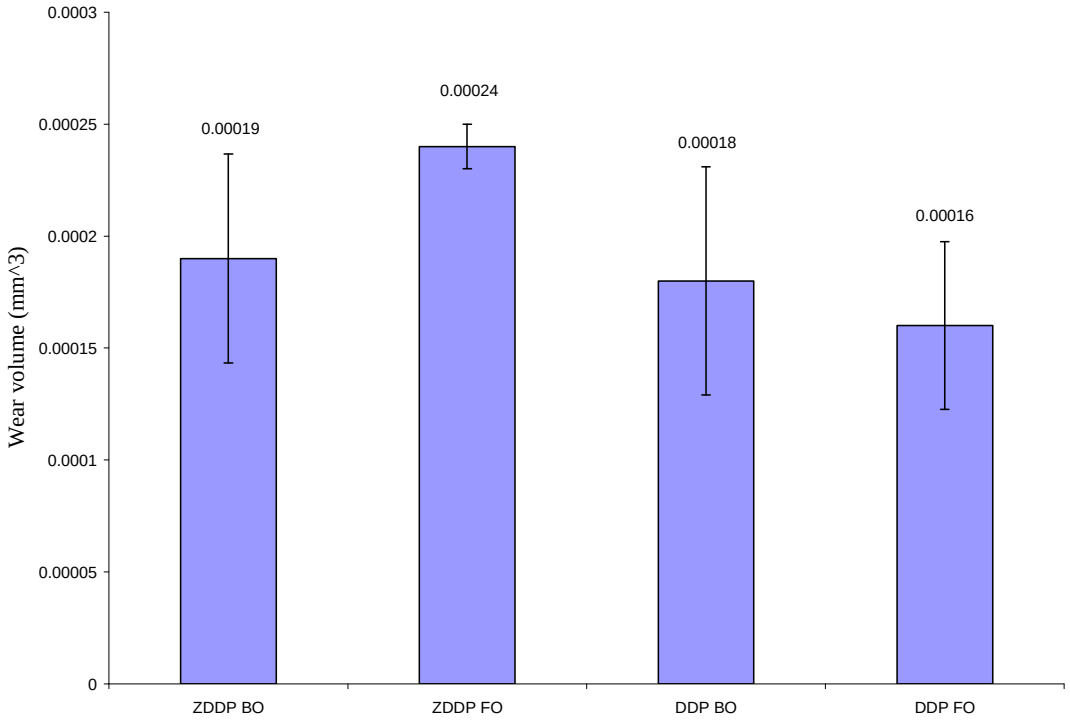

Figure 4.3 wear volume data for tests on four different formulations, containing ZDDP, DDP in base oil/fully formulated oil.

4.2.3 Ashless Dialkyl Dithiophosphate Compared with Ashless Amine Phosphates:

Figure 4.4 shows that DDP is much better than Amine phosphates in antiwear performance, when DDP is used in lubricating steel surface the Fe from the underlying substrate has shown to be a critical component in help to the formation of polyphosphate film. The presence of S helps in the formation of FeS that also protects the surface [55].On the other hand, it has been shown that the absence of S in the amine phosphates results in poor wear performance in steel. This trend appears to follow in the case of Al alloys as well.

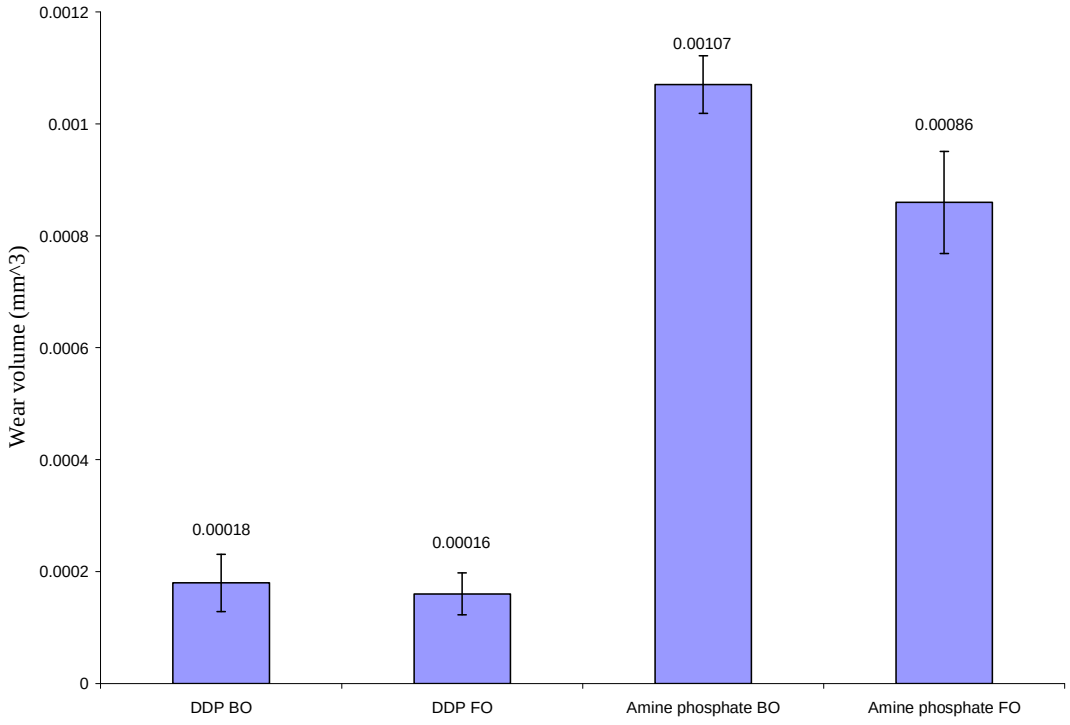

Figure 4.4 wear volume data for tests on four different formulations, containing Amine phosphate, DDP in base oil/fully formulated oil.

4.2.4 Thiadiazole Compared with Amine Phosphates:

Thiadiazole is a sulfur ashless antiwear additive, Amine phosphates is a phosphorus ashless antiwear additive. In base oil condition, Amine phosphate is better than Thiadiazole in antiwear performance. Compared with steel where presence of phosphorus results in formation of Fe-phosphate protective film with Amine phosphate but this is absent when Thiadiazole is used. Thiadiazole in fully formulated oil exhibits good synergistic antiwear effect with other constituents in fully formulated oil.

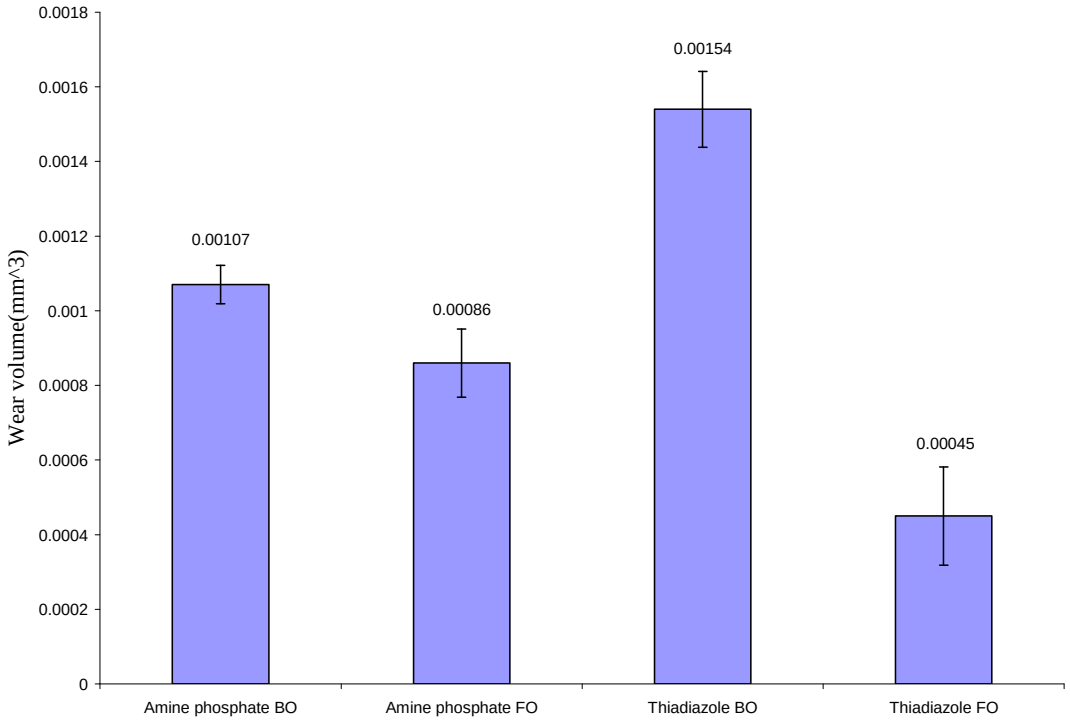

Figure 4.5 wear volume data for tests on four different formulations, containing Amine phosphate, Thiadiazole in base oil/fully formulated oil.

4.3 XANES Spectroscopy

XANES spectroscopy was performed for energy ranges covering sulfur, phosphorus ,iron, aluminum, and oxygen K-absorption edges (SGM beamline) and L-absorption edges (VLS-PGM beamline).In both cases XANES spectra were recorded in fluorescence yield (FLY) and total electron yield (TEY) modes. To compare the acquired XANES spectra from antiwear film samples to those of model compounds to understand the chemical nature of the antiwear film by identifying the structural environment of these atoms in the antiwear film.

4.3.1 Zinc Dialkyl-dithiophosphate Compared with Antimony 0, 0-dialkylphosphorodithioate: Effect of Cation

Al L-edge

Figure 4.6 and 4.7 show Al L-edge spectra record in TEY (surface sensitive) and FLY (bulk sensitive) modes respectively. In figures, the XANES spectra in TEY and FLY modes are shown for samples containing Zinc dialkyl-dithiophosphate in base oil/fully formulated oil and

Antimony 0, 0-dialkylphosphorodithiatae in base oil alongside the same spectra for the model compounds: Al- foil,$AlPO_4$,Al_2O_3,$Al_2(SO_4)_3$.

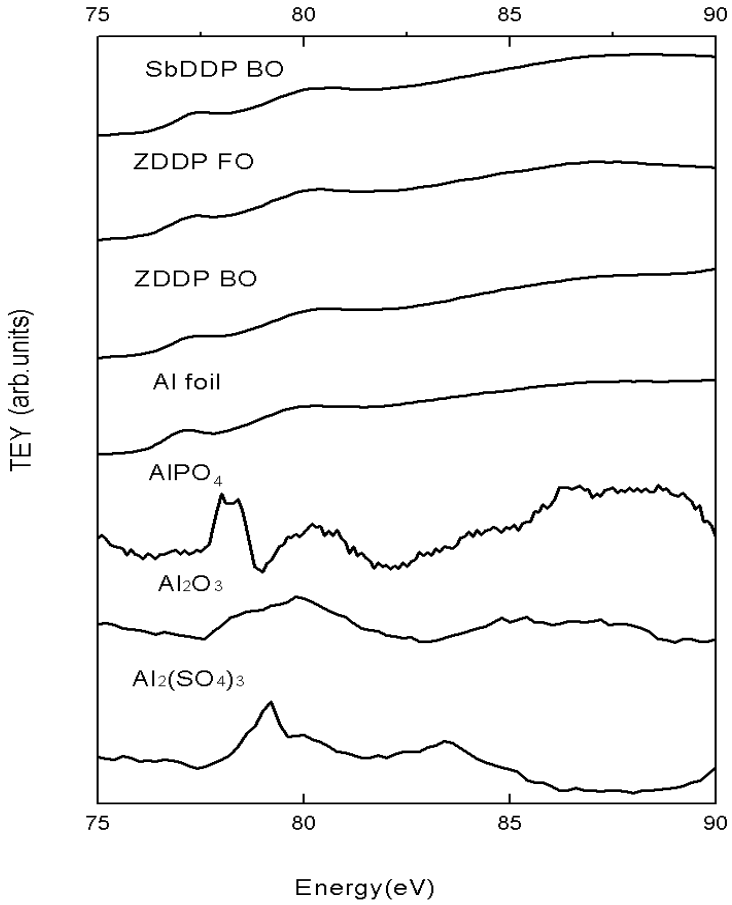

Figure 4.6 Al L-edge XANES spectra collected in TEY mode for transfer film generated by samples containing Zinc dialkyl-dithiophosphate in base oil/fully formulated oil and Antimony 0, 0-dialkylphosphorodithiatae in base oil under 0.5 kg loads and the same spectra record for model compounds, Al- foil,$AlPO_4$,Al_2O_3,$Al_2(SO_4)_3$.

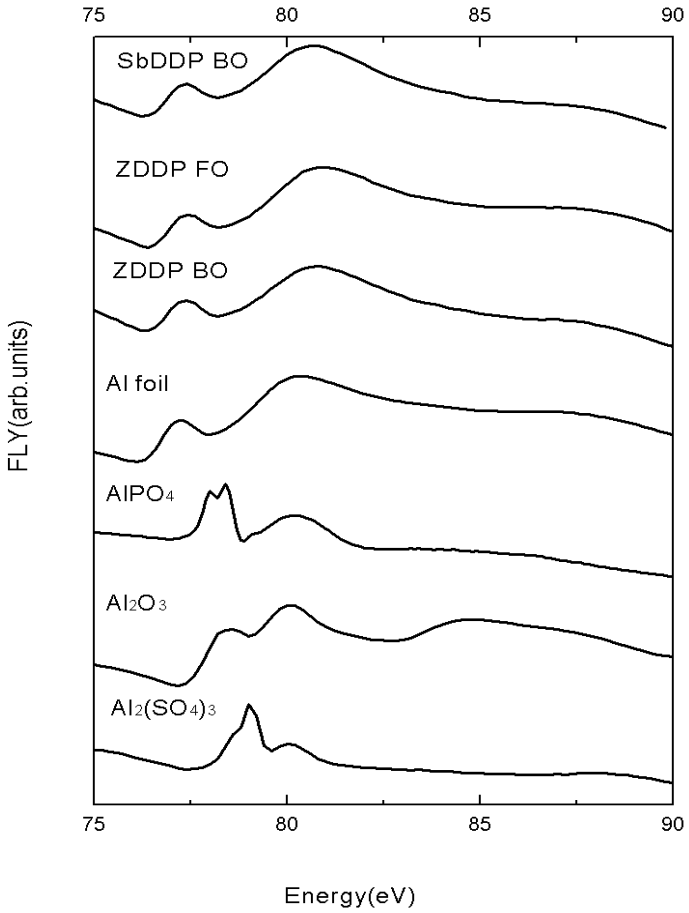

Figure 4.7 Al L-edge XANES spectra collected in FLY mode for transfer film generated by samples containing Zinc dialkyl-dithiophosphate in base oil/fully formulated oil and Antimony 0, 0-dialkylphosphorodithiatae in base oil under 0.5 kg loads and the same spectra record for model compounds, Al- foil,$AlPO_4$,Al_2O_3,$Al_2(SO_4)_3$.

It is clearly evident from both TEY and FLY of the Al L-edge that the spectra resembles that which was acquired from a plain Al foil indicating that Al does not participate in the formation of either a tribofilm or a transfer film on the surface. The similarity between the Al L-edge Spectra for the Al foil which contains thin native oxide and the wear surface suggests that in the bulk of the wear surface where Al in present alone it exists in the form of native oxide. There is no evidence to suggest the formation of Al-phosphate, sulfide and sulfate. Martin H. Müser et.al [56] in their study of ZDDP and its ability to form protective polyphosphate films

suggest that there is a critical pressure and temperature requires for the decomposition and formation of long chain polyphosphates. In the case of Al matrix the lower modulus and yield strength results in excessive plastic deformation and the Hertzian contact pressure are not sufficient for the formation of polyphosphate tribofilms on Al.

Fe L-edge

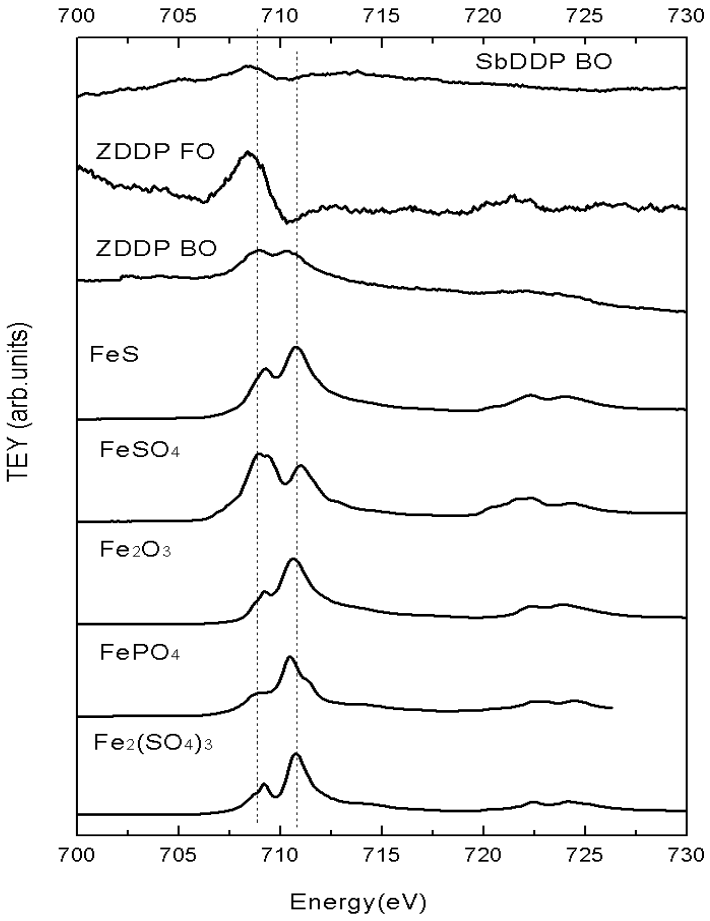

Figure 4.8 Fe L-edge XANES spectra collected in TEY mode for transfer film generated by samples containing Zinc dialkyl-dithiophosphate in base oil/fully formulated oil and Antimony 0, 0-dialkylphosphorodithiatae in base oil under 0.5 kg loads and the same spectra record for model compounds, FeS,$FeSO_4$,Fe_2O_3,$FePO_4$,$Fe_2(SO_4)_3$.

Figure 4.8 and 4.9 show Fe L-edge spectra record in TEY (surface sensitive) and FLY (bulk sensitive) modes respectively. In figures ,the XANES spectra in TEY and FLY modes are shown for samples containing Zinc dialkyl-dithiophosphate in base oil/fully formulated oil and

Antimony 0, 0-dialkylphosphorodithiatae in base oil alongside the same spectra for the model compounds:FeS,$FeSO_4$,Fe_2O_3,$FePO_4$,$Fe_2(SO_4)_3$.

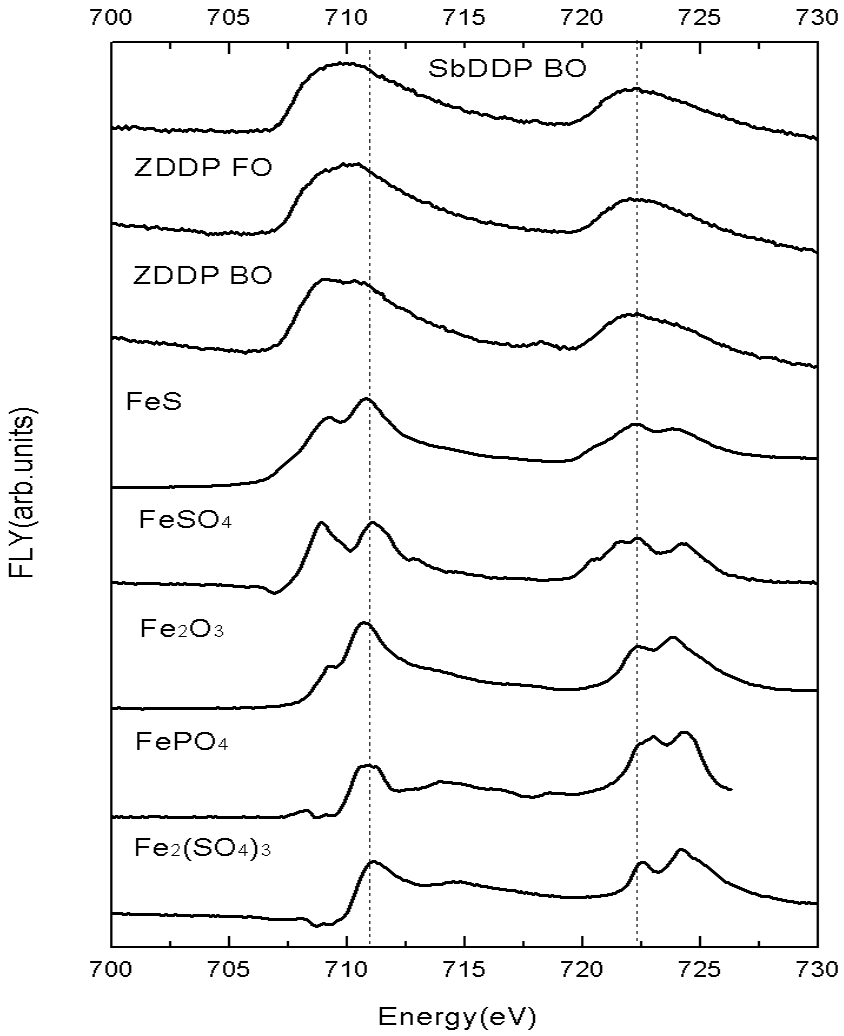

Figure 4.9 Fe L-edge XANES spectra collected in FLY mode for transfer film generated by samples containing Zinc dialkyl-dithiophosphate in base oil/fully formulated oil and Antimony 0, 0-dialkylphosphorodithiatae in base oil under 0.5 kg loads and the same spectra record for model compounds, FeS,$FeSO_4$,Fe_2O_3,$FePO_4$,$Fe_2(SO_4)_3$.

The TEY spectra for the wear surfaces indicate that in the case of ZDDP in base oil, the near surface region contains $FeSO_4$ while the fully formulated oil appears to contain a mixture of sulfates and sulfides. The peaks for Fe when SbDDP is used are weaker in TEY indicating limited presence of Fe near the surfaces. On the other hand in FLY mode there is a distinctive

peak associated with Fe in all cases indicating that there is well developed transfer film on the surface that contains Fe. However, the peak is diffuse suggesting that the transfer film may indeed contain a mixture of phosphates, sulfides and sulfates of Fe in the transfer film.

S L-edge

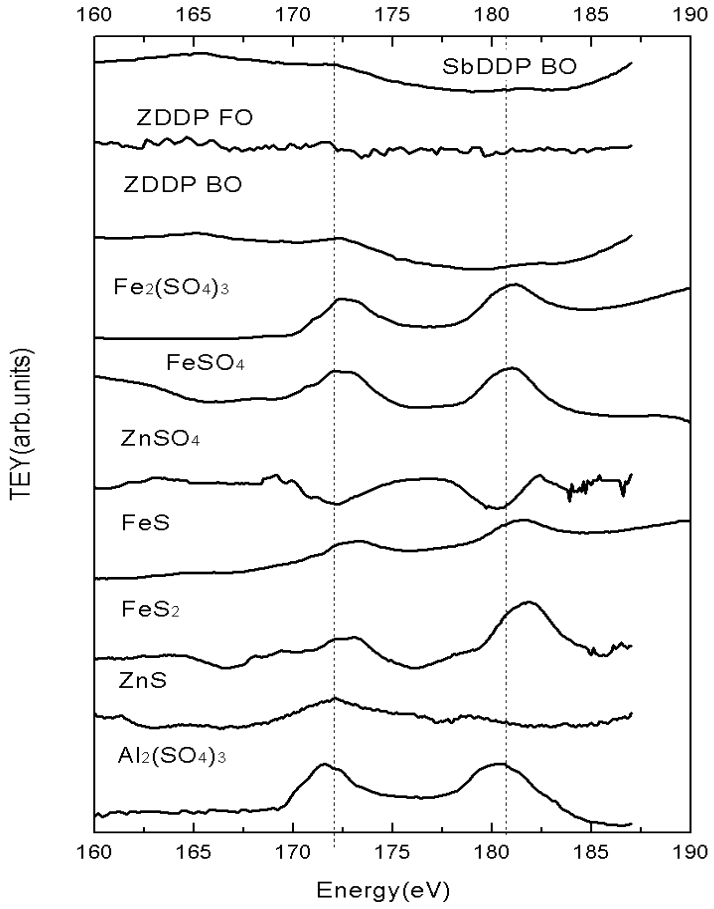

Figure 4.10 S L-edge XANES spectra collected in TEY mode for transfer film generated by samples containing Zinc dialkyl-dithiophosphate in base oil/fully formulated oil and Antimony 0, 0-dialkylphosphorodithiatae in base oil under 0.5 kg loads and the same spectra record for model compounds, $FeSO_4$,FeS,FeS_2,$Fe_2(SO_4)_3$,$ZnSO_4$,ZnS,$Al_2(SO_4)_3$.

Figure 4.10 and 4.11 show S L-edge spectra record in TEY (surface sensitive) and FLY (bulk sensitive) modes respectively. In figures, the XANES spectra in TEY and FLY modes are shown for samples containing Zinc dialkyl-dithiophosphate in base oil/fully formulated oil and

Antimony 0,0-dialkylphosphorodithiatae in base oil alongside the same spectra for the model compounds: $FeSO_4$,FeS,FeS_2,$Fe_2(SO_4)_3$,$ZnSO_4$,ZnS,$Al_2(SO_4)_3$.

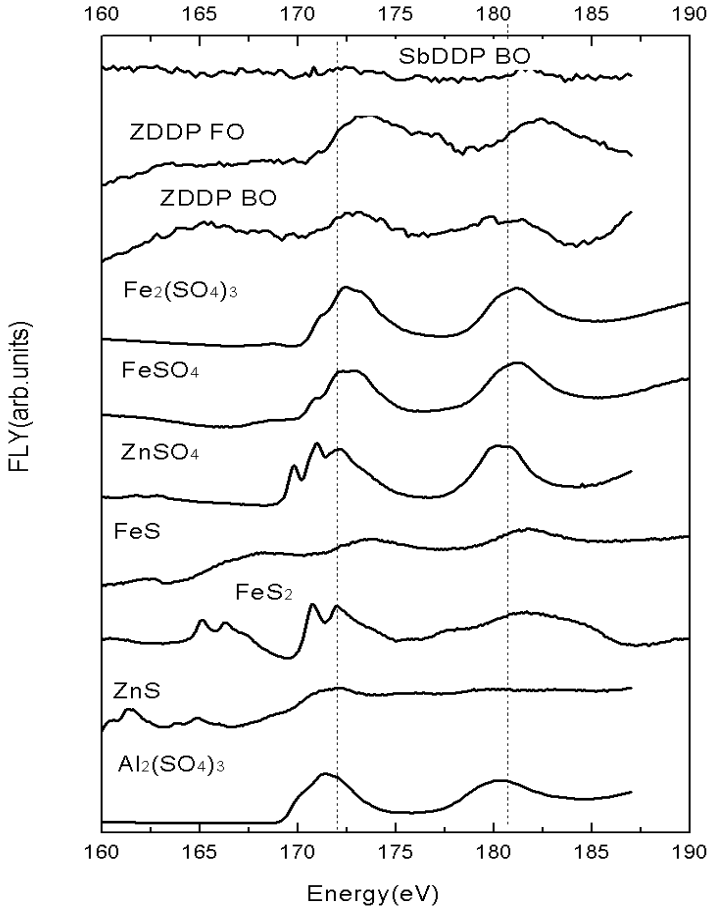

Figure 4.11 S L-edge XANES spectra collected in FLY mode for transfer film generated by samples containing Zinc dialkyl-dithiophosphate in base oil/fully formulated oil and Antimony 0, 0-dialkylphosphorodithiatae in base oil under 0.5 kg loads and the same spectra record for model compounds, $FeSO_4$,FeS,FeS_2,$Fe_2(SO_4)_3$,$ZnSO_4$,ZnS,$Al_2(SO_4)_3$.

Both TEY and FLY of the S-Ledge indicate that very weak presence of S in transfer film. This weak presence of S may be attributed to the fact that the energy flux in the VLS-PGM beamline at the S L-edge is relatively low and the signal strength from the S L-edge is relatively weak.

In the FLY mode, in the transfer film formed when ZDDP is used, the dominant peak position matches with the peak position for $ZnSO_4$, with a little $FeSO_4$. The presence of sulfates as opposed to sulfides indicated poorer protection of the surfaces. In the case of SbDDP, very

little evidence of the presence of sulfide, sulfate is apparent. The spectra collected in TEY mode did not yield conclusive data.

P L-edge

Figure 4.12 and 4.13 show P L-edge spectra record in TEY (surface sensitive) and FLY (bulk sensitive) modes respectively. In figures , the XANES spectra in TEY and FLY modes are shown for samples containing Zinc dialkyl-dithiophosphate in base oil/fully formulated oil and Antimony 0, 0-dialkylphosphorodithiatae in base oil alongside the same spectra for the model compounds:$Zn_3(PO_4)_2$,$Fe_4(P_2O_7)_3$,$FePO_4$,$AlPO_4$.

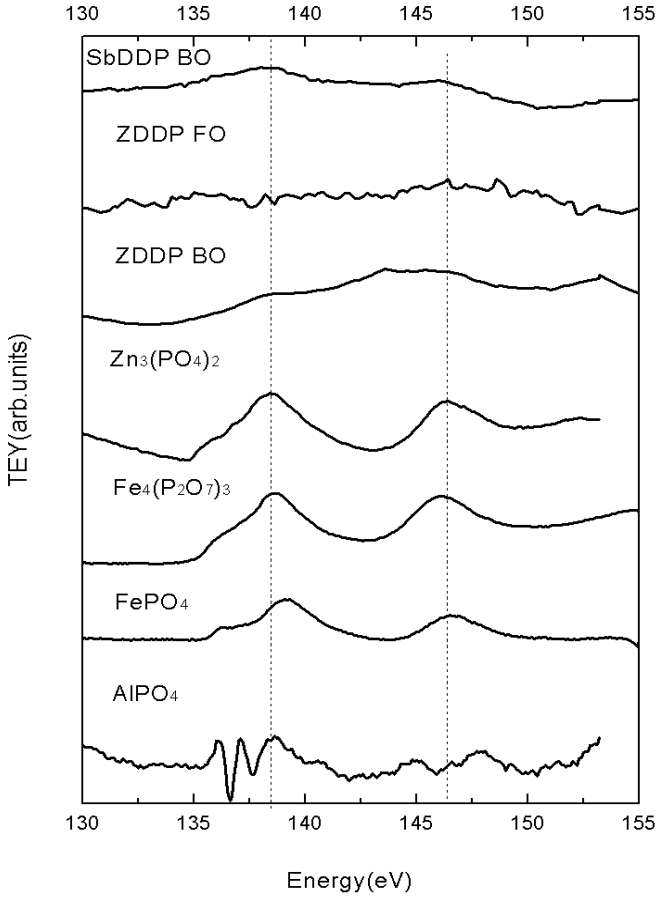

Figure 4.12 P L-edge XANES spectra collected in TEY mode for transfer film generated by samples containing Zinc dialkyl-dithiophosphate in base oil/fully formulated oil and Antimony 0, 0-dialkylphosphorodithiatae in base oil under 0.5 kg loads and the same spectra record for model compounds, $Zn_3(PO_4)_2$,$Fe_4(P_2O_7)_3$,$FePO_4$,$AlPO_4$.

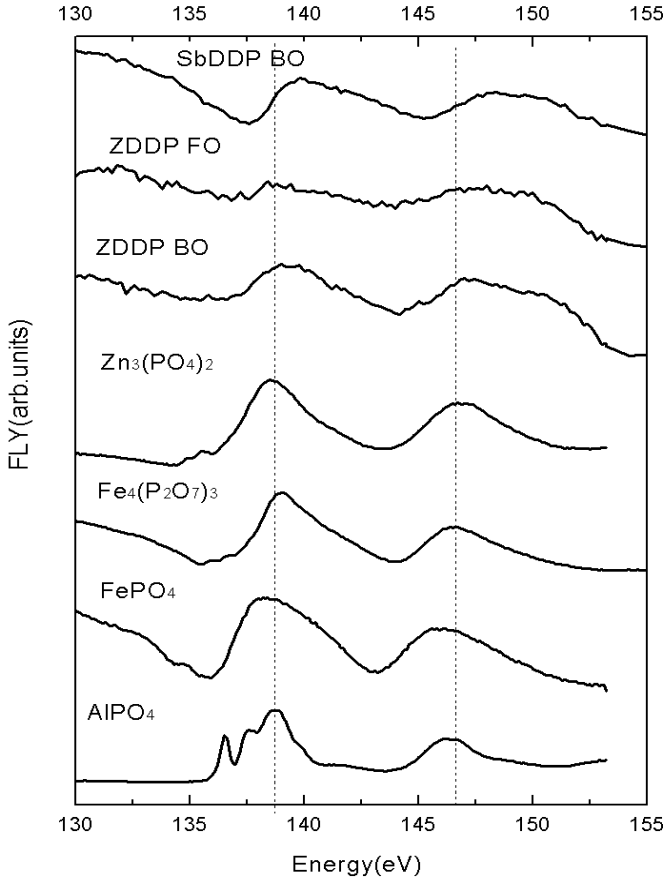

Figure 4.13 P L-edge XANES spectra collected in FLY mode for transfer film generated by samples containing Zinc dialkyl-dithiophosphate in base oil/fully formulated oil and Antimony 0, 0-dialkylphosphorodithiatae in base oil under 0.5 kg loads and the same spectra record for model compounds, $Zn_3(PO_4)_2$,$Fe_4(P_2O_7)_3$,$FePO_4$,$AlPO_4$.

The TEY spectra with ZDDP and SbDDP in base oil indicate the weak presence of P in the transfer film near the surface; however, the peak intensities are very weak indicating that not much P is present near the surface. On the other hand the FLY spectra of the transfer film indicate a stonger presence of P in the transfer film with the base oil compositions exhibiting strong evidence for the presence of Zn-phosphates when ZDDP was used and Sb-phosphates when SbDDP is used. However, due to the close proximity of the Fe-phosphate peaks and the diffuse nature of the P L-edge spectra from the tribofilm we cannot discount the presence of Fe-phosphates in the tribofilms and transfer films. This evidence supports the Fe-Ledge spectra which indicated the strong presence of Fe in FLY mode.

O K-edge

Figure 4.14 and 4.15 show O K-edge spectra record in TEY (surface sensitive) and FLY (bulk sensitive) modes respectively. In figures , the XANES spectra in TEY and FLY modes are shown for samples containing Zinc dialkyl-dithiophosphate in base oil/fully formulated oil and Antimony 0, 0-dialkylphosphorodithiatae in base oil alongside the same spectra for the model compounds: $Zn_3(PO_4)_2$, $FeSO_4$,Fe_2O_3, $FePO_4$,$Fe_2(SO_4)_3$,$AlPO_4$,Al_2O_3,$Al_2(SO_4)_3$.

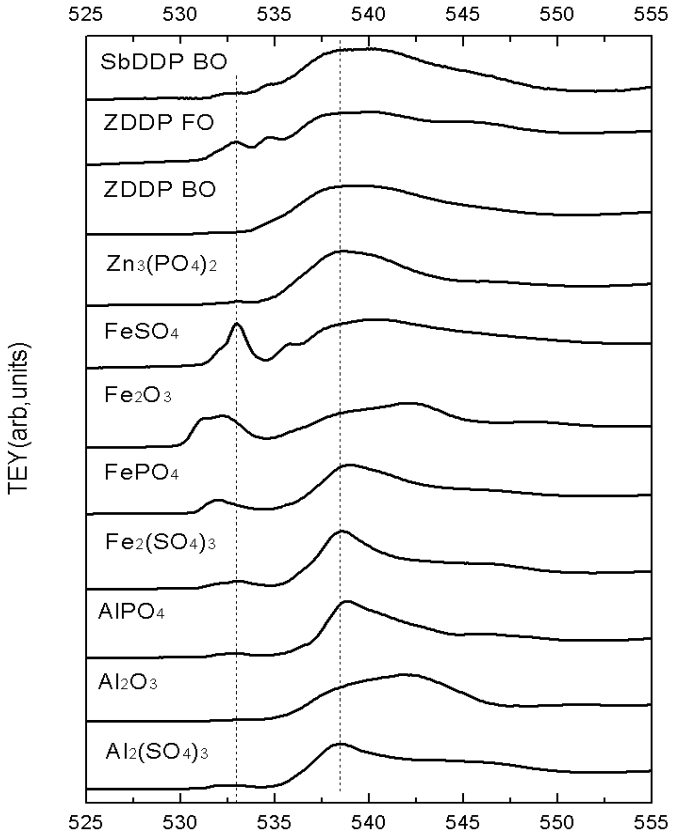

Figure 4.14 O K-edge XANES spectra collected in TEY mode for transfer film generated by samples containing Zinc dialkyl-dithiophosphate in base oil/fully formulated oil and Antimony 0, 0-dialkylphosphorodithiatae in base oil under 0.5 kg loads and the same spectra record for model compounds, $Zn_3(PO_4)_2$, $FeSO_4$, Fe_2O_3, $FePO_4$, $Fe_2(SO_4)_3$, $AlPO_4$, Al_2O_3, $Al_2(SO_4)_3$.

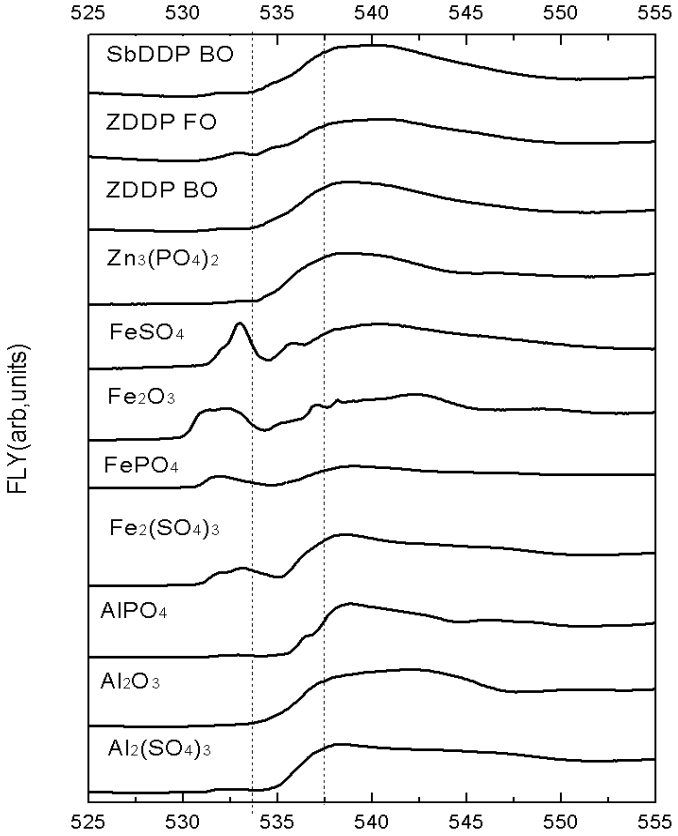

Figure 4.15 O K-edge XANES spectra collected in FLY mode for transfer film generated by samples containing Zinc dialkyl-dithiophosphate in base oil/fully formulated oil and Antimony 0, 0-dialkylphosphorodithiatae in base oil under 0.5 kg loads and the same spectra record for model compounds, $Zn_3(PO_4)_2$, $FeSO_4$, Fe_2O_3, $FePO_4$, $Fe_2(SO_4)_3$, $AlPO_4$, Al_2O_3, $Al_2(SO_4)_3$.

Both TEY and FLY spectra show that the transfer film from ZDDP in base oil/fully formulated oil ,the major peak match the Al_2O_3,and it contains minor $Zn_3(PO_4)_2$, $FeSO_4$.The transfer film from SbDDP in base oil ,the major peak matches the Al_2O_3,and it contains a little $FeSO_4$.

4.3.2 Zinc Dialkyl-dithiophosphate Compared with Ashless Dialkyl Dithiophosphate:

These Two Antiwear Chemistries Were Compared to Examine the Role Played by the Metal Cation Zn on Formation of Protective Tribofilms and Transfer Film.

Al L-edge

Figure 4.16 and 4.17 show Al L-edge spectra record in TEY (surface sensitive) and FLY (bulk sensitive) modes respectively. In figures , the XANES spectra in TEY and FLY modes are shown for samples containing Zinc dialkyl-dithiophosphate in base oil/fully formulated oil and Dialkyl dithiophosphate in base oil /fully formulated oil alongside the same spectra for the model compounds: Al foil,$AlPO_4$,Al_2O_3,$Al_2(SO_4)_3$.

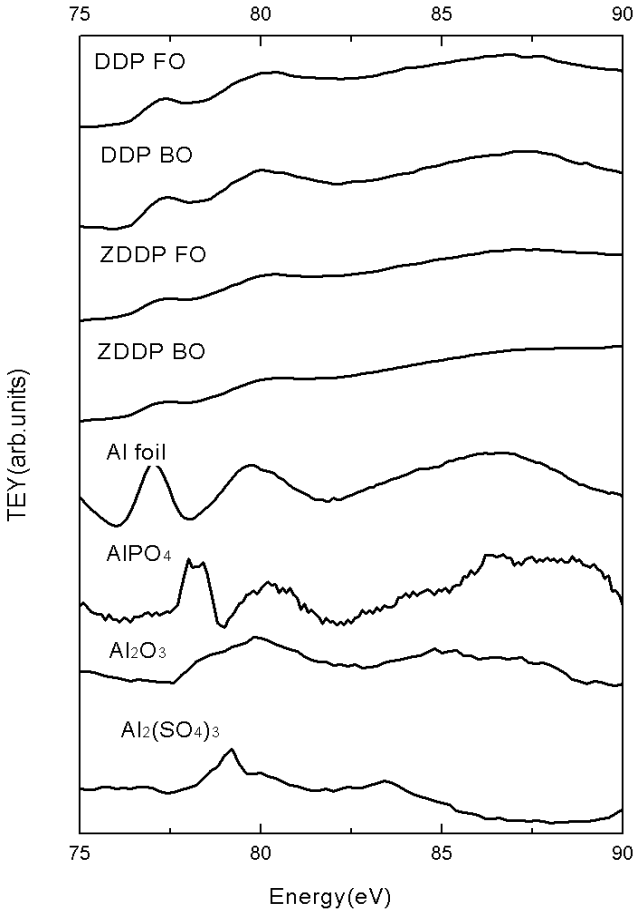

Figure 4.16 Al L-edge XANES spectra collected in TEY mode for transfer film generated by samples containing Zinc dialkyl-dithiophosphate in base oil/fully formulated oil and Dialkyl dithiophosphate in base oil/fully formulated oil under 0.5 kg loads and the same spectra record for model compounds, Al- foil,$AlPO_4$,Al_2O_3,$Al_2(SO_4)_3$.

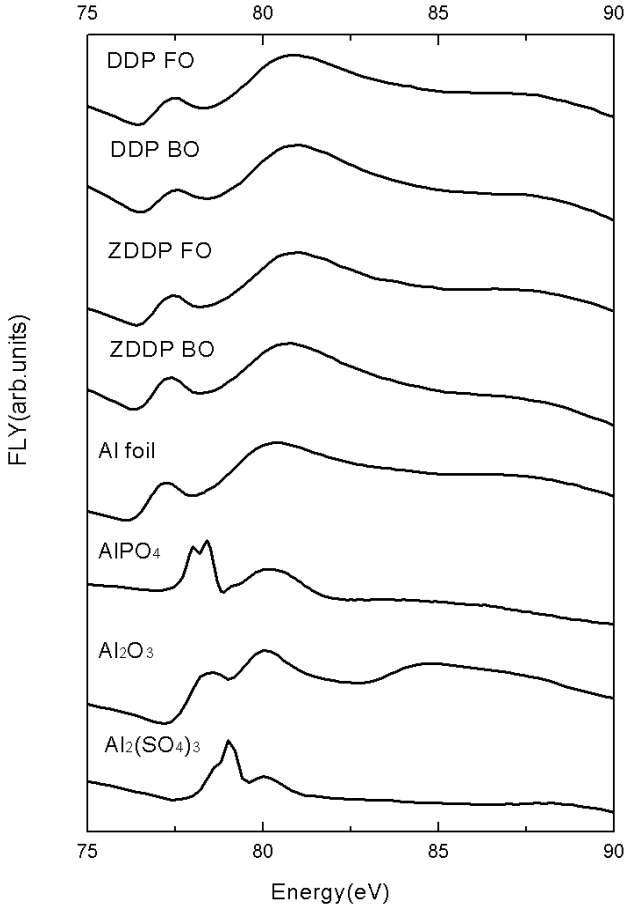

Figure 4.17 Al L-edge XANES spectra collected in FLY mode for transfer film generated by samples containing Zinc dialkyl-dithiophosphate in base oil/fully formulated oil and Dialkyl dithiophosphate in base oil/fully formulated oil under 0.5 kg loads and the same spectra record for model compounds, Al- foil,$AlPO_4$,Al_2O_3,$Al_2(SO_4)_3$.

It is clearly evident from both TEY and FLY of the Al-Ledge that the spectra resembles that which was acquired from a plain Al foil indicating that Al does not participate in the formation of either a tribofilm or a transfer film on the surface.

Fe L-edge

Figure 4.18 and 4.19 show Fe L-edge spectra record in TEY (surface sensitive) and FLY (bulk sensitive) modes respectively. In figures, the XANES spectra in TEY and FLY modes are shown for samples containing Zinc dialkyl-dithiophosphate in base oil/fully formulated oil

and Dialkyl dithiophosphate in base oil /fully formulated oil alongside the same spectra for the model compounds:FeS,$FeSO_4$,Fe_2O_3,$FePO_4$,$Fe_2(SO_4)_3$.

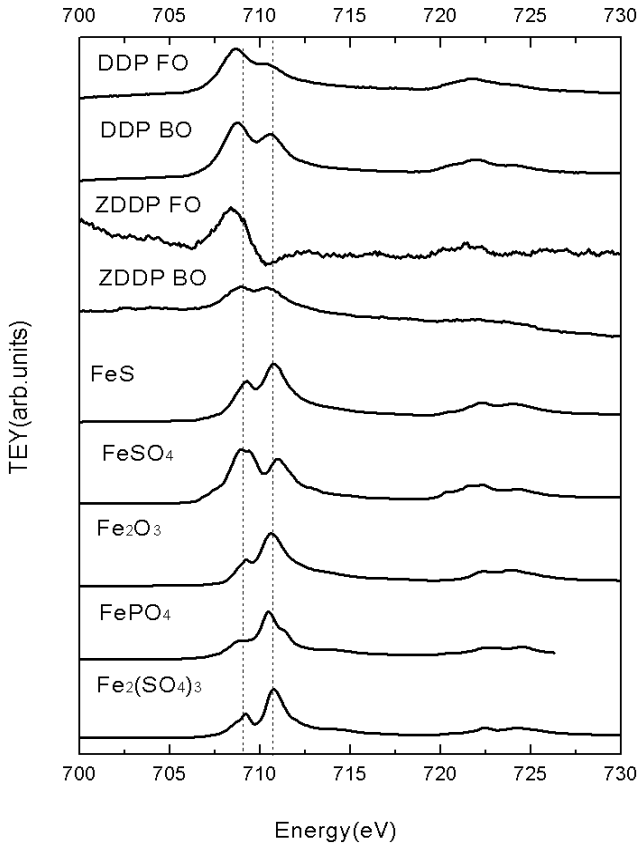

Figure 4.18 Fe L-edge XANES spectra collected in TEY mode for transfer film generated by samples containing Zinc dialkyl-dithiophosphate in base oil/fully formulated oil and Dialkyl dithiophosphate in base oil/fully formulated oil under 0.5 kg loads and the same spectra record for model compounds, FeS,$FeSO_4$,Fe_2O_3,$FePO_4$,$Fe_2(SO_4)_3$.

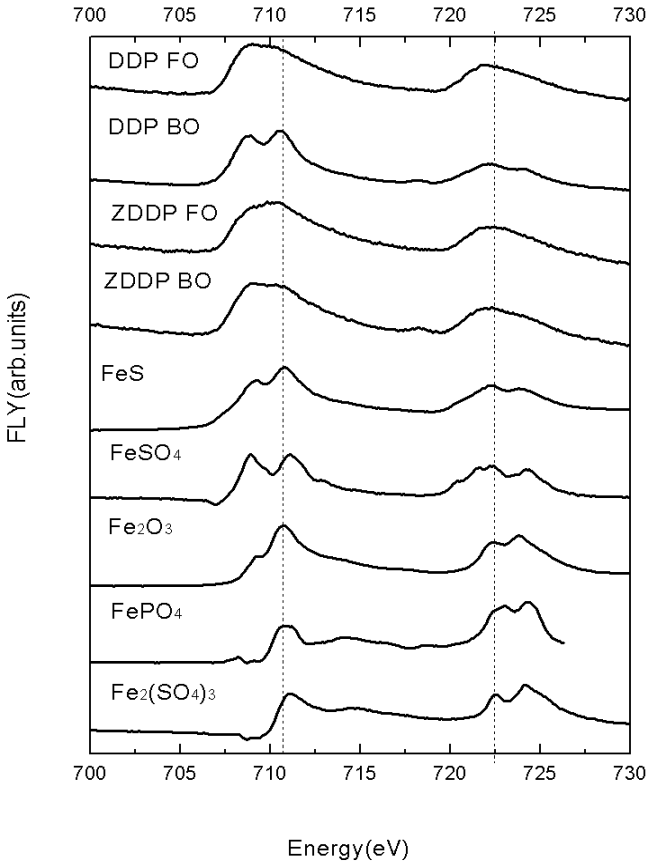

Figure 4.19 Fe L-edge XANES spectra collected in FLY mode for transfer film generated by samples containing Zinc dialkyl-dithiophosphate in base oil/fully formulated oil and Dialkyl dithiophosphate in base oil/fully formulated oil under 0.5 kg loads and the same spectra record for model compounds, FeS,$FeSO_4$,Fe_2O_3,$FePO_4$,$Fe_2(SO_4)_3$.

The TEY spectra for the surface indicate that in the case of ZDDP in base oil, the near surface region contains $FeSO_4$ while the fully formulated oil appears to contain a mixture of sulfates and sulfides. On the peaks for Fe when DDP is used indicates presence of $FeSO_4$ .In FLY mode, In the case of DDP in base oil, the film contains $FeSO_4$, On the other hand there is a distinctive peak associated with Fe in other case indicating that there is well developed transfer film on the surface that contains Fe. However, the peak is diffuse suggesting that the transfer film may indeed contain a mixture of phosphates, sulfides and sulfides of Fe in the transfer film.

S L-edge

Figure 4.20 and 4.21 show S L-edge spectra record in TEY (surface sensitive) and FLY (bulk sensitive) modes respectively. In figures, the XANES spectra in TEY and FLY modes are shown for samples containing Zinc dialkyl-dithiophosphate in base oil/fully formulated oil and Dialkyl dithiophosphate in base oil /fully formulated oil alongside the same spectra for the model compounds: $FeSO_4$,FeS,FeS_2,$Fe_2(SO_4)_3$,$ZnSO_4$,ZnS,$Al_2(SO_4)_3$.

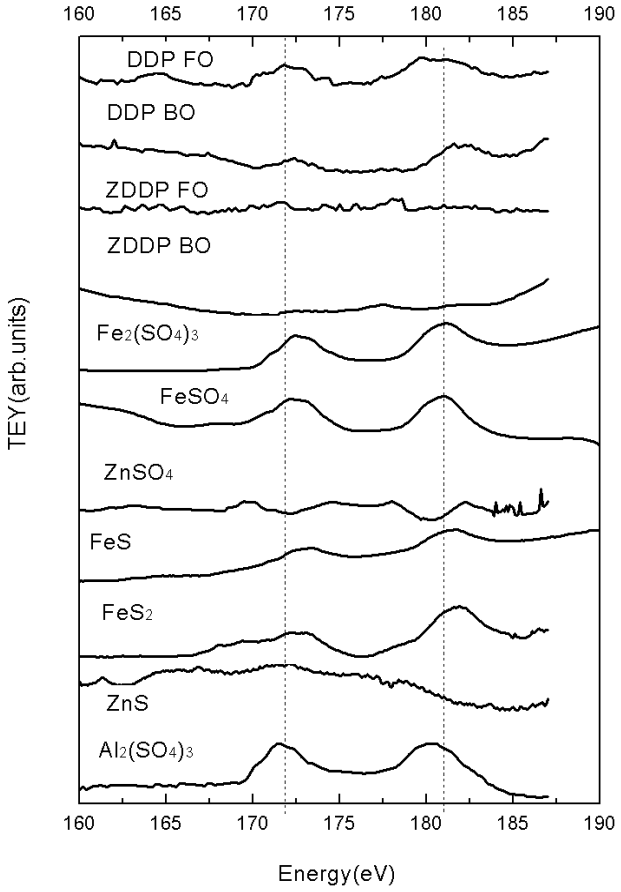

Figure 4.20 S L-edge XANES spectra collected in TEY mode for transfer film generated by samples containing Zinc dialkyl-dithiophosphate in base oil/fully formulated oil and Dialkyl dithiophosphate in base oil/fully formulated oil under 0.5 kg loads and the same spectra record for model compounds, $FeSO_4$,FeS,FeS_2,$Fe_2(SO_4)_3$,$ZnSO_4$,ZnS,$Al_2(SO_4)_3$.

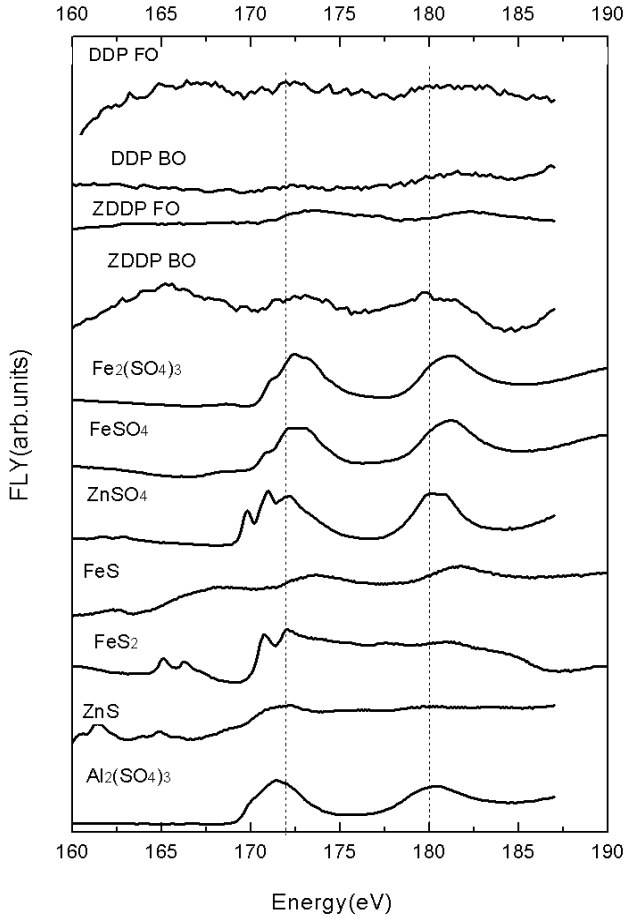

Figure 4.21 S L-edge XANES spectra collected in FLY mode for transfer film generated by samples containing Zinc dialkyl-dithiophosphate in base oil/fully formulated oil and Dialkyl dithiophosphate in base oil/fully formulated oil under 0.5 kg loads and the same spectra record for model compounds, $FeSO_4$,FeS,FeS_2,$Fe_2(SO_4)_3$,$ZnSO_4$,ZnS,$Al_2(SO_4)_3$.

Both TEY and FLY of the S-Ledge indicate that very weak presence of S in transfer film. This weak presence of S may be attributed to the fact that the energy flux in the VLS-PGM beamline at the S L-edge is relatively low and the signal strength from the S L-edge is relatively weak.

In the TEY mode, in the transfer film formed when DDP is used, the dominant peak position matches with the peak position for $FeSO_4$.The presence of sulfates as opposed to sulfides indicated poorer protection of the surface. In the case of ZDDP, very little evidence of

the presence of sulfide, sulfate is apparent. The spectra collected in FLY mode did not yield conclusive data.

P L-edge

Figure 4.22 and 4.23 show P L-edge spectra record in TEY (surface sensitive) and FLY (bulk sensitive) modes respectively. In figures, the XANES spectra in TEY and FLY modes are shown for samples containing Zinc dialkyl-dithiophosphate in base oil/fully formulated oil and Dialkyl dithiophosphate in base oil /fully formulated oil alongside the same spectra for the model compounds:$Zn_3(PO_4)_2$,$Fe_4(P_2O_7)_3$,$FePO_4$,$AlPO_4$.

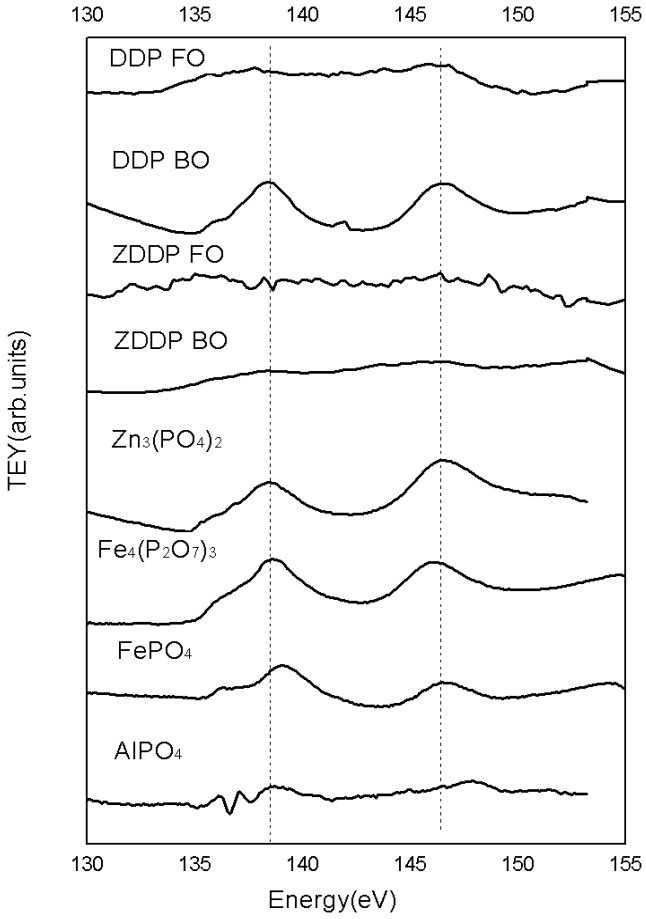

Figure 4.22 P L-edge XANES spectra collected in TEY mode for transfer film generated by samples containing Zinc dialkyl-dithiophosphate in base oil/fully formulated oil and Dialkyl dithiophosphate in base oil/fully formulated oil under 0.5 kg loads and the same spectra record for model compounds, $Zn_3(PO_4)_2$,$Fe_4(P_2O_7)_3$,$FePO_4$,$AlPO_4$.

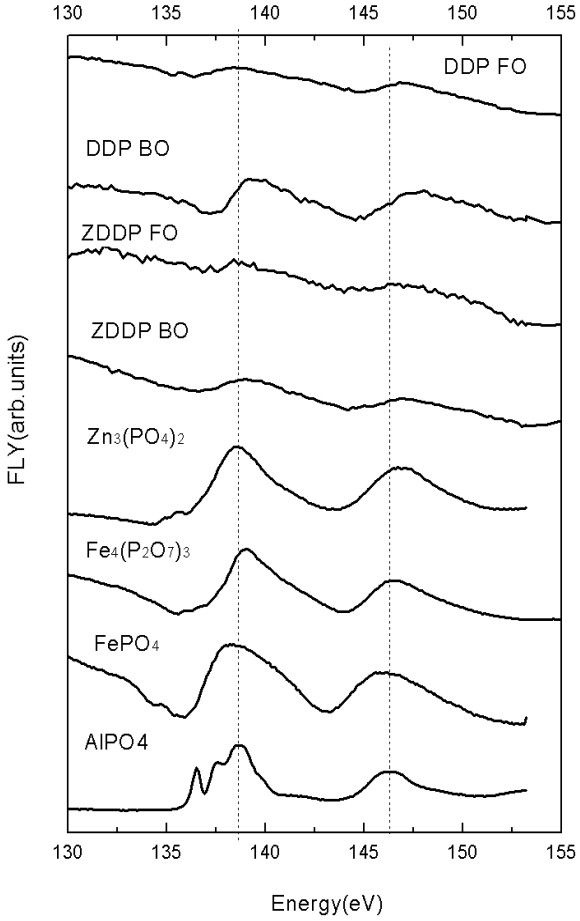

Figure 4.23 P L-edge XANES spectra collected in FLY mode for transfer film generated by samples containing Zinc dialkyl-dithiophosphate in base oil/fully formulated oil and Dialkyl dithiophosphate in base oil/fully formulated oil under 0.5 kg loads and the same spectra record for model compounds, $Zn_3(PO_4)_2$,$Fe_4(P_2O_7)_3$,$FePO_4$,$AlPO_4$.

TEY spectra with ZDDP and DDP indicate the weak presence of P in the transfer film near the surface; however, the peak intensities are very weak indicating that not much P is present near the surface. In the case of DDP in base oil, the peak intensity is very strong indicating that near surface region contains iron-phosphates. On the other hand the FLY spectra of the transfer film indicate a presence of P in the transfer film with the base oil compositions exhibiting the evidence for the presence of iron-phosphates when DDP was used. In the case of ZDDP in base oil, for FLY, it indicates that the film contains little zinc-phosphates, and for TEY, very little evidence of the presence of phosphates is apparent. Comparing the wear performance of oils with ZDDP and DDP shown in Fig 4.2.2, it is evident that DDP results in

better wear protection that can be partially explained by its ability form protective polyphosphate films on the surface.

O K-edge

Figure 4.24 and 4.25 show O K-edge spectra record in TEY (surface sensitive) and FLY (bulk sensitive) modes respectively. In figures , the XANES spectra in TEY and FLY modes are shown for samples containing Zinc dialkyl-dithiophosphate in base oil/fully formulated oil and Dialkyl dithiophosphate in base oil /fully formulated oil alongside the same spectra for the model compounds: $Zn_3(PO_4)_2$, $FeSO_4$,Fe_2O_3, $FePO_4$,$Fe_2(SO_4)_3$,$AlPO_4$,Al_2O_3,$Al_2(SO_4)_3$.

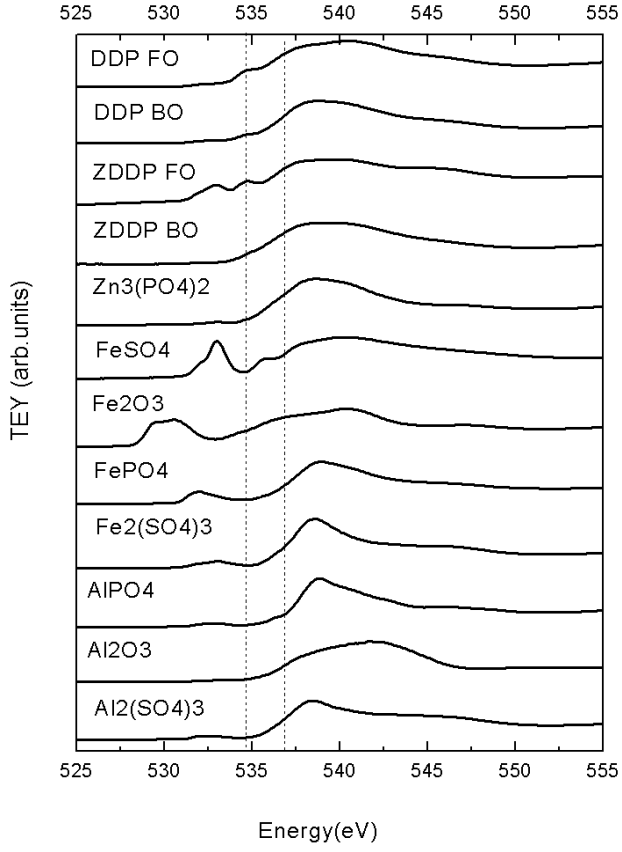

Figure 4.24 O K-edge XANES spectra collected in TEY mode for transfer film generated by samples containing Zinc dialkyl-dithiophosphate in base oil/fully formulated oil and Dialkyl dithiophosphate in base oil under 0.5 kg loads and the same spectra record for model compounds, $Zn_3(PO_4)_2$, $FeSO_4$, Fe_2O_3, $FePO_4$, $Fe_2(SO_4)_3$, $AlPO_4$, Al_2O_3, $Al_2(SO_4)_3$.

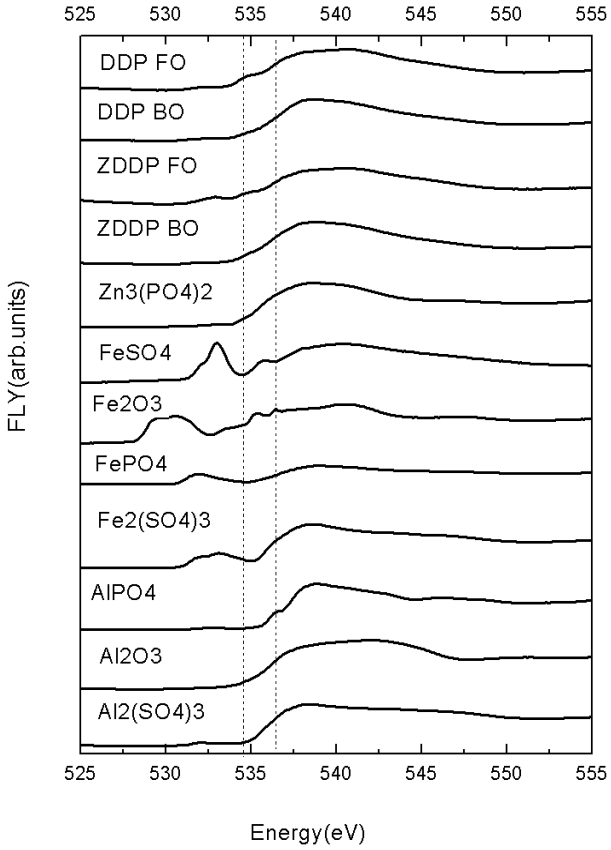

Figure 4.25 O K-edge XANES spectra collected in FLY mode for transfer film generated by samples containing Zinc dialkyl-dithiophosphate in base oil/fully formulated oil and Dialkyl dithiophosphate in base oil under 0.5 kg loads and the same spectra record for model compounds, $Zn_3(PO_4)_2$, $FeSO_4$, Fe_2O_3, $FePO_4$, $Fe_2(SO_4)_3$, $AlPO_4$, Al_2O_3, $Al_2(SO_4)_3$.

Both TEY and FLY spectra show that the transfer film from ZDDP in base oil/fully formulated oil ,the major peak match the Al_2O_3,and it contains minor $Zn_3(PO_4)_2$, $FeSO_4$.The transfer film from DDP, the major peak matches the Al_2O_3,and it contains a little $FeSO_4$, $FePO_4$.However,from the P L-edge it is evident that larger amount of O is present in the form of $FePO_4$ when DDP is used compared to ZDDP indicating that O is cross-linked in the form of polyphosphate chain results in better wear performance.

4.3.3 Ashless Dialkyl Dithiophosphate Compared with Ashless Amine Phosphate:

Both Amine phosphate and DDP are ashless antiwear additives without a metal cation. They were compared to examine the role played by “S” on the wear and formation of tribofilms.

Al L-edge

Figure 4.26 and 4.27 show Al L-edge spectra record in TEY (surface sensitive) and FLY (bulk sensitive) modes respectively. In figures, the XANES spectra in TEY and FLY modes are shown for samples containing Amine phosphate in base oil/fully formulated oil and Dialkyl dithiophosphate in base oil /fully formulated oil alongside the same spectra for the model compounds: Al foil,$AlPO_4$,Al_2O_3,$Al_2(SO_4)_3$.

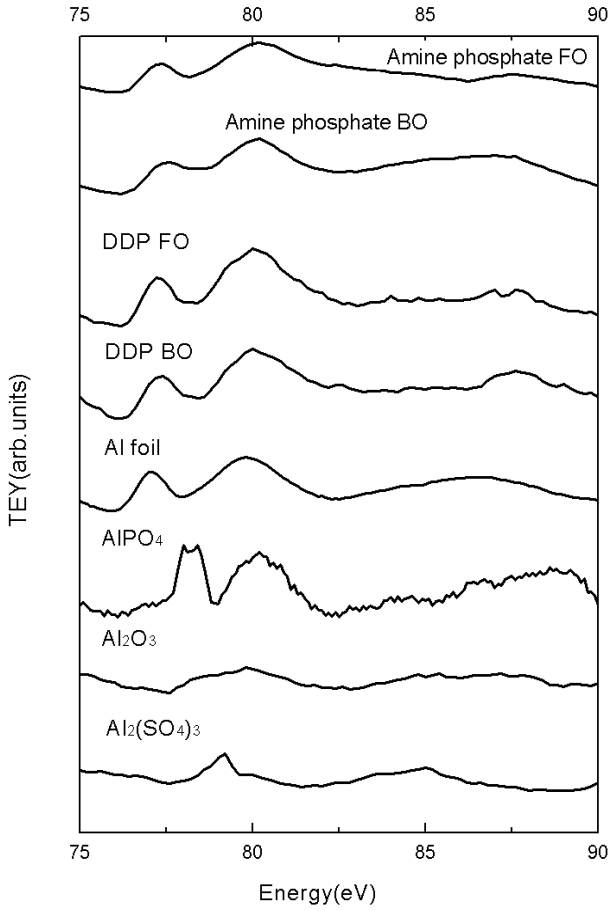

Figure 4.26 Al L-edge XANES spectra collected in TEY mode for transfer film generated by samples containing Amine phosphates in base oil/fully formulated oil and Dialkyl dithiophosphate in base oil/fully formulated oil under 0.5 kg loads and the same spectra record for model compounds, Al- foil,$AlPO_4$,Al_2O_3,$Al_2(SO_4)_3$.

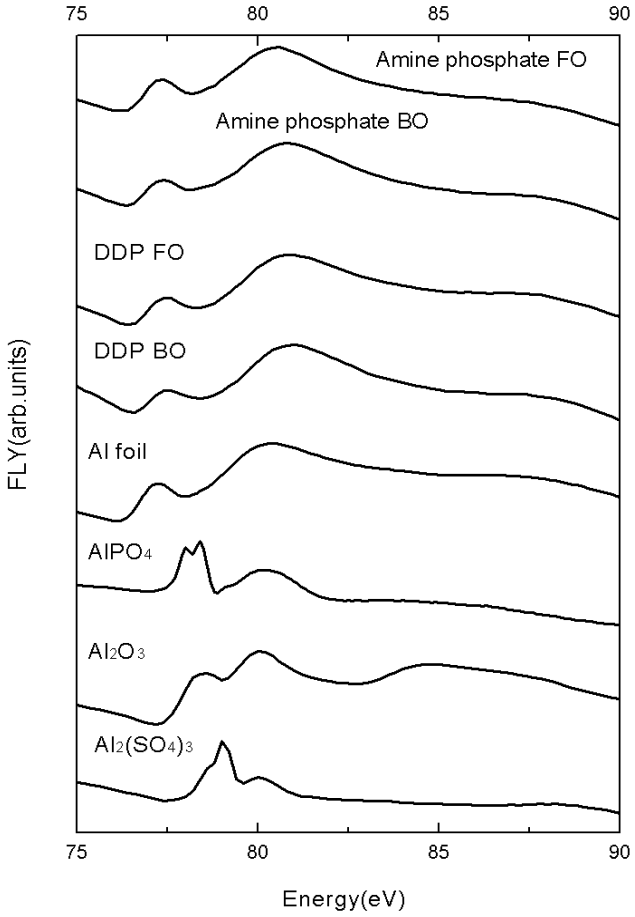

Figure 4.27 Al L-edge XANES spectra collected in FLY mode for transfer film generated by samples containing Amine phosphate in base oil/fully formulated oil and Dialkyl dithiophosphate in base oil/fully formulated oil under 0.5 kg loads and the same spectra record for model compounds, Al- foil,$AlPO_4$,Al_2O_3,$Al_2(SO_4)_3$.

It is clearly evident from both TEY and FLY of the Al-Ledge that the spectra resembles that which was acquired from a plain Al foil indicating that Al does not participate in the formation of either a tribofilm or a transfer film on the surface.

Fe L-edge

Figure 4.28 and 4.29 show Fe L-edge spectra record in TEY (surface sensitive) and FLY (bulk sensitive) modes respectively. In figures, the XANES spectra in TEY and FLY modes are shown for samples containing Amine phosphate in base oil/fully formulated oil and Dialkyl dithiophosphate in base oil /fully formulated oil alongside the same spectra for the model compounds:FeS,$FeSO_4$,Fe_2O_3,$FePO_4$,$Fe_2(SO_4)_3$.

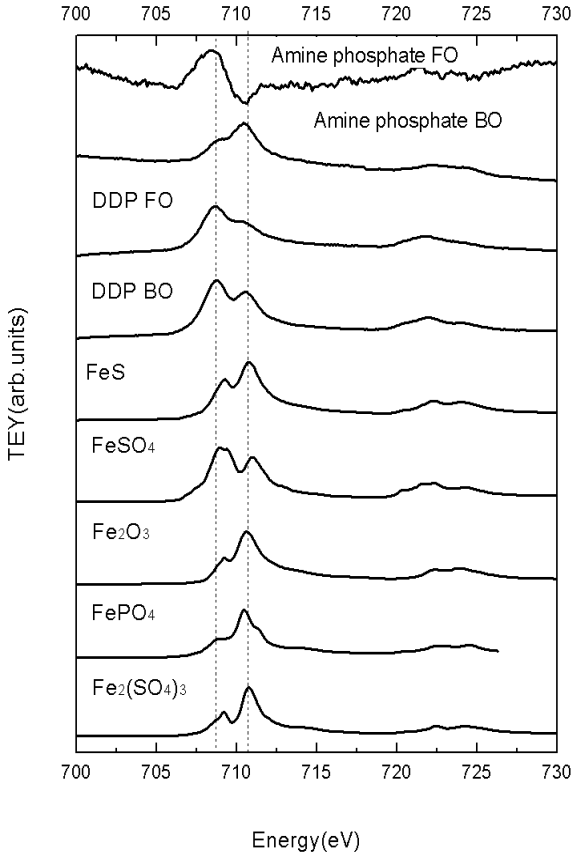

Figure 4.28 Fe L-edge XANES spectra collected in TEY mode for transfer film generated by samples containing Amine phosphate in base oil/fully formulated oil and Dialkyl dithiophosphate in base oil/fully formulated oil under 0.5 kg loads and the same spectra record for model compounds, FeS,$FeSO_4$,Fe_2O_3,$FePO_4$,$Fe_2(SO_4)_3$.

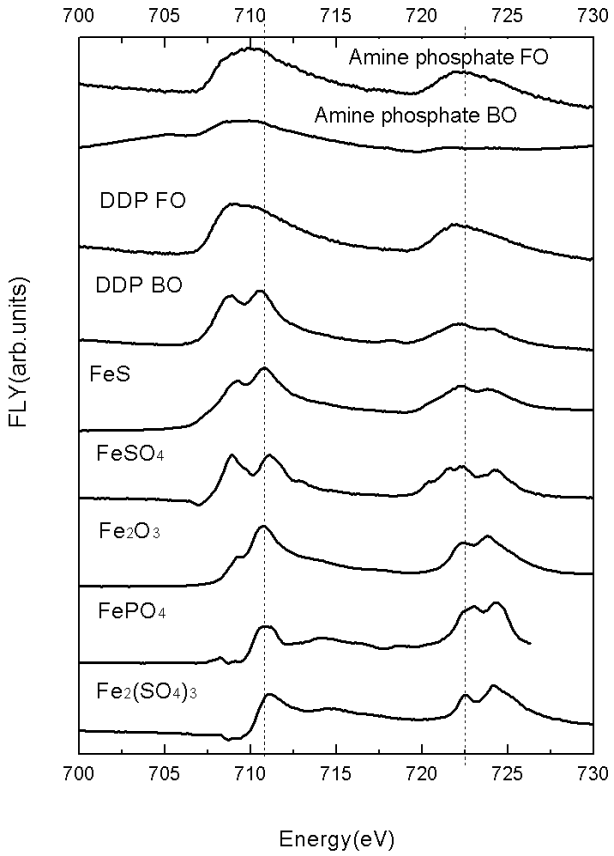

Figure 4.29 Fe L-edge XANES spectra collected in FLY mode for transfer film generated by samples containing Amine phosphate in base oil/fully formulated oil and Dialkyl dithiophosphate in base oil/fully formulated oil under 0.5 kg loads and the same spectra record for model compounds, FeS,$FeSO_4$,Fe_2O_3,$FePO_4$,$Fe_2(SO_4)_3$.

The TEY spectra for the wear surface indicate that in the case of DDP, the near surface region contains $FeSO_4$ .On the peaks for Fe when amine phosphate is used in TEY indicate that the presence of $FePO_4$, in the case of amine phosphate in fully formulated oil, the surface region contains a little $FeSO_4$, it may come from the detergent(Calcium Sulfonate). In FLY mode, DDP in base oil, the spectra indicates that the film contains $FeSO_4$ and $FePO_4$, on the other hand, there is a distinctive peak associated with Fe in other case indicating that there is well developed transfer film on the surface that contains Fe. However, the peak is diffuse suggesting that the transfer film may indeed contain a mixture of phosphates, sulfides and sulfides of Fe in the transfer film.

S L-edge

Figure 4.30 and 4.31 show S L-edge spectra record in TEY (surface sensitive) and FLY (bulk sensitive) modes respectively. In figures, the XANES spectra in TEY and FLY modes are shown for samples containing Amine phosphate in base oil/fully formulated oil and Dialkyl dithiophosphate in base oil /fully formulated oil alongside the same spectra for the model compounds: $FeSO_4$,FeS,FeS_2,$Fe_2(SO_4)_3$,Zn SO_4,ZnS,$Al_2(SO_4)_3$.

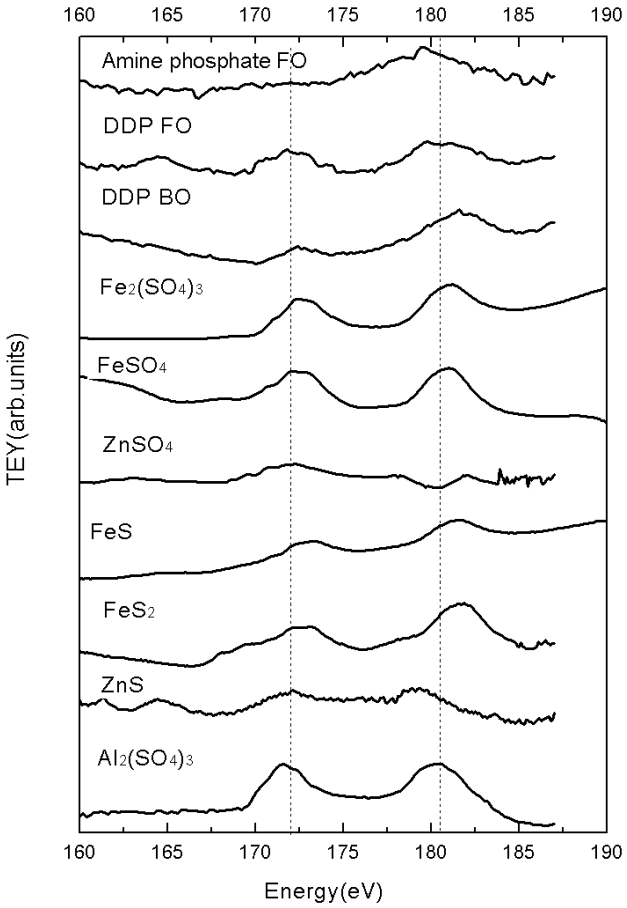

Figure 4.30 S L-edge XANES spectra collected in TEY mode for transfer film generated by samples containing Amine phosphate in base oil/fully formulated oil and Dialkyl dithiophosphate in base oil/fully formulated oil under 0.5 kg loads and the same spectra record for model compounds, $FeSO_4$,FeS ,FeS_2,$Fe_2(SO_4)_3$,Zn SO_4,ZnS,$Al_2(SO_4)_3$.

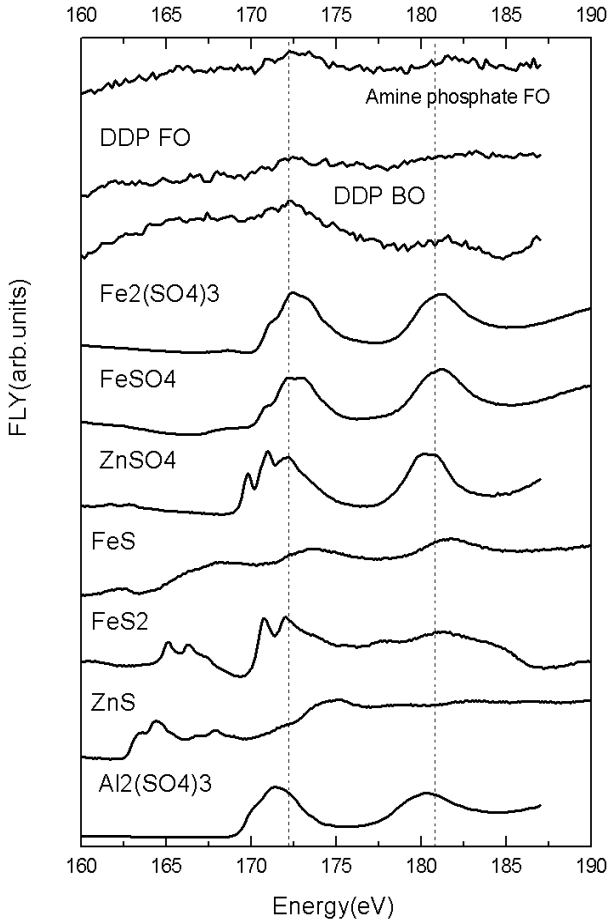

Figure 4.31 S L-edge XANES spectra collected in FLY mode for transfer film generated by samples containing Amine phosphate in base oil/fully formulated oil and Dialkyl dithiophosphate in base oil/fully formulated oil under 0.5 kg loads and the same spectra record for model compounds, $FeSO_4$,FeS ,FeS_2,$Fe_2(SO_4)_3$,Zn SO_4,ZnS,$Al_2(SO_4)_3$.

Both TEY and FLY of the S-Ledge indicate that very weak presence of S in transfer film. This weak presence of S may be attributed to the fact that the energy flux in the VLS-PGM beamline at the S L-edge is relatively low and the signal strength from the S L-edge is relatively weak.

In the TEY mode, in the transfer film formed when DDP is used, the dominant peak position matches with the peak position for $FeSO_4$.The presence of sulfates as opposed to sulfides indicated poorer protection of the surface. In the case of amine phosphates, it has no sulfur. The spectra collected in FLY mode did not yield conclusive data.

P L-edge

Figure 4.32 and 4.33 show P L-edge spectra record in TEY (surface sensitive) and FLY (bulk sensitive) modes respectively. In figures, the XANES spectra in TEY and FLY modes are shown for samples containing Amine phosphate in base oil/fully formulated oil and Dialkyl dithiophosphate in base oil /fully formulated oil alongside the same spectra for the model compounds:$Zn_3(PO_4)_2$,$Fe_4(P_2O_7)_3$,$FePO_4$,$AlPO_4$.

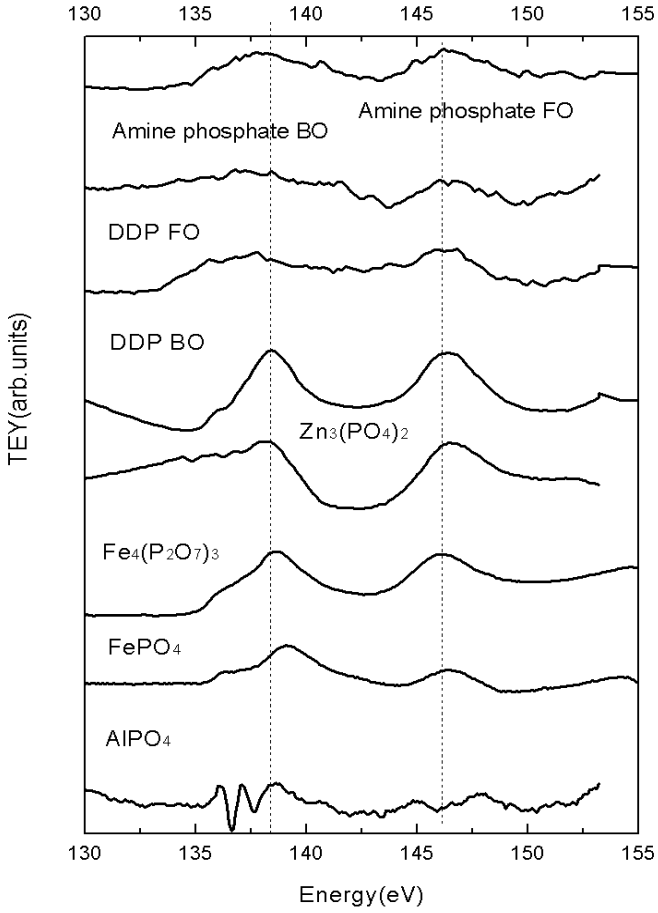

Figure 4.32 P L-edge XANES spectra collected in TEY mode for transfer film generated by samples containing Amine phosphate in base oil/fully formulated oil and Dialkyl dithiophosphate in base oil/fully formulated oil under 0.5 kg loads and the same spectra record for model compounds, $Zn_3(PO_4)_2$,$Fe_4(P_2O_7)_3$,$FePO_4$,$AlPO_4$.

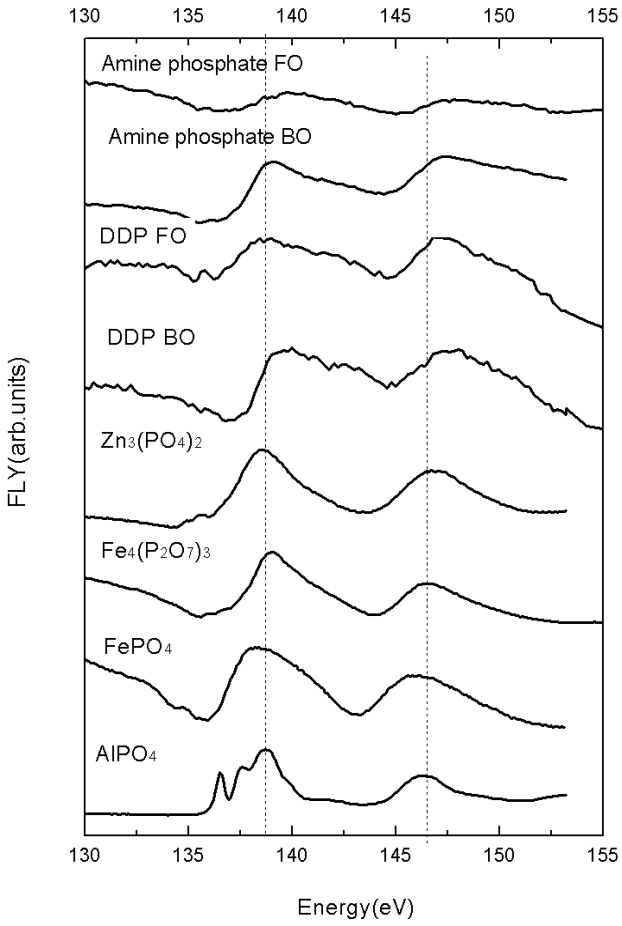

Figure 4.33 P L-edge XANES spectra collected in FLY mode for transfer film generated by samples containing Amine phosphate in base oil/fully formulated oil and Dialkyl dithiophosphate in base oil/fully formulated oil under 0.5 kg loads and the same spectra record for model compounds, $Zn_3(PO_4)_2$,$Fe_4(P_2O_7)_3$,$FePO_4$,$AlPO_4$.

TEY spectra with DDP and amine phospates indicate the weak presence of P in the transfer film near the surface; however, the peak intensities are very weak indicating that not much P is present near the surface. In the case of DDP in base oil, the peak intensity is very strong indicating that near surface region contains iron-phosphates. On the other hand the FLY spectra of the transfer film indicate a presence of P in the transfer film with the base oil and fully formulated oil compositions exhibiting the evidence for the presence of iron-phosphates when DDP and amine phosphates were used. The wear performance of the amine phosphate antiwear additive is much poorer than the DDP additive and that is evident by the weaker phosphate film on the surface and absence of S in the amine phosphate.

O K-edge

Figure 4.34 and 4.35 show O K-edge spectra record in TEY (surface sensitive) and FLY (bulk sensitive) modes respectively. In figures , the XANES spectra in TEY and FLY modes are shown for samples containing Amine phosphate in base oil/fully formulated oil and Dialkyl dithiophosphate in base oil /fully formulated oil alongside the same spectra for the model compounds: $Zn_3(PO_4)_2$, $FeSO_4$,Fe_2O_3, $FePO_4$,$Fe_2(SO_4)_3$,$AlPO_4$,Al_2O_3,$Al_2(SO_4)_3$.

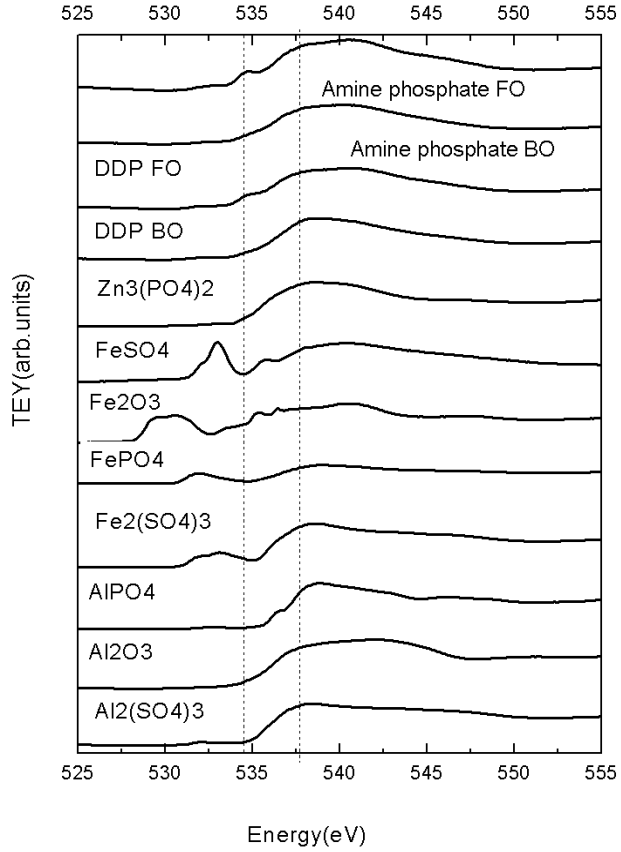

Figure 4.34 O K-edge XANES spectra collected in TEY mode for transfer film generated by samples containing Amine phosphate in base oil/fully formulated oil and Dialkyl dithiophosphate in base oil under 0.5 kg loads and the same spectra record for model compounds, $Zn_3(PO_4)_2$, $FeSO_4$, Fe_2O_3, $FePO_4$, $Fe_2(SO_4)_3$, $AlPO_4$, Al_2O_3, $Al_2(SO_4)_3$.

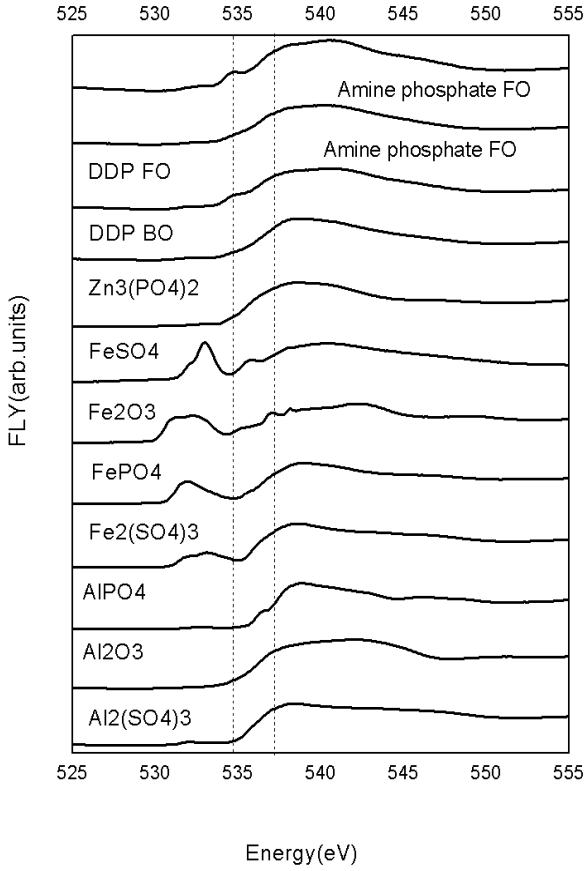

Figure 4.35 O K-edge XANES spectra collected in FLY mode for transfer film generated by samples containing Amine phosphate in base oil/fully formulated oil and Dialkyl dithiophosphate in base oil under 0.5 kg loads and the same spectra record for model compounds, $Zn_3(PO_4)_2$, $FeSO_4$, Fe_2O_3, $FePO_4$, $Fe_2(SO_4)_3$, $AlPO_4$, Al_2O_3, $Al_2(SO_4)_3$.

Both TEY and FLY spectra show that the transfer film from Amine phosphate in base oil, the major peak match the Al_2O_3,and it contains minor $FePO_4$, for the film formed with Amine phosphate in fully formulated oil, it also contains a little $FeSO_4$,$FeSO_4$ when S comes from the detergent. The transfer film from DDP, the major peak matches the Al_2O_3, and it contains a little $FeSO_4$, $FePO_4$.However the stronger P L-edge spectra in FLY mode when DDP is used indicates that the presence of both sulfur and phosphorus in the antiwear chemistry is essential for protective transfer film formation.

4.3.4 Thiadiazole Compared with Amine Phosphates:

Compare the Sulfur Ashless Antiwear Additives with Phosphate Ashless Antiwear Additives

Al L-edge

Figure 4.36 and 4.37 show Al L-edge spectra record in TEY (surface sensitive) and FLY (bulk sensitive) modes respectively. In figures, the XANES spectra in TEY and FLY mode are shown for samples containing Thiadiazole in base oil/fully formulated oil and Amine phosphate in base oil /fully formulated oil alongside the same spectra for the model compounds: Al foil,$AlPO_4$,Al_2O_3,$Al_2(SO_4)_3$.

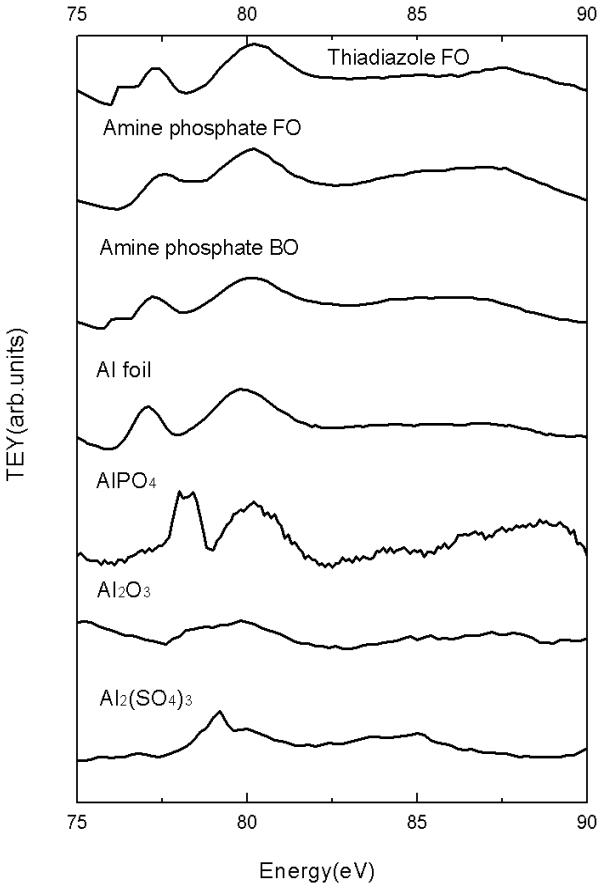

Figure 4.36 Al L-edge XANES spectra collected in TEY mode for transfer film generated by samples containing Thiadiazole in base oil/fully formulated oil and Amine phosphates in base oil/fully formulated oil under 0.5 kg loads and the same spectra record for model compounds, Al- foil, $AlPO_4$, Al_2O_3, $Al_2 (SO_4)_3$.

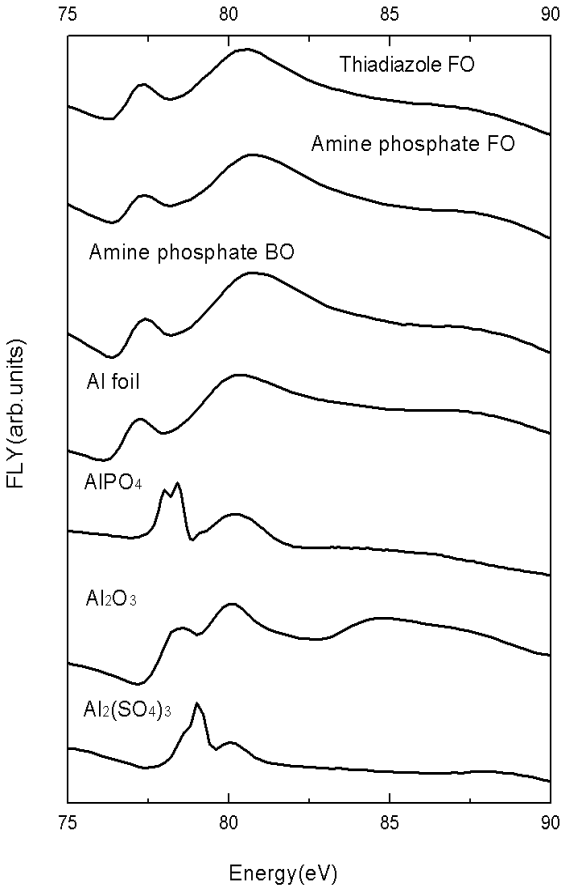

Figure 4.37 Al L-edge XANES spectra collected in FLY mode for transfer film generated by samples containing Thiadiazole in base oil/fully formulated oil and Amine phosphate in base oil/fully formulated oil under 0.5 kg loads and the same spectra record for model compounds, Al- foil, $AlPO_4$, Al_2O_3, $Al_2 (SO_4)_3$.

It is clearly evident from both TEY and FLY of the Al-Ledge that the spectra resembles that which was acquired from a plain Al foil indicating that Al does not participate in the formation of either a tribofilm or a transfer film on the surface.

Fe L-edge

Figure 4.38 and 4.39 show Fe L-edge spectra record in TEY (surface sensitive) and FLY (bulk sensitive) modes respectively. In figures, the XANES spectra in TEY and FLY modes are shown for samples containing Amine phosphate in base oil/fully formulated oil and Thiadiazole in base oil /fully formulated oil alongside the same spectra for the model compounds:FeS,$FeSO_4$,Fe_2O_3,$FePO_4$,$Fe_2(SO_4)_3$.

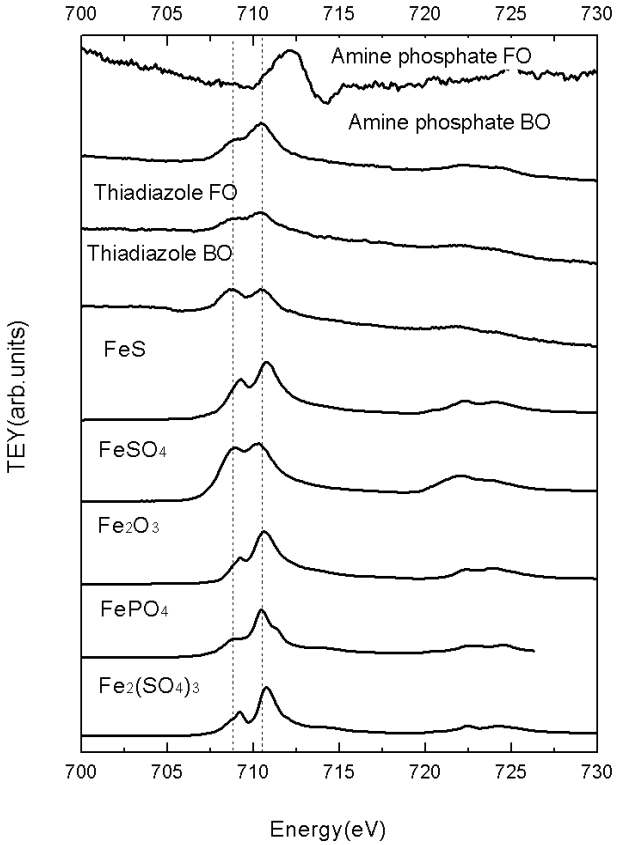

Figure 4.38 Fe L-edge XANES spectra collected in TEY mode for transfer film generated by samples containing Thiadiazole in base oil/fully formulated oil and Amine phosphate in base oil/fully formulated oil under 0.5 kg loads and the same spectra record for model compounds, FeS, $FeSO_4$, Fe_2O_3, $FePO_4$, $Fe_2(SO_4)_3$.

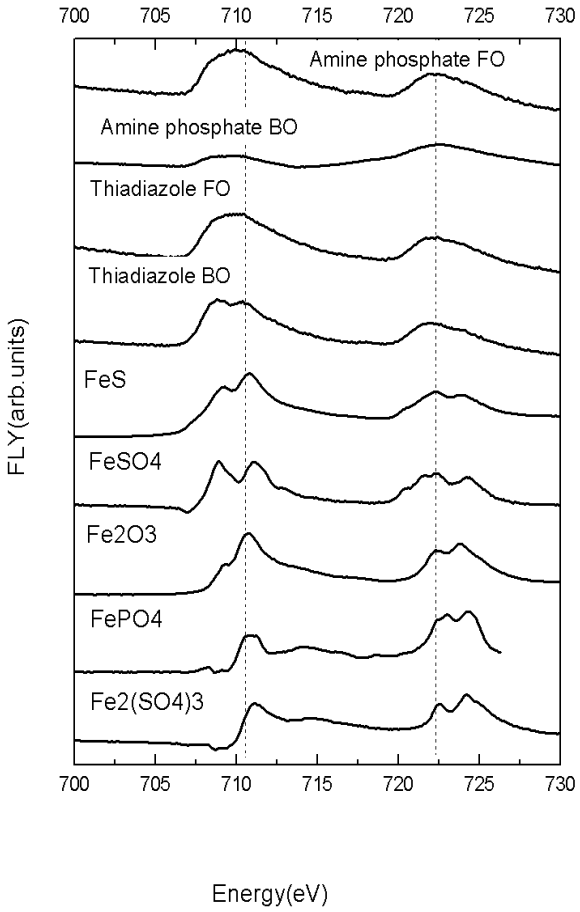

Figure 4.39 Fe L-edge XANES spectra collected in FLY mode for transfer film generated by samples containing Thiadiazole in base oil/fully formulated oil and Amine phosphate in base oil/fully formulated oil under 0.5 kg loads and the same spectra record for model compounds, FeS, $FeSO_4$, Fe_2O_3, $FePO_4$, $Fe_2(SO_4)_3$.

The TEY spectra for the wear surface indicate that in the case of thiadiazole, the near surface region contains $FeSO_4$ .On the peaks for Fe when amine phosphate is used in TEY indicate that the presence of $FePO_4$, in the case of amine phosphate in fully formulated oil, the surface region contains a little $FeSO_4$,it comes from the detergent(Calcium sulfonate). On the other hand in FLY mode there is a distinctive peak associated with Fe in all case indicating that there is well developed transfer film on the surface that contains Fe. However, the peak is diffuse suggesting that the transfer film may indeed contain a mixture of phosphates, sulfides and sulfides of Fe in the transfer film.

S L-edge

Figure 4.40 and 4.41 show S L-edge spectra record in TEY (surface sensitive) and FLY (bulk sensitive) modes respectively. In figures, the XANES spectra in TEY and FLY modes are shown for samples containing Amine phosphate in base oil/fully formulated oil and Thiadiazole in base oil /fully formulated oil alongside the same spectra for the model compounds: $FeSO_4$,FeS,FeS_2,$Fe_2(SO_4)_3$,Zn SO_4,ZnS,$Al_2(SO_4)_3$.

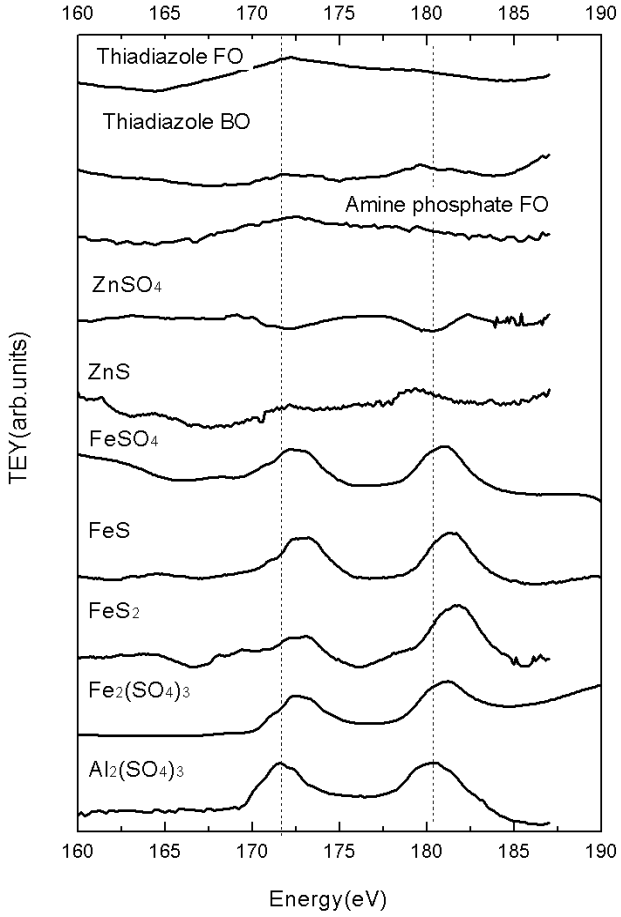

Figure 4.40 S L-edge XANES spectra collected in TEY mode for transfer film generated by samples containing Thiadiazole in base oil/fully formulated oil and Amine phosphate in base oil/fully formulated oil under 0.5 kg loads and the same spectra record for model compounds, $FeSO_4$,FeS ,FeS_2,$Fe_2(SO_4)_3$,Zn SO_4,ZnS,$Al_2(SO_4)_3$.

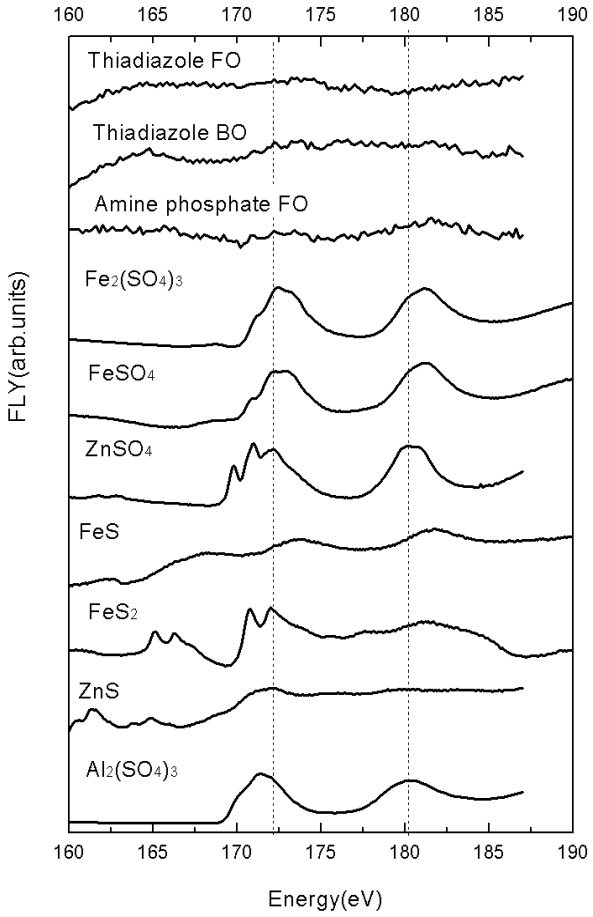

Figure 4.41 S L-edge XANES spectra collected in FLY mode for transfer film generated by samples containing Thiadiazole in base oil/fully formulated oil and Amine phosphate in base oil/fully formulated oil under 0.5 kg loads and the same spectra record for model compounds, $FeSO_4$,FeS ,FeS_2,$Fe_2(SO_4)_3$,$ZnSO_4$,ZnS,$Al_2(SO_4)_3$.

Both TEY and FLY of the S-Ledge indicate that very weak presence of S in transfer film. This weak presence of S may be attributed to the fact that the energy flux in the VLS-PGM beamline at the S L-edge is relatively low and the signal strength from the S L-edge is relatively weak.

In the TEY mode, in the transfer film formed when thiadiazole is used, the dominant peak position matches with the peak position for $FeSO_4$.The presence of sulfates as opposed to sulfides indicated poorer protection of the surface. In the case of amine phosphates, it has no sulfur. The spectra collected in FLY mode did not yield conclusive data.

P L-edge

Figure 4.42 and 4.43 show P L-edge spectra record in TEY (surface sensitive) and FLY (bulk sensitive) modes respectively. In figures, the XANES spectra in TEY and FLY modes are shown for samples containing Amine phosphate in base oil/fully formulated oil and Thiadiazole in base oil /fully formulated oil alongside the same spectra for the model compounds:$Zn_3(PO_4)_2$,$Fe_4(P_2O_7)_3$,$FePO_4$,$AlPO_4$.

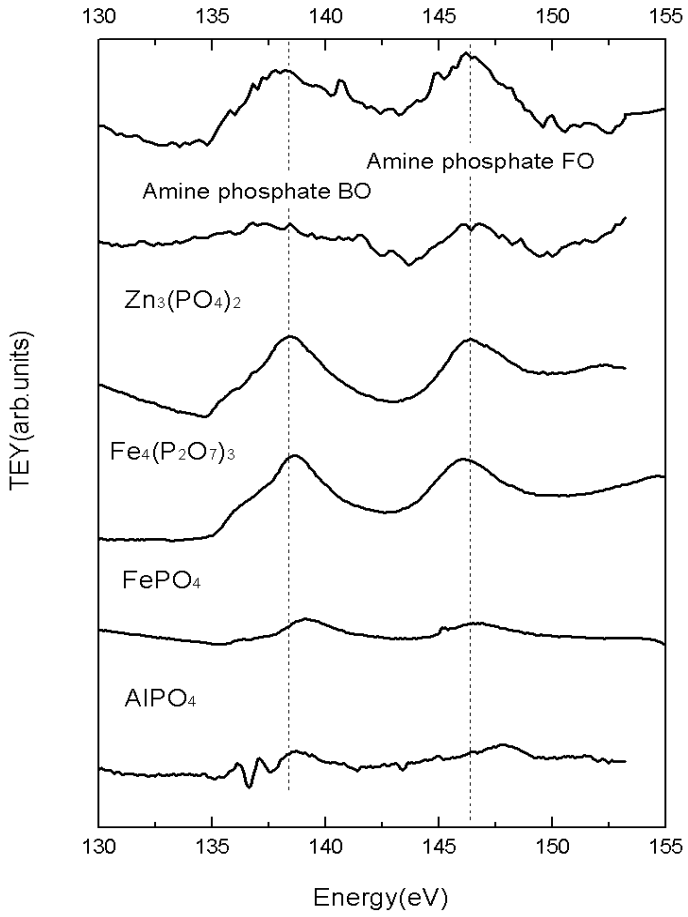

Figure 4.42 P L-edge XANES spectra collected in FLY mode for transfer film generated by samples containing Thiadiazole in base oil/fully formulated oil and Amine phosphate in base oil/fully formulated oil under 0.5 kg loads and the same spectra record for model compounds, $Zn_3(PO_4)_2$, $Fe_4(P_2O_7)_3$,$FePO_4$,$AlPO_4$.

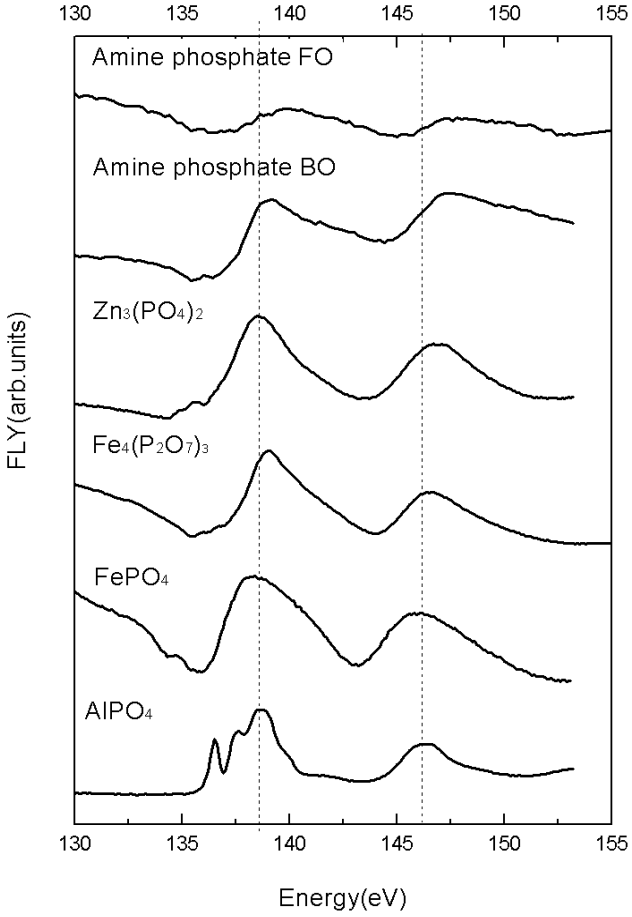

Figure 4.43 P L-edge XANES spectra collected in TEY mode for transfer film generated by samples containing Thiadiazole in base oil/fully formulated oil and Amine phosphate in base oil/fully formulated oil under 0.5 kg loads and the same spectra record for model compounds, $Zn_3(PO_4)_2$, $Fe_4(P_2O_7)_3$, $FePO_4$, $AlPO_4$.

TEY spectra with amine phosphates in base oil indicate the wear presence of P in the transfer film near the surface; however, the peak intensities are very weak indicating that not much P is present near the surface. In the case of amine phosphates in fully formulated oil, the peak intensity is very strong indicating that near surface region contains iron-phosphates. On the other hand the FLY spectra of the transfer film indicate a presence of P in the transfer film with the base oil and fully formulated oil compositions exhibiting the evidence for the presence of iron-phosphates when amine phosphates were used. For thiadiazole, it has no phosphorus.

O L-edge

Figure 4.44 and 4.45 show O K-edge spectra record in TEY (surface sensitive) and FLY (bulk sensitive) modes respectively. In figures, the XANES spectra in TEY and FLY modes are shown for samples containing Amine phosphate in base oil/fully formulated oil and Thiadiazole in base oil /fully formulated oil alongside the same spectra for the model compounds: $Zn_3(PO_4)_2$, $FeSO_4$,Fe_2O_3, $FePO_4$,$Fe_2(SO_4)_3$,$AlPO_4$,Al_2O_3,$Al_2(SO_4)_3$.

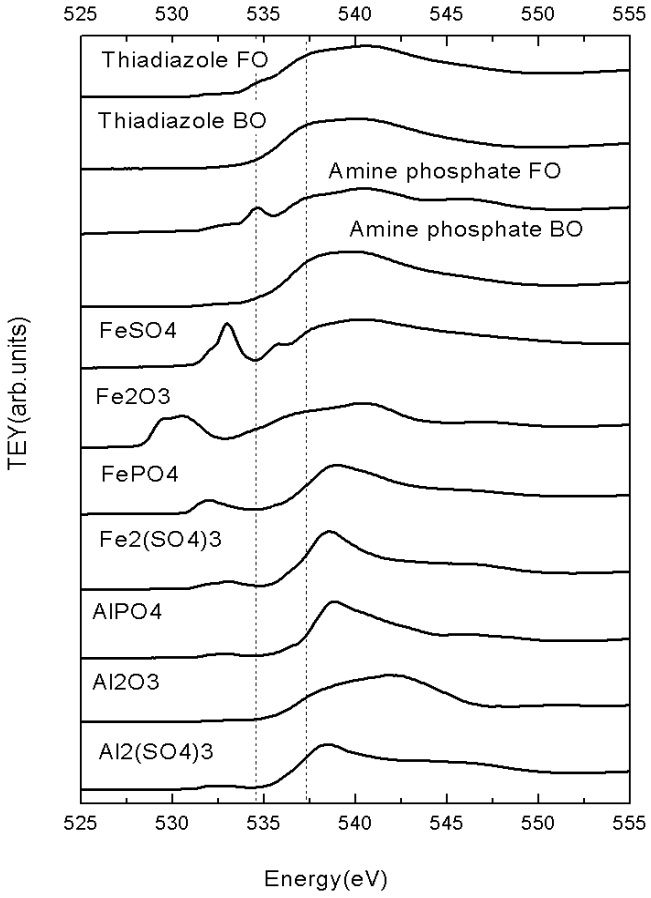

Figure 4.44 O K-edge XANES spectra collected in TEY mode for transfer film generated by samples containing Amine phosphate in base oil/fully formulated oil and Thiadiazole in base oil under 0.5 kg loads and the same spectra record for model compounds, $Zn_3(PO_4)_2$, $FeSO_4$, Fe_2O_3, $FePO_4$, $Fe_2(SO_4)_3$, $AlPO_4$, Al_2O_3, $Al_2(SO_4)_3$.

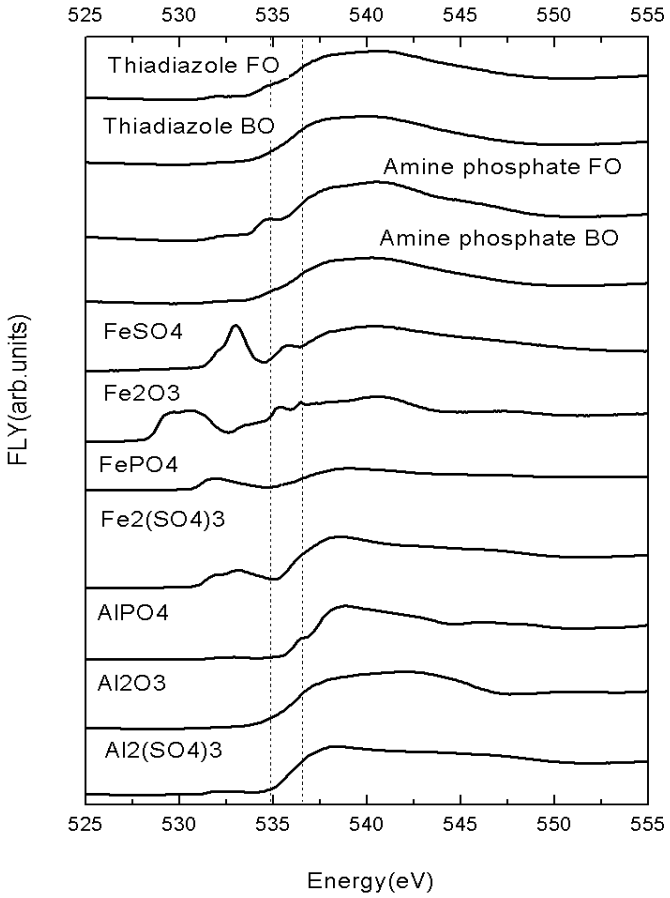

Figure 4.45 O K-edge XANES spectra collected in FLY mode for transfer film generated by samples containing Amine phosphate in base oil/fully formulated oil and Thiadiazole in base oil under 0.5 kg loads and the same spectra record for model compounds, $Zn_3(PO_4)_2$, $FeSO_4$, Fe_2O_3, $FePO_4$, $Fe_2(SO_4)_3$, $AlPO_4$, Al_2O_3, $Al_2(SO_4)_3$.

Both TEY and FLY spectra show that the transfer film from Amine phosphate in base oil ,the major peak match the Al_2O_3,and it contains minor $FePO_4$, for fully formulated oil, the film also contains a little $FePO_4$, $FeSO_4$, $FeSO_4$ comes from the detergent. The transfer film from Thiadiazole, the major peak matches the Al_2O_3, and it contains a little $FeSO_4$.Comparision of wear results shown in Fig 4.2.4 indicate that when either amine phosphate or thiadiazole is used the wear performance is poorer than when an antiwear chemistry that contains both S and P is used (eg. DDP).Hence it can be summarized that only S or P in the antiwear chemistry is insufficient to form protective films on the surface.

4.4 SEM/EDS Analysis of Tribofilms

4.4.1 ZDDP (Zinc Dialkyl-dithiophosphate)

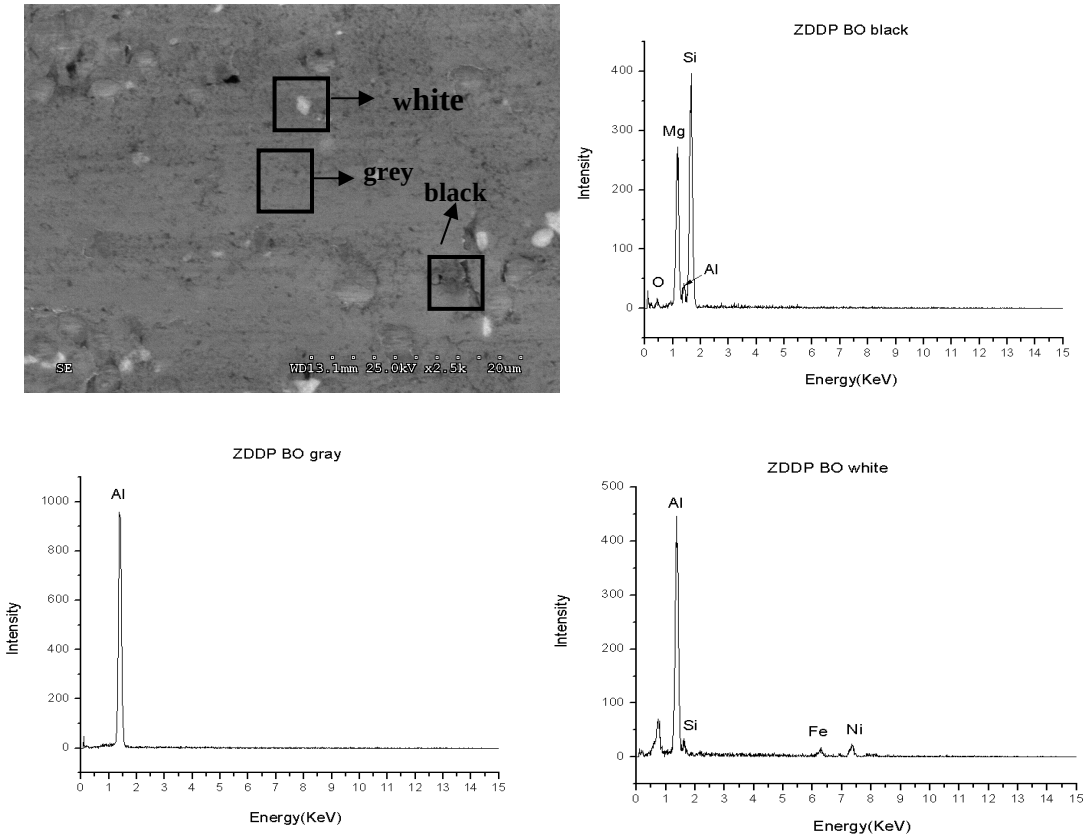

Figure 4.46 Scanning electron micrograph of the middle of the wear scar on the aluminum alloy disk at 2500x magnification for the HFRB wear test run under 0.5kg normal load for 50Hz on oil sample containing ZDDP (0.10wt%P) in base oil and EDS spectra obtained from the black, gray, white area of the film.

Fig 4.46 is a scanning electron micrograph from within the wear scar from ZDDP in base oil. It shows the relatively smooth surface with the presence of precipitates on the surface. EDS analysis was conducted in the matrix region (gray) and where the precipitates were present (white and black).The EDS spectra from the matrix region only indicates the presence of Al confirming the XANES data which indicates that Al is present only in its native oxide state. On the other hand the black particles are Mg_2Si precipitates which do not show any presence of Fe, P, S, while the white precipitates indicate the presence of Al, Si, Fe and Ni. This precipitate is Nickel Aluminide with some Si in it, and the Fe present is from the transfer film. The absence

of S or P indicates that the transfer film is relatively thin on the precipitate. The fact that the transfer film is only present on the precipitate and not in the matrix clearly indicates that the harder precipitate can sustain higher loads without plastic deformation and can be local region where transfer films can be deposited.

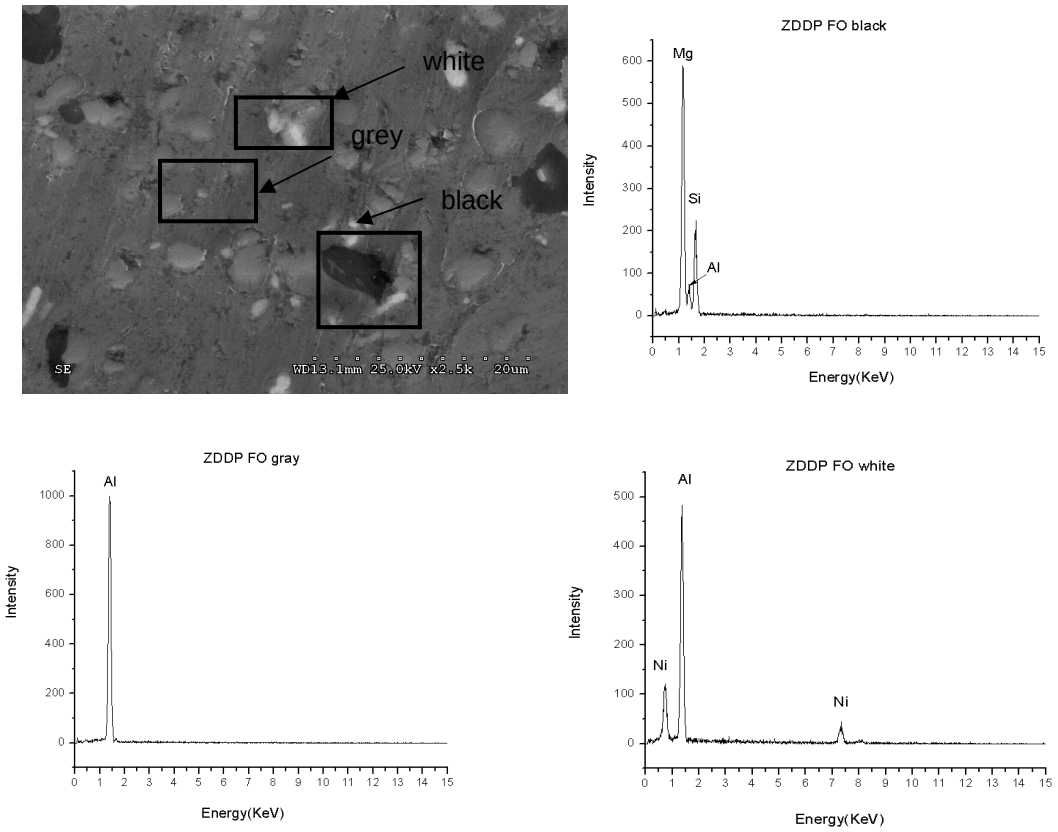

Figure 4.47 Scanning electron micrograph of the middle of the wear scar on the aluminum alloy disk at 2500x magnification for the HFRB wear test run under 0.5kg normal load for 50 Hz on oil sample containing ZDDP(0.10wt%P) in fully formulated oil and EDS spectra obtained from the black, gray, white area of the film.

Fig 4.47 is a scanning electron micrograph from within the wear scar from ZDDP in fully formulated oil. It shows the relatively smooth surface with the presence of precipitates on the surface. EDS analysis was conducted in the matrix region (gray and white) and where the precipitates were present (black).The EDS spectra from the matrix region only indicates the presence of Al confirming the XANES data which indicates that Al is present only in its native oxide state. On the other hand the black particles are Mg_2Si precipitates which do not show any

presence of Fe, P, S, while the white region indicates the presence of Al, and Ni. This is Al_3Ni precipitate. The absence of S or P indicates that the transfer film is relatively thin on the precipitate.

4.4.2 Antimony 0, 0-dialkylphosphorodithioate

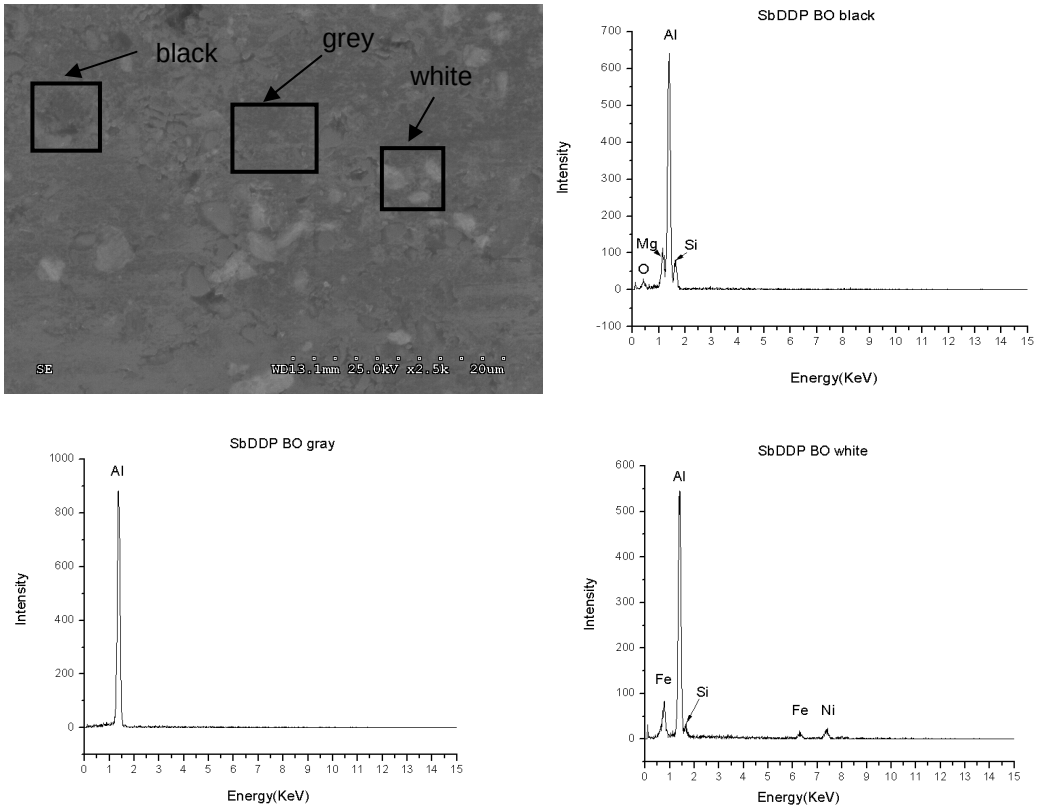

Figure 4.48 Scanning electron micrograph of the middle of the wear scar on the aluminum alloy disk at 2500x magnification for the HFRB wear test run under 0.5kg normal load for 50 Hz on oil sample containing SbDDP(0.10wt%P) in base oil and EDS spectra obtained from the black, gray, white area of the film.

Fig 4.48 is a scanning electron micrograph from within the wear scar from SbDDP in base oil. It shows the relatively smooth surface with the presence of precipitates on the surface. EDS analysis was conducted in the matrix region (gray) and where the precipitates were present (white and black).The EDS spectra from the matrix region only indicates the presence of Al confirming the XANES data which indicates that Al is present only in its native oxide state. On the other hand the black particles are Mg_2Si in Al-matrix which do not show any presence of

Fe, P, S, while the white precipitates indicate the presence of Al, Si, Fe and Ni. This precipitate is Nickel Aluminide with some Si in it and the Fe present is from the transfer film. The absence of S or P indicates that the transfer film is relatively thin on the precipitate. The fact that the transfer film is only present on the precipitate and not in the matrix clearly indicates that the harder precipitate can sustain higher loads without plastic deformation and can be local region where transfer films can be deposited.

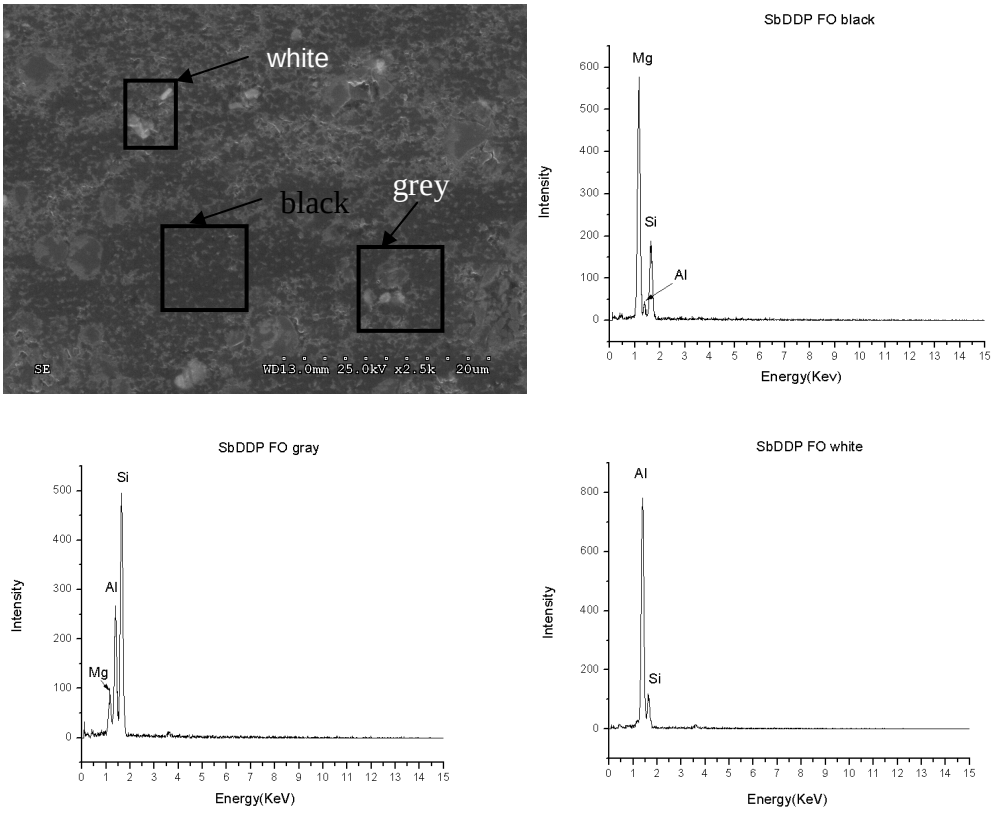

Figure 4.49 Scanning electron micrograph of the middle of the wear scar on the aluminum alloy disk at 2500x magnification for the HFRB wear test run under 0.5kg normal load for 50 Hz on oil sample containing SbDDP(0.10wt%P) in fully formulated oil and EDS spectra obtained from the black, gray, white area of the film.

Fig 4.49 is a scanning electron micrograph from within the wear scar from SbDDP in fully formulated oil. It shows the relatively smooth surface with the presence of precipitates on the surface. EDS analysis was conducted in the matrix region (gray and white) and where the precipitates were present (black).The EDS spectra from the matrix region indicates the

presence of Mg_2Si in Al-matrix, while the white spot indicates the presence of Al, Si. This is the limited solubility of Si in the Al-matrix. On the other hand the black particles are Mg_2Si which do not show any presence of Fe, P, S, The absence of S or P indicates that the transfer film is relatively thin on the precipitate.

4.4.3 Dialkyl Dithiophosphate

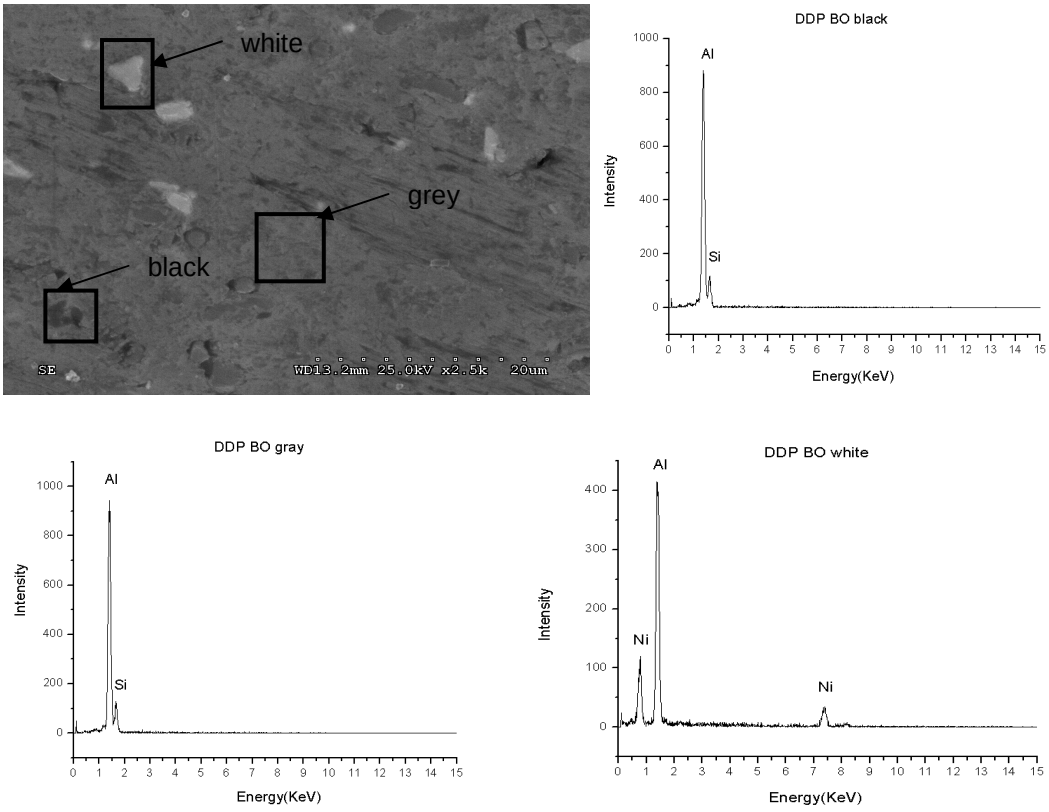

Figure 4.50 Scanning electron micrographs of the middle of the wear scar on the aluminum alloy disk at 2500x magnification for the HFRB wear tests run under 0.5kg normal load for 50 Hz on oil sample containing DDP (0.10wt%P) in base oil and EDS spectra obtained from the black, gray, white area of the film.

Fig 4.50 is a scanning electron micrograph from within the wear scar from DDP in base oil. It shows the relatively smooth surface with the presence of precipitates on the surface. EDS analysis was conducted in the matrix region (black, gray and white).The EDS spectra from the black and gray spots indicate limited solubility of Si in the Al-matrix. On the other hand the white

particle is Al_3Ni precipitates, which do not show any presence of Fe, P, S, The absence of S or P indicates that the transfer film is relatively thin on the precipitate.

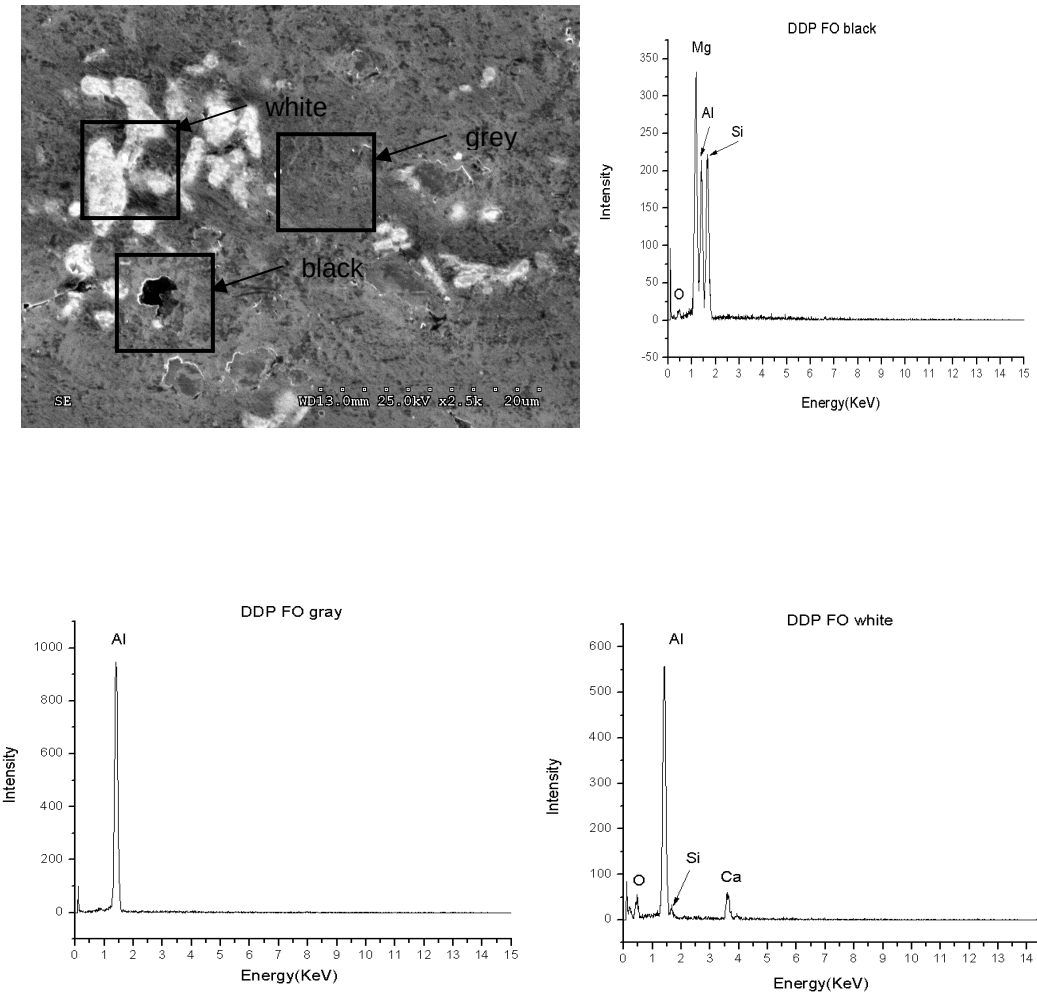

Figure 4.51 Scanning electron micrographs of the middle of the wear scar on the aluminum alloy disk at 2500x magnification for the HFRB wear tests run under 0.5kg normal load for 50 Hz on oil sample containing DDP (0.10wt%P) in fully formulated oil and EDS spectra obtained from the black, gray, white area of tribofilms.

Fig 4.51 is a scanning electron micrograph from within the wear scar from DDP in fully formulated oil. It shows the relatively smooth surface with the presence of precipitates on the surface. EDS analysis was conducted in the matrix region (gray, white) and where the precipitates were present (black).The EDS spectra from the matrix region only indicates the

presence of Al confirming the XANES data which indicates that Al is present only in its native oxide state. On the other hand the black particle is Mg_2Si in the Al-matrix which do not show any presence of Fe, P, S, while the white particle indicates the presence of Al, Si, and Ca. This shows limited solubility Si in Al-matrix and the Ca present is from the detergent. The absence of S or P indicates that the transfer film is relatively thin on the precipitate.

4.4.4 Amine Phosphate

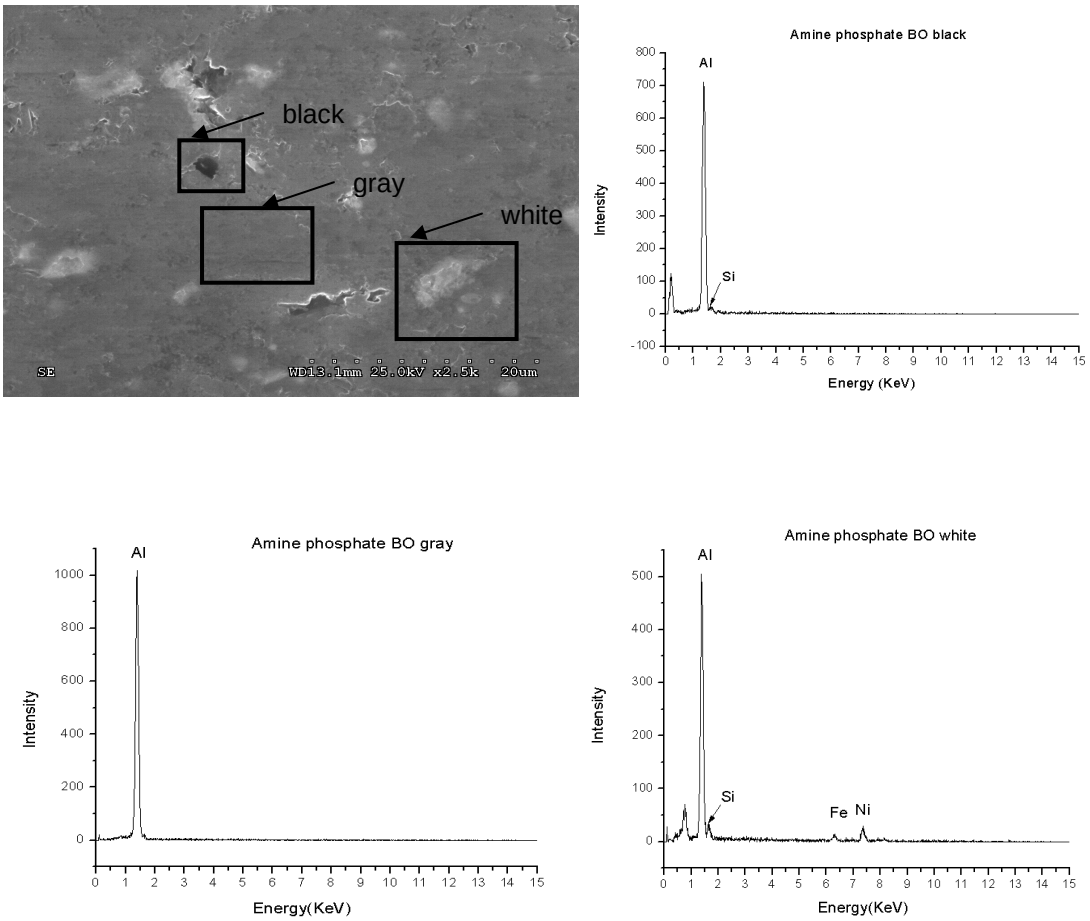

Figure 4.52 Scanning electron micrographs of the middle of the wear scar on the aluminum alloy disk at 2500x magnification for the HFRB wear tests run under 0.5kg normal load for 50 Hz on oil sample containing Amine phosphate(0.10wt%P) in base oil and EDS spectra obtained from the black, gray, white area of the film.

Fig 4.52 is a scanning electron micrograph from within the wear scar from Amine phosphate in base oil. It shows the relatively smooth surface with the presence of precipitates on the surface. EDS analysis was conducted in the matrix region (black, gray) and where the

precipitates were present (white).The EDS spectra from the matrix region only indicates the presence of Al confirming the XANES data which indicates that Al is present only in its native oxide state. On the other hand the black particle is limited solubility Si in Al-matrix which do not show any presence of Fe, P, S, while the white precipitates indicate the presence of Al, Si, Fe and Ni. This precipitate is Nickel Aluminide with some Si in it and the Fe present is from the transfer film. The absence of S or P indicates that the transfer film is relatively thin on the precipitate. The fact that the transfer film is only present on the precipitate and not in the matrix clearly indicates that the harder precipitate can sustain higher loads without plastic deformation and can be local region where transfer films can be deposited.

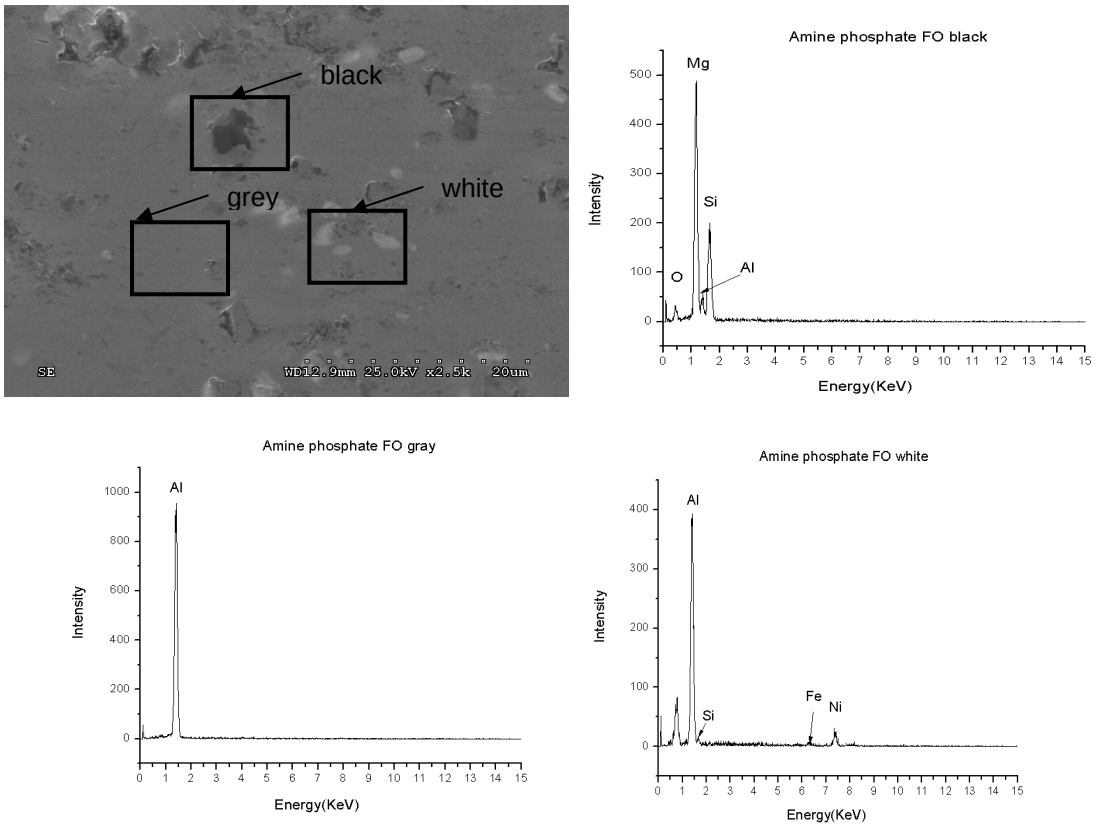

Figure 4.53 Scanning electron micrographs of the middle of the wear scar on the aluminum alloy disk at 2500x magnification for the HFRB wear tests run under 0.5kg normal load for 50Hz on oil sample containing Amine phosphate(0.10wt%P) in fully formulated oil and EDS spectra obtained from the black, gray, white area of the film.

Fig 4.53 is a scanning electron micrograph from within the wear scar from Amine phosphate in fully formulated oil. It shows the relatively smooth surface with the presence of precipitates on the surface. EDS analysis was conducted in the matrix region (gray) and where the precipitates were present (white and black).The EDS spectra from the matrix region only indicates the presence of Al confirming the XANES data which indicates that Al is present only in its native oxide state. On the other hand the black particles are Mg_2Si precipitates which do not show any presence of Fe, P, S, while the white precipitates indicate the presence of Al, Si, Fe and Ni. This precipitate is a complex of Nickel Aluminide with some Si in it and the Fe present is from the transfer film. The absence of S or P indicates that the transfer film is relatively thin on the precipitate. The fact that the transfer film is only present on the precipitate and not in the matrix clearly indicates that the harder precipitate can sustain higher loads without plastic deformation and can be local region where transfer films can be deposited.

4.4.5 Thiadiazole

Fig 4.54 is a scanning electron micrograph from within the wear scar from Thiadiazole in base oil. It shows the relatively smooth surface with the presence of precipitates on the surface. EDS analysis was conducted in the matrix region (black, gray) and where the precipitates were present (white).The EDS spectra from the matrix region indicates limited solubility of Mg in Al-matrix. On the other hand the black particles are Al-matrix only which do not show any presence of Fe, P, S, while the white precipitates indicate the presence of Al, Si, Fe and Ni. This precipitate is a complex of Nickel Aluminide with some Si in it and the Fe present is from the transfer film. The absence of S or P indicates that the transfer film is relatively thin on the precipitate. The fact that the transfer film is only present on the precipitate and not in the matrix clearly indicates that the harder precipitate can sustain higher loads without plastic deformation and can be local region where transfer films can be deposited.

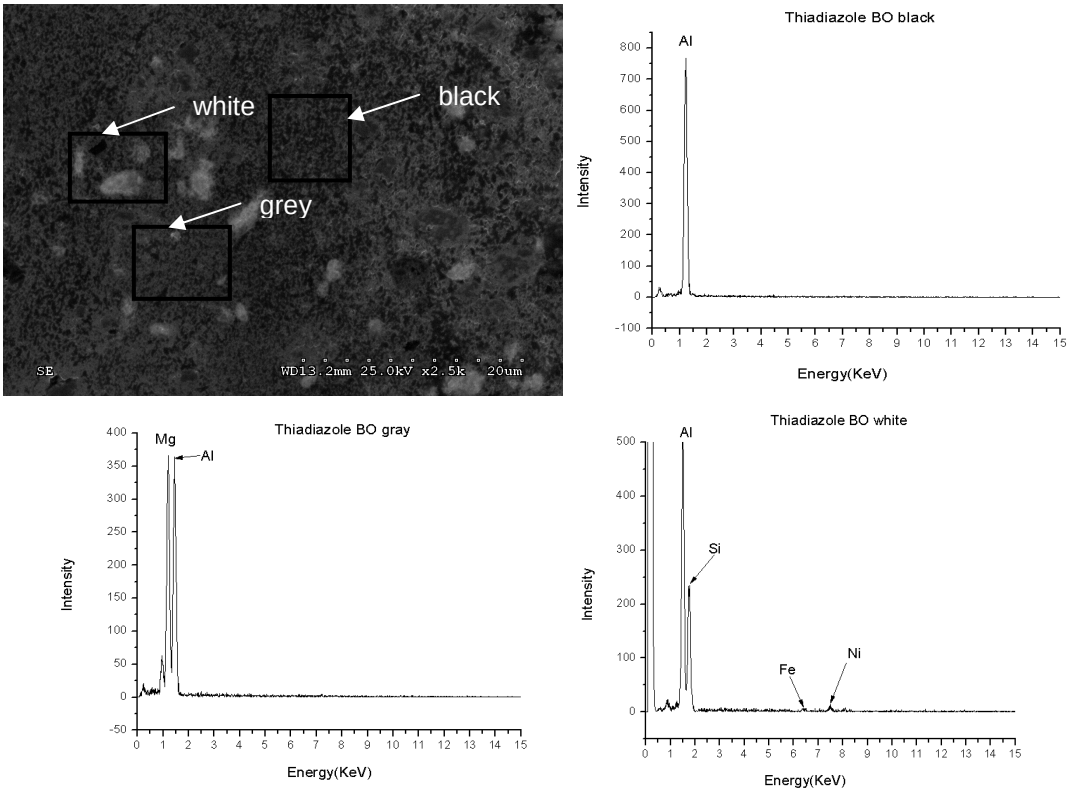

Figure 4.54 Scanning electron micrographs of the middle of the wear scar on the aluminum alloy disk at 2500x magnification for the HFRB wear tests run under 0.5kg normal load for 50 Hz on oil sample containing Thiadiazole (0.20wt%S) in base oil and EDS spectra obtained from the black, gray, white area of tribofilms.

Fig 4.55 is a scanning electron micrograph from within the wear scar from Thiadiazole in fully formulated oil. It shows the relatively smooth surface with the presence of precipitates on the surface. EDS analysis was conducted in the matrix region (black, gray and white) .The EDS spectra from the matrix region only indicates the presence of Al confirming the XANES data which indicates that Al is present only in its native oxide state. On the other hand the black, white regions indicate limited solubility of Si in Al-matrix which do not show any presence of Fe, P, S. The absence of S or P indicates that the transfer film is relatively thin on the precipitate.

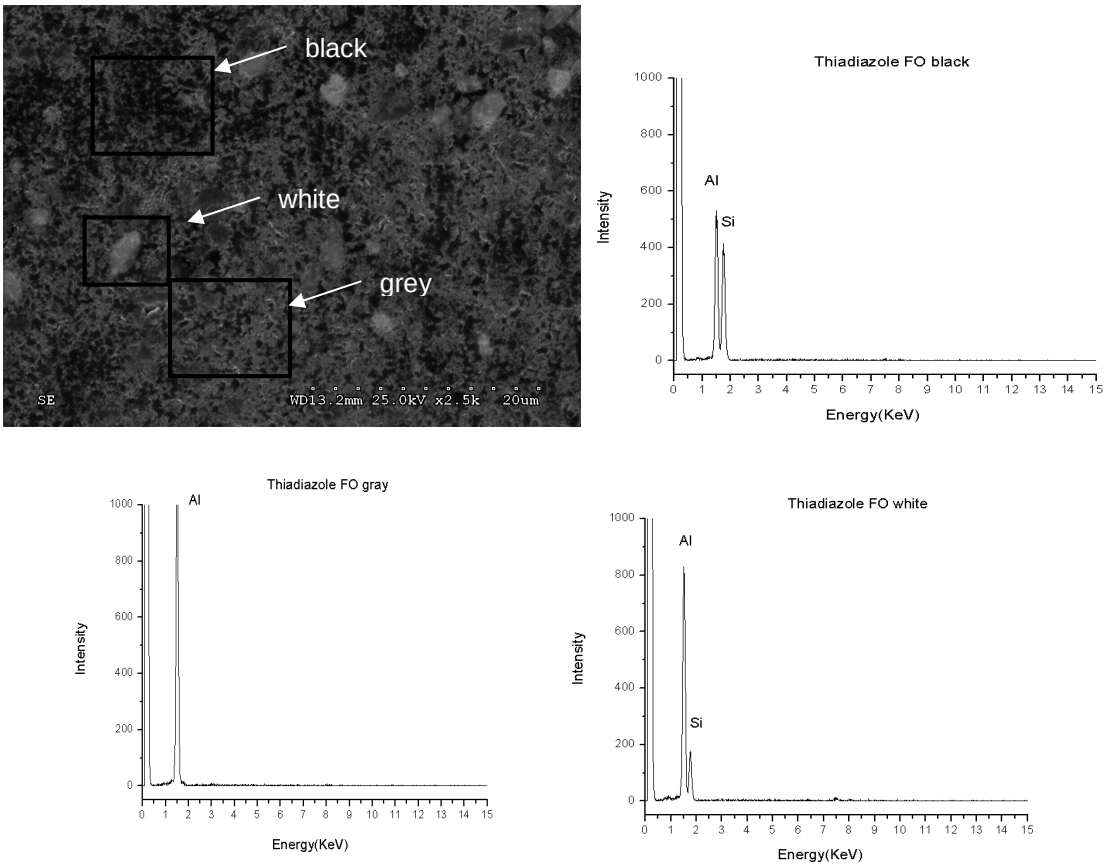

Figure 4.55 Scanning electron micrographs of the middle of the wear scar on the aluminum alloy disk at 2500x magnification for the HFRB wear tests run under 0.5kg normal load for 50 Hz on oil sample containing Thiadiazole (0.20wt%S) in fully formulated and EDS spectra obtained from the black, gray, white area of tribofilms.

CHAPTER 5

MECHANISM

The transfer films formed with these additives show that they contain Fe-phosphates, Fe-sulfates and Fe-sulfides respectively. The P, S from the antiwear additives play a role in wear protection by reacting with Fe in steel. See Table 5.1.

Figure 5.1 shows the cross section of Al alloy, the matrix of this alloy is primarily pure Al with minor a mount of Cu and Mg dissolved in solid solution with the precipitates being made up of pure Si and Mg_2Si, Al_3Ni. The fact that the transfer film is only present on the Nickel Aluminide precipitate and not on the matrix clearly indicates that the harder precipitate can sustain higher loads without plastic deformation and can be local region where transfer films can be deposited.

Table 5.1 The chemistry of the films

Chemistry	Compounds of Transfer Film
ZDDP in base oil	Sulfide, Sulfate ,$FeSO_4$, $ZnSO_4$, Zn-phosphate
ZDDP in fully formulated oil	Sulfide, Sulfate, $ZnSO_4$, $FeSO_4$,Zn-phosphate
SbDDP in base oil	Sulfide, Sulfate, Sb-phosphate
DDP in base oil	$FeSO_4$, iron-phosphate, Al_2O_3, $FePO_4$
DDP in fully formulated oil	$FeSO_4$, iron-phosphate, Al_2O_3, $FePO_4$
Amine phosphate in base oil	$FePO_4$, Al_2O_3
Amine phosphate in fully formulated oil	$FePO_4$,$FeSO_4$, Al_2O_3
Thiadiazole in base oil	$FeSO_4$, Al_2O_3
Thiadiazole in fully formulated oil	$FeSO_4$, Al_2O_3

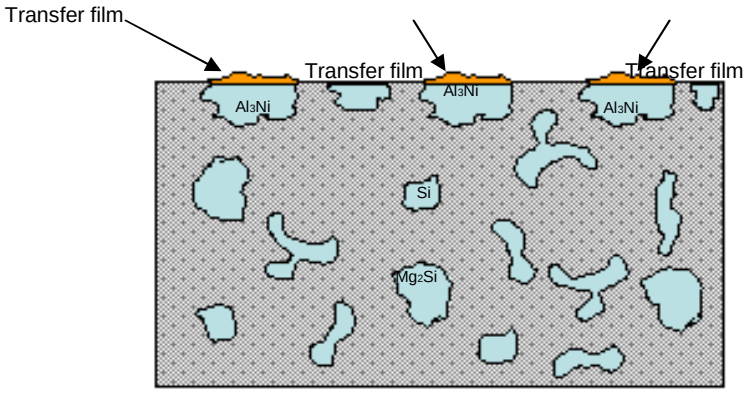

Figure 5.1 The cross section of Al alloy

CHAPTER 6

CONCLUSION

In this study, ZDDP, SbDDP, DDP, Amine phosphate, and Thiadiazole, five antiwear additives wear used for Al-alloy and the mechanism of wear protection was examined using XANES, SEM/EDS and Surface Profiler.

ZDDP and SbDDP are ash antiwear additives because they contain the metal Zn and Sb. The different cation species have the influence on the formation of antiwear film. SbDDP is better than ZDDP in antiwear performance. DDP is an ashless antiwear additive, compared to ZDDP, it can form thicker and better tribofilms and improved wear performance because the Fe from the substrate helps in the cross-linking of polyphosphate film[55].It has been shown that the absence of S and P in the antiwear chemistry results in poor wear performance in steel. P and S play the important role in wear protection by reacting with Fe in steel to form the transfer film containing Fe-sulfates, Fe-sulfides and Fe-phosphates. Amine phosphate and thiadiazole are also the ashless antiwear additives, compared with steel where absence of sulfur or phosphorus results in poor wears protection.

From XANES data, it is shown that Al does not participate in the formation of either a tribofilms or a transfer film on the surface and Al is present alone in the form of native oxide in the bulk of the wear surface. The film is formed on the Ni-silicides precipitates and there is no evidence to suggest the formation of Al-phosphate, sulfide and sulfate. Martin H. Müser et. al [56] in their study of ZDDP and its ability to form protective polyphosphate films suggest that there is a critical pressure and temperature requires for the deposition and formation of long chain polyphosphates. In the case of Al matrix the lower modulus and yield strength results in excessive plastic deformation and the Hertzian contact pressure are not sufficient for the

formation of polyphosphate tribofilms on Al. The transfer films formed with these additives show that they contain Fe-phosphates, Fe-sulfates and Fe-sulfides respectively. The P, S from the antiwear additives play a role in wear protection by reacting with Fe in steel. An antiwear chemistry that contains both S and P is used (eg. DDP), it has better antiwear performance. Hence it can be summarized that either S or P is insufficient to form protective films on the surface.

From the SEM/EDS data, the wear surface is relatively smooth with the presence of precipitates on the surface. EDS analysis was conducted in the matrix region and where the precipitates were present. The EDS spectra from the matrix region only indicate the presence of Al confirming the XANES data which indicates that Al is present only in its native oxide state. On the other hand the precipitates are Mg_2Si and Nickel Aluminide with some Si in it. The absence of S and P indicates that the transfer film is relatively thin on the precipitate. The fact that the transfer film is only present on the Nickel Aluminide precipitate and not on the matrix clearly indicates that the harder precipitate can sustain higher loads without plastic deformation and can be local region where transfer films can be deposited.

APPENDIX A

CHEMICAL STRUCTURES OF ANTIWEAR ADDITIVES

a) ZDDP (Zinc dialkyl-dithiophosphate)

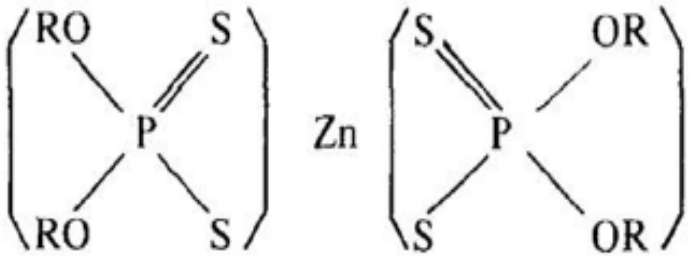

b) VANLUBE 622(Antimony 0, 0-dialkylphosphorodithioate)

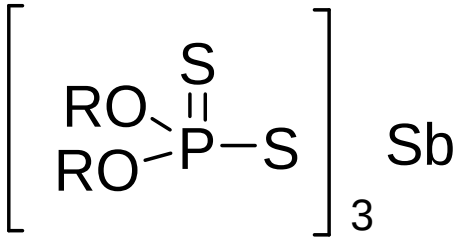

c) IRGALUBE 353 (Dialkyl dithiophosphate)

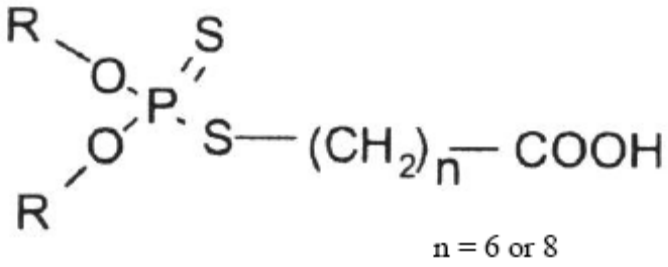

d) IRGALUBE 349 (Amine phosphates)

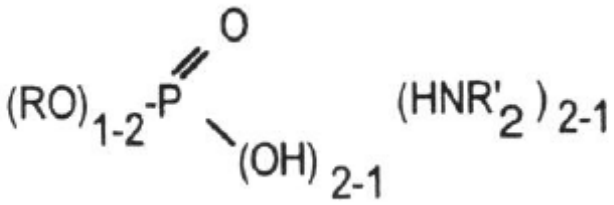

e) VANLUBE 972 (Thiadiazole derivative triethylene glycol monobutyl ether)

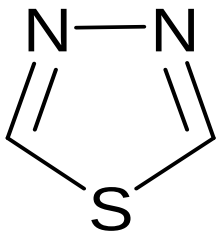

1, 3, 4-thiadiazole derivative 40% by weight

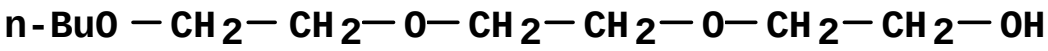

butoxytriglycol 45% by weight

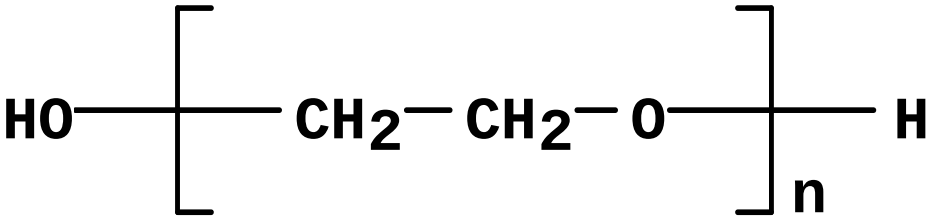

Polyethylene glycol 15% by weight

REFERENCES

1 Mark A. Nicholls, “Micro-scale chemical and mechanical characterization of ZDDP antiwear films on steel and Al-Si alloys.”

2 Barnes, A. M., Bartle, K.D., and Thibon, V.R.A., 2001, “A Review of Zinc Dialkyldithiophosphates (ZDDPS): Characterisation and Role in the Lubrication Oil” Tribology International, 34(6) pp.389-395.

3 Minfray,C.,Martin,J.M.,Esnouf,C.,2004, “A multi-technique approach of tribofilm characterization,” Proceedings of the 30th International Conference on Metallurgie, Apr 28-May 2 2002,Elsevier,San Diego, CA, United States,447-448,pp.272-277.

4 Nicholls, M.A., Do, T., Norton, P.R., 2005, “Review of the Lubrication of Metallic Surfaces by Zinc Dialkyl-Dithiophosphates,” Tribology International, 38pp.15-39.

5 So,H.,Lin,Y.C.,Huang,G.G.S.,1993, “Antiwear Mechanism of Zinc DialkylDithiophosphates Added to a Paraffinic Oil in the Boundary Lubrication Condition,” Wear,166(1)pp.17-26.

6 Sheasby, J.S., Caughlin, T.A., and Habeeb, J.J., 1991, “Observation of the Antiwear Activity of Zinc Dialkyldithiophosphate Additives,” Wear, 150(1-2) pp.247-257.

7 Willermet,P.A.,Dailey,D.P.,Carter,R.O.,III,1995, “Mechanism of Formation of Antiwear Films from Zinc Dialkyldithiophosphates,” Tribology International,28(3)pp.177-187.

8 Neville, A., and Kollia-Rafailidi, V., 2002, “A Comparison of Boundary Wear Film Formation on Steel and a Thermal Sprayed Co/Cr/Mo Coating under Sliding Conditions,” Wear, 252(3-4) pp.227-239.

9 I.M.Hutching, Tribology: Friction and Wear of Engineering Materials, CRC Press, London, 1992.

10 Kapsa, P., Martin, J.M., Blanc, C., 1981, “Antiwear Mechanism of ZDDP in the Presence of Calcium Sulfonate Detergent.”Journal of Lubrication Technology, Transactions ASME, 103(4) pp.486-496.

11 S.Hironaka and T.Sakurai, Wear 50(1978) 105.

12 L.T.Hu, J.M.Chen, W.M.Liu, Q.J.Xue, and C.Kajdas, Wear 243(2000) 60.

13 M.Kawamura and K.Fujita, Wear 89(1983) 99.

14 R.S.Montgomery, Wear 8 (1965) 289.

15 P.C.Nautiyal and J.A.Schey, J.Trib.112 (1990) 282.

16 M.Fuller, M.Kasrai, J.S.Sheasby, G.M.Bancroft, K.Fyfe, and K.H.Tan, Trib.Lett.1 (1995)367.

17 T.Konishi, E.E.Klaus, and J.L.Duda, Trib.Trans.39 (1996)811.

18 Y.Wan, L.L.Cao, and Q.J.Xue, Trib.Int.30 (1997)767.

19 M.Kawamura and K.Fujita, Wear 89(1983)99.

20 Gwidon W. Stachowiak, Engineering tribology.

21 Ajay Kapoor, Simon C. Tung, Shirley E. Schwartz, Martin Priest, Rob S.Dwyer-joyce, Modern Tribology Handbook.

22 Bhushan, B., 2000, “Modern Tribology Handbook, Volume 1,”C R C Press LLC, United States of America, pp.1760.

23 Chattopadhyay, R. (2001). Surface Wear - Analysis, Treatment, and Prevention. OH, USA: ASM-International. ISBN 0-87170-702-0.

24 Parekh, K., 2006, “Interactions between Antiwear Agent and Novel Additive in Engine Oils”

25 Tonck,A.,Martin,J.M.,Kapsa,P.,1979, “Boundary Lubrication with Anti-Wear Additives; Study of Interface Film Formation by Electrical Contact Resistance,” Tribology International,12(5)pp.209-213.

26 Khorramian, B.A., Iyer, G.R., Kodali, S., 1993, “Review of Antiwear Additives for Crankcase Oils,” Wear, 169(1) pp.87-95.

27 Allyson M. Barnes, Keith D. Bartle, Vincent R. A. Thibon, A review of zinc diakyldithiophosphates (ZDDPS); characterization and role in the lubricating oil.

28 Fuller, M., Z., Kasrai, M., 1997, “Chemical Characterization of Tribochemical and Thermal Films Generated from Neutral and Basic ZDDPs using X-Ray Absorption Spectroscopy,” Tribology International, 30(4) pp.305-315.

29 Li,Y.,Pereira,G.,Kasrai,M.,2007, “Studies on ZDDP Anti-Wear Films Formed Under Different Conditions by XANES Spectroscopy, Atomic Force Microscopy and 31 P NMR,” Tribology Letters,28(3)pp.319-328.

30Harrison,J.J.,Chan,C.Y.,Onopchenko,A.,2007,Neutral Zinc(II)O,O-Di-Alkyldithiophosphates-Variable Temperature 31P NMR and Quantum Chemical Study of the ZDDP Monomer-Dimer Equilibrium,” Magnetic Reonace in Chemistry,46(2)pp.115-115-124.

31 Spikes, H.A., 2004, “The History and Mechanisms of ZDDP,” Tribology Letters, 17(3) pp.469-489.

32 K.J.Bird and G.D.Galvin, Wear 37(1976)143.

33 S.Jahanmir, J.Trib.109 (1987)577.

34 M.I.De Barros, J.Bouchet, I.Raoult, T.Le Mogne, J.M.Martin, M.Kasrai, and Y.Yamada, Wear 254(2003)863.

35 E.S.Ferrari, K.J.Roberts, M.Sansone, and D.Adams, Wear 236(1999)259.

36 J.M.Martin, J.L.Mansot, I.Berbezier, and H.Dexpert, Wear 93(1984)117.

37 F.G.Rounds, ASLE Trans.18 (1975)79.

38 C.Westerfield and S.Agnew, Wear 181(1995)805.

39 C.Grossiord, J.M.Martin, T.Le Mogne, and T.Palermo, Trib.Lett.6 (1999)171.

40 E.S.Ferrari, K.J.Roberts, and D.Adams, Wear 253(2002)759.

41 D.R.Armstrong, E.S.Ferrari, K.J.Roberts, and D.Adams, Wear 208(1997)138.

42 D.R.Armstrong, E.S.Ferrari, K.J.Roberts, and D.Adams, Wear208 (1997)138.

43 D.R.Armstrong, E.S.Ferrari, K.J.Roberts, and D.Adams, Wear217 (1998)276.

44 C.Westerfield and S.Agnew, Wear 181(1995) 805.

45 P.A.Willermet,J.M.Pieprzak,D.P.Dailey,R.O.Carter III,N.E.Lindsay,L.P.Haack,and J.E.de Vries,J.Trib.113(1991)38.

46 Z.Yin, M.Kasrai, G.M.Bancroft, K.F.Laycock, and K.H.Tan, Trib.Int.26 (1993)383.

47 Z.Yin, M.Kasrai, G.M.Bancroft, K.F.Laycock, and K.H.Tan, Trib.Int.26 (1993)383.

48 P.A.Willermet,J.M.Pieprzak,D.P.Dailey,R.O.Carter III,N.E.Lindsay,L.P.Haack,and J.E.de Vries,J.Trib.113(1991)38.

49 55 M.L.Suominen Fuller, M.Kasrai, G.M.Bancroft, K.Fyfe, and K.H.Tan, Trib.Int.31 (1998)627.

50 E.S Ferrari, K.J.Roberts, M.Sansone, and D.Adams, Wear 236(1999)259.

51 J.M.Martin, C.Grossiord, K.Varlot, B.Vacher, and J.Igarashi, Trib.Lett.8 (2000)193.

52 J.M.Martin, Trib.Lett.6 (1999) 1.

53 70 Ye, Z., Zhang, C., Wang, Y., 2004, “An Experimental Investigation of Piston Skirt Scuffing: A Piston Scuffing Apparatus, Experiments, and Scuffing Mechanism Analysis,” Wear, 257(1-2) pp.8-31.

54 The Canadian Light Source; www.lightsource.ca.

55 Bohoon Kim, Properties of Tribofilm formed with Ashless Dithiophosphate and Zinc Dialkyl Dithiophosphate under Extreme Pressure Conditions.

56 Nicholas J. Mosey, Martin H. Müser, Tom K. Woo “Molecular Mechanism for the Functionality of Lubricant Additives” Science 307, 1612(2005) DOI:10.1126/science.1107895

BIOGRAPHICAL INFORMATION

Beibei Wang received her B.Sc. in Materials Science and Engineering from the Beijing Technology and Business University. She started graduate studies at UT Arlington in fall 2007 .She did her research towards a master degree under the supervision of professor Pranesh B. Aswath. Her research focuses on aluminum tribology.